

SMC Bulletin

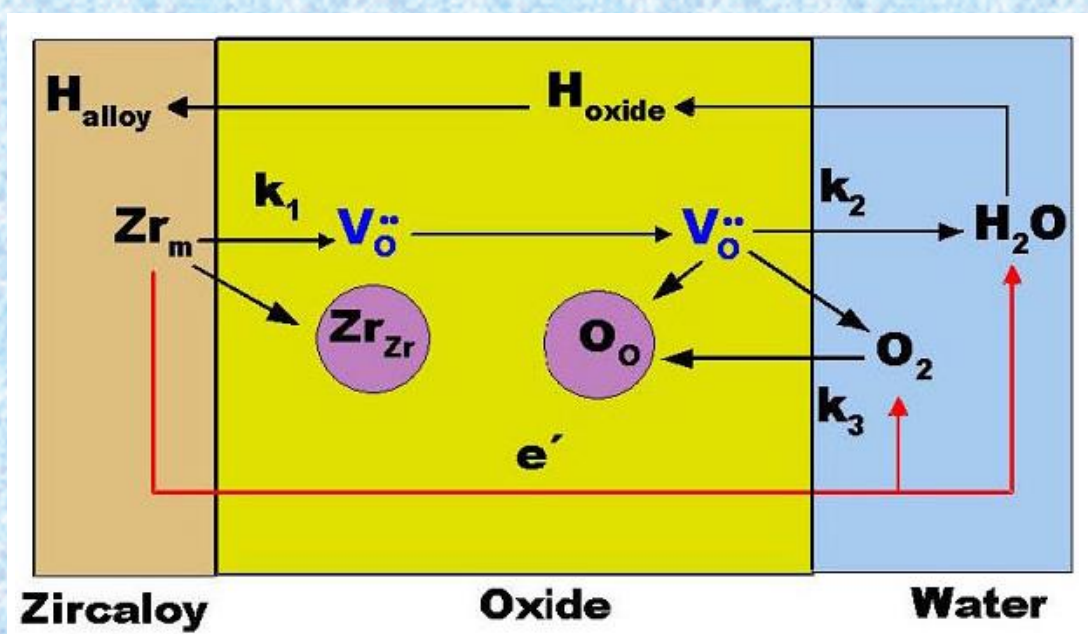
ISSN 2394-5087

A Publication of the Society for Materials Chemistry

Volume 15

No. 1

April 2024



Special Issue on
Electrochemistry for Nuclear and Other Application.



Society for Materials Chemistry

Society for Materials Chemistry was mooted in 2007 with following aims and objectives:

- (a) to help the advancement, dissemination and application of the knowledge in the field of materials chemistry,
- (b) to promote active interaction among all material scientists, bodies, institutions and industries interested in achieving the advancement, dissemination and application of the knowledge of materials chemistry,
- (c) to disseminate information in the field of materials chemistry by publication of bulletins, reports, newsletters, journals.
- (d) to provide a common platform to young researchers and active scientists by arranging seminars, lectures, workshops, conferences on current research topics in the area of materials chemistry,
- (e) to provide financial and other assistance to needy deserving researchers for participation to present their work in symposia, conference, etc.
- (f) to provide an incentive by way of cash awards to researchers for best thesis, best paper published in journal/national/international conferences for the advancement of materials chemistry,
- (g) to undertake and execute all other acts as mentioned in the constitution of SMC.

Executive Committee

President

Dr. A. K. Tyagi

Bhabha Atomic Research Centre
Trombay, Mumbai – 400 085
Email: aktyagi@barc.gov.in

Vice-Presidents

Prof. Kulamani Parida

Siksha 'O' Anusandhan University
Bhubaneswar – 751 030, Odisha
Email: kulamaniparida@soa.ac.in

Dr. P. A. Hassan

Bhabha Atomic Research Centre
Trombay, Mumbai – 400 085
Email: hassan@barc.gov.in

Secretary

Dr. Sandeep Nigam

Bhabha Atomic Research Centre
Trombay, Mumbai – 400 085
Email: snigam@barc.gov.in

Treasurer

Dr. K. C. Barick

Bhabha Atomic Research Centre
Trombay, Mumbai – 400 085
Email: kcbarick@barc.gov.in

Members

D Prof. Amreesh Chandra

Indian Institute of Technology
Kharagpur Kharagpur – 721 302

Dr. Chandra N. Patra

Bhabha Atomic Research Centre
Trombay, Mumbai – 400 085

Dr. Deepak Tyagi

Bhabha Atomic Research Centre
Trombay, Mumbai – 400 085

Prof. (Smt.) Kanchana V.

Indian Institute of Technology
Hyderabad Kandi-502284, Sangareddy,
Telangana

Dr. (Smt.) Mrinal R. Pai

Bhabha Atomic Research Centre
Trombay, Mumbai – 400 085

Dr. Pranesh Senguta

Bhabha Atomic Research Centre
Trombay, Mumbai – 400 085

Dr. R. K. Vatsa

Department of Atomic Energy Mumbai
Mumbai – 400 001

Dr. Sukhendu Nath

Bhabha Atomic Research Centre
Trombay, Mumbai – 400 085

Prof. Tokeer Ahmad

Jamia Millia Islamia
Jamia Nagar, New Delhi – 110 025

Dr. V. K. Jain,

UM-DAE Centre for Excellence in Basic
Sciences, University of Mumbai
Kalina Campus, Mumbai – 400098

Dr.(Smt.) Vinita G. Gupta

Bhabha Atomic Research Centre
Trombay, Mumbai – 400 085

Prof. Vivek Polshettiwar

Tata Institute of Fundamental
Research Mumbai – 400 005

Dr. Y. K. Bhardwaj

Bhabha Atomic Research Centre
Trombay, Mumbai – 400 085

Co-opted Members

Dr. Adish Tyagi

Bhabha Atomic Research Centre
Trombay, Mumbai – 400 085

Prof. G. Mugesh

Indian Institute of Science Bangalore
Bangalore – 560 012

Dr. Pramod Sharma

Bhabha Atomic Research Centre
Trombay, Mumbai – 400 085

Prof. Sandeep Verma

Indian Institute of Technology Kanpur
Kanpur – 208 016

Contact address

Society for Materials Chemistry

C/o Chemistry Division

Bhabha Atomic Research Centre, Trombay, Mumbai, 400 085, India

Tel: +91-22-25592001, E-mail: socmatchem@gmail.com

SMC Bulletin

A Publication of the Society for Materials Chemistry

Volume 15

No. 1

April 2024

Special Issue on
Electrochemistry for Nuclear and Other Application.



SMC Bulletin

Vol. 15

No. 1

April 2024

Guest Editor

V S Tripathi

Radiation & Photochemistry Division
Bhabha Atomic Research Centre
Trombay, Mumbai-400085
Email: vst_apcd@barc.gov.in

Editorial Board	
<p>Dr. C. Majumder (Editor-in-Chief) Chemistry Division Bhabha Atomic Research Centre Trombay, Mumbai - 400 085 Email: chimaju@barc.gov.in</p>	<p>Dr. Arvind Kumar Tripathi Chemistry Division Bhabha Atomic Research Centre Trombay, Mumbai, 400 085 e-mail: catal@barc.gov.in</p>
<p>Dr. (Smt.) S. N. Sawant Chemistry Division Bhabha Atomic Research Centre Trombay, Mumbai - 400 085 Email: stawde@barc.gov.in</p>	<p>Dr. (Smt.) Mrinal Pai Chemistry Division Bhabha Atomic Research Centre Trombay, Mumbai - 400 085 Email: mrinalr@barc.gov.in</p>
<p>Dr. (Kum.) Manidipa Basu Chemistry Division Bhabha Atomic Research Centre Trombay, Mumbai, 400 085 e-mail: deepa@barc.gov.in</p>	<p>Prof. (Smt.) Kanchana V. Department of Physics Indian Institute of Technology Hyderabad Kandi-502284, Sangareddy, Telangana Email: kanchana@phy.iith.ac.in</p>
<p>Dr. Kaustava Bhattacharyya Chemistry Division Bhabha Atomic Research Centre Trombay, Mumbai - 400 085 Email: kaustava@barc.gov.in</p>	<p>Dr. (Smt.) Gunjan Verma Chemistry Division Bhabha Atomic Research Centre Trombay, Mumbai - 400 085 Email: gunjanv@barc.gov.in</p>

Published by

Society for Materials Chemistry
C/o. Chemistry Division
Bhabha Atomic Research Centre, Trombay, Mumbai, 400 085
E-mail: socmatchem@gmail.com,
Tel: +91-22-25592001

Please note that the authors of the paper are alone responsible for the technical contents of papers and references cited therein.

Guest Editorial



V S Tripathi

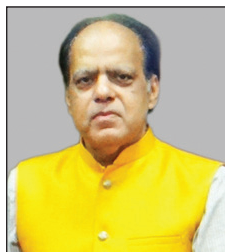
It is a privilege for me to present the thematic issue of SMC bulletin on “Electrochemistry for Nuclear and Other Application.” Electrochemistry deals with the transfer of charge across the interface between different chemical phases, most commonly between a solid electrode phase and a dissolved electrolyte phase. Traditionally electrochemistry has been more relevant in the field of corrosion evaluation under equilibrium conditions, electrowinning and electrorefining of common and reactive metals and energy storage using cells. The discernment of fundamentals of kinetic and thermodynamic processes of the electrochemical reactions has led to spread of electrochemistry in broader areas and now it has become a truly multidisciplinary field. The present issue provides a glimpse of recent applications of electrochemistry in nuclear field along with its application in generation of green fuel and sensing at trace levels.

Evaluating the electrochemical behavior of structural materials in a very low conductivity medium under high temperature and high pressure conditions is unique challenge. Contact Distance Electrochemistry (CDE) is a tool to carry out electrochemical measurement in such a challenging medium. In-situ evaluation of corrosion behavior using this system in conjunction with electrochemical impedance spectroscopy (EIS) is elaborated in the first article. The application of EIS in evaluating the corrosion behavior is nicely elaborated in the second article which deals with the decontamination studies related with stellite. The impedance measurements carried out over the entire duration of decontamination has been used to elucidate the selective dissolutions in different decontamination media. An overview of the applications of electrochemistry in the nuclear fuel cycle is presented in the third article. The advanced electrochemical methods which are used in chemical quality control of nuclear fuel, spent-fuel reprocessing, pyroprocessing of spent nuclear fuel etc are discussed in this article. A variation of redox potential measurement for monitoring the progress of an electrochemical synthesis process is presented in the fourth article. Herein, the application of a high frequency alternating voltage to overcome the polarization of the electrode is described. The fifth article provides a review of the electrochemical water splitting methodologies which are being hotly pursued towards meeting the sustainable energy requirements. The recent advances in the field of bifunctional electrocatalysts based on nanoparticles, conducting polymers and metal organic frameworks is nicely presented in this article. The use of electrochemistry for sensing applications is presented in the sixth article. Application of zinc oxide nanoparticle modified carbon paste electrode for determination of vanillin is described in this article.

These articles give a flavor of the work carried out in some of the labs but it does not cover the extensive field of applications of electrochemistry. However, we are confident that depth of the subject portrayed and diverse nature of the field presented in the bulletin would inspire the young researchers to explore field to further depths.

I sincerely acknowledge the active cooperation received from all the contributors of the articles appearing herein. I also thank the Society for Materials Chemistry for entrusting the guest editorial responsibility on me.

From the desks of the President and Secretary



Dr. A. K. Tyagi



Dr. Sandeep Nigam

Dear SMC Members, Colleagues and Readers,

Warm greetings from the Executive Council of the Society for Materials Chemistry (SMC)!

There has been continuous effort of our editorial team to bring out contemporary thematic issues. The multidisciplinary nature of these issues makes them relevant to the researchers of different scientific background. In the same direction, current issue entitled “Electrochemistry for nuclear and other applications” is another marching step.

First article of this thematic issue presents Controlled Distance Electrochemistry (CDE) for High Temperature Oxidation Studies of nuclear materials in reactor simulated condition. Another article presents the utilization of Electrochemical Impedance Spectroscopy to elucidate the mechanism of Stellite corrosion in permanganate based decontaminating formulations. Rapid and sensitive redox speciation method for vanadium during electro-synthesis of V(II) formate has been described in one of the chapter. Fabrication of a voltammetrically effective Vanillin sensor at a ZnO-modified carbon paste electrode has been presented in another chapter. Other two chapters also beautifully present the use of electrochemistry for targeted applications.

We gratefully acknowledge Dr. V. S. Tripathi who agreed to be the guest editor of this issue and put in efforts to bring out this special issue. We also acknowledge the efforts of all the contributing authors for submitting their informative articles. We also thank all the members of SMC for their continued support and cooperation in the growth of the Society for Materials Chemistry.

CONTENTS

Sr. No	Feature Articles	Page No.
1.	Controlled Distance Electrochemistry (CDE) for High Temperature Oxidation Studies of nuclear materials in reactor simulated condition <i>Kiran K Mandapaka and Supratik Roychowdhury</i>	1
2.	Electrochemical Impedance Spectroscopy to elucidate the mechanism of Stellite #3 corrosion in permanganate based decontaminating formulations <i>Veena Subramanian, Sinu Chandran, S.V. Narasimhan, and T.V. Krishnamohan</i>	7
3.	Electrochemistry in Nuclear Fuel Cycle <i>Manoj Kumar Sharma</i>	15
4.	Rapid and sensitive redox speciation method for vanadium during electro-synthesis of V(II) formate <i>K. K. Bairwa and V. S. Tripathi</i>	27
5.	Advancing Green Hydrogen Revolution: A Comprehensive Review of Bifunctional Electrocatalysts and Hybrid Materials for Water Electrolysis <i>Naseem Kousar, Gouthami Patil, Lokesh Koodlur Sannegowda*</i>	33
6.	Fabrication of a voltammetrically effective Vanillin sensor at a ZnO-modified carbon paste electrode: A cyclic voltammetric study <i>G.S. Sumanth, B.E. Kumara Swamy*, K. Chetankumar</i>	42

Controlled Distance Electrochemistry (CDE) for High Temperature Oxidation Studies of nuclear materials in reactor simulated condition

Kiran K Mandapaka and Supratik Roychowdhury

Corrosion Engineering Section, Materials Processing and Corrosion Engineering Division,
Bhabha Atomic Research Centre, Trombay, Mumbai – 400 085, India

Email: supratik@barc.gov.in

Abstract

Oxidation of metals and alloys in nuclear reactor aqueous environment is an electrochemical phenomenon and a mechanistic understanding of the same necessitates study of in-situ electrical/electronic properties of oxide. Majority of in-core structural components in nuclear reactors are exposed to a variety of water chemistry at high temperature and high pressure (HTHP) including demineralised (DM) water. The challenge is to perform electrochemical measurements in-situ during oxidation in poor conductivity DM water. This paper presents the technique of controlled distance electrochemistry (CDE) and its efficacy to conduct electrochemical measurements using contact electric resistance (CER) and electrochemical impedance spectroscopy (EIS) in DM water. Illustrations are presented from oxidation of carbon steel, stainless steel and zirconium alloys.

Introduction

Oxidation of metals and alloys is an electrochemical phenomenon and electrochemical experiments in the environment of interest gives insights into the mechanism. Figure 1 is an illustration of mixed conduction model of oxidation behaviour of zirconium (Zr) and its alloys [1-2]. The rate controlling step in the process of oxidation is the diffusion of oxygen anions (O^{2-}) through anionic vacancy across the surface oxide layer [2-3]. The factors affecting oxidation would be the diffusion coefficient of such anions, electric field gradient across the oxide layer and/or electric resistance / impedance of the oxide. A thorough mechanistic insight into the phenomenon of oxidation can be obtained if electrochemical measurements can be obtained in-situ during oxidation [4-6]; such as electrochemical impedance spectroscopy in the actual environmental conditions to which the alloy is exposed to during service. In-core structural components in nuclear power reactors get exposed to a variety of water chemistry, depending on the reactor type, at high temperature and high pressure (HTHP). The primary coolant in boiling water reactor (BWR) [1] and Advanced heavy water reactor (AHWR) [7] is DM water with a specific conductivity of $0.055 \mu\text{Scm}^{-1}$ without any chemical addition. The nature of oxide and the oxidation kinetics do play vital role in the material degradation in such environments; for example, intergranular stress corrosion cracking (IGSCC) [8-9] of stainless steel (SS) or oxidation of zirconium (Zr) base alloys (both localized and uniform oxidation) and consequent hydrogen pick-up leading to hydrogen related damages [1, 3, 10].

Nevertheless, the major challenge posed in in-situ high temperature electrochemical measurements in simulated BWR/AHWR environment is the large solution resistance leading to high ohmic (IR) drop. The advent of controlled distance electrochemistry (CDE) approach [4-6] facilitates oxidation studies in low conductivity electrolytes (such as DM water). The CDE arrangement maintains a very close distances (of the order of $\sim 5 \mu\text{m}$) between working (WE) and counter electrodes (CE) throughout the duration of electrochemical measurements which reduces the IR drop enabling electrochemical measurements in HTHP DM water. A combination of recirculation test loop capable of maintaining desired water chemistry and an autoclave equipped with CDE arrangement is an ideal set up for in-situ mechanistic studies of the oxidation behavior of

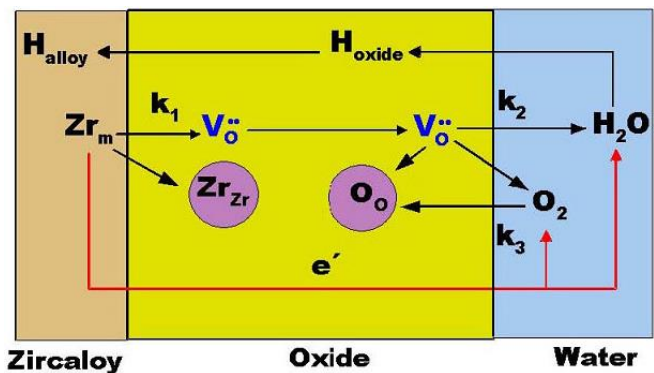


Figure 1. Oxidation of zirconium alloys as an electrochemical phenomenon; the symbols used are Zr_m = zirconium atom in the metal, Zr_{Zr} = zirconium ion in oxide oxide lattice, $V_o^{\bullet\bullet}$ = oxygen ion vacancy and O_o = oxygen ion in the oxide lattice [2].

materials in BWR/AHWR simulated environment. This paper presents the application of CDE approach to the study of in-situ HTHP oxidation behavior of carbon steel, SS and Zr alloys with varying material condition in high purity water environment. The techniques used are contact electric resistance (CER) [4-6] and electrochemical impedance spectroscopy (EIS) coupled with oxide morphological characterization. The advantage of CDE approach over conventional gravimetric method is highlighted.

Experimental Methodology

The schematic representation of CDE set-up inside the autoclave is shown in Fig.2. It uses a stepper motor controller to control the movement of a calibrated stiff spring which in turn allows maintaining a desired distance between the counter electrode (CE) and working electrode (WE). A shunt resistor parallel to the CE-WE is used to discriminate between contact and break position. The wire penetrations through the autoclave pressure boundary are connected to a potentiostat and frequency response analyzer (FRA). The autoclave with the CDE arrangement was connected to a recirculation loop and was refreshed continuously with desired chemistry water.

The in-situ characterization of the oxide films was done using CER and EIS techniques. The 3 mm discs required for fitting into the CDE holder [4-6] were prepared from the alloys to be studied. Iridium (Ir) tip with a diameter of 3 mm was used as a counter electrode for both CER and CDE-EIS measurements performed in-situ during the exposures in the recirculation autoclave system. The EIS measurements were done in a two-electrode configuration in which the Ir probe was connected to both the reference and the counter electrode terminals. The CER technique is based on the measurement of the electrical resistance across a solid-solid contact surface using direct current [4-6]. During the measurement, the surfaces of the Ir and the working sample were brought in contact and pulled apart to a distance of 10 μm at regular intervals. The surfaces of the working electrode and the Ir electrode came in contact with the environment when the probes were pulled apart. When the surfaces were brought into contact, a direct current was passed through the contact surfaces and the resulting potential was measured in order to determine the resistance (CER) of the surface film. All the resistance measured in this arrangement is due to the surface film (oxide) formed on the working electrode as Ir remains inert in the environment and does not contribute to the resistance. Application of potential to

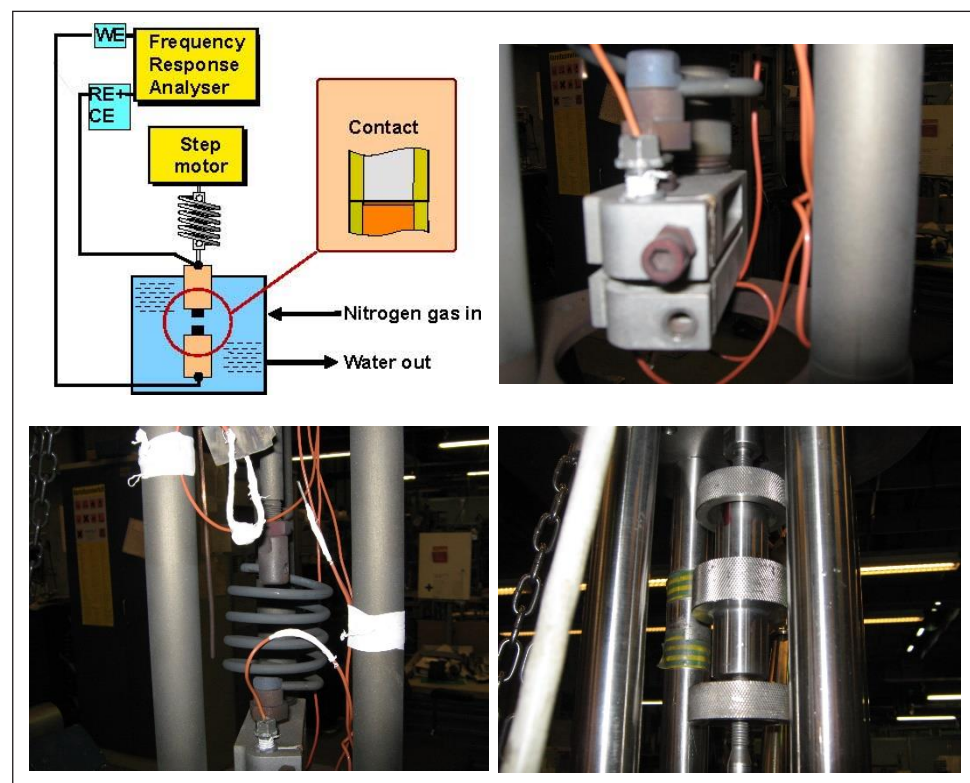


Figure 2. The CDE set-up inside an autoclave attached to a recirculation loop: (a) schematic showing CE-WE arrangement, (b) the specimen holder for Ir tip CE and WE, (c) stiff spring with holder (d) pull rod controlling the movement of spring through a stepper motor across autoclave pressure boundary.

the sample was not feasible as the measurements were done in high purity water (conductivity < 0.10 $\mu\text{S cm}^{-1}$). The resistance of the film was recorded with increasing time of exposure until a film with stable CER value was formed. The Ir tip was then positioned at 10 μm from the sample surface by the help of a stepper motor arrangement and impedance spectra of the film were recorded. In the EIS measurements, an a.c. voltage perturbation of 20 mV was applied over a frequency ranging from 10^{-3} to 10^6 Hz. The response in current was recorded in terms of changes in impedance and phase angle shift. All the impedance measurements in this study have been carried out at the open circuit potential. The spectra thus obtained were modeled using equivalent circuit approach. The kinetic parameters (corresponding to processes contributing towards

oxidation) derived from the modeling were used to compare the oxidation behavior. The uniqueness of this study lies in the fact that all the impedance measurements done were in high purity demineralized water (conductivity $< 0.1 \mu\text{S cm}^{-1}$) which has been possible by the CDE arrangement allowing the measurements to be taken at a very small distance from the sample surface ($\sim 10 \mu\text{m}$) thereby minimizing the solution resistance and hence the IR drop.

Results and Discussion

In the present paper, few applications of the CDE technique in nuclear reactor simulated environment are demonstrated. The results are presented and discussed with few illustrative examples from oxidation of stainless steel, carbon steel and Zr alloys.

Stainless Steel

The IGSCC of SS304L material [8] in core shroud

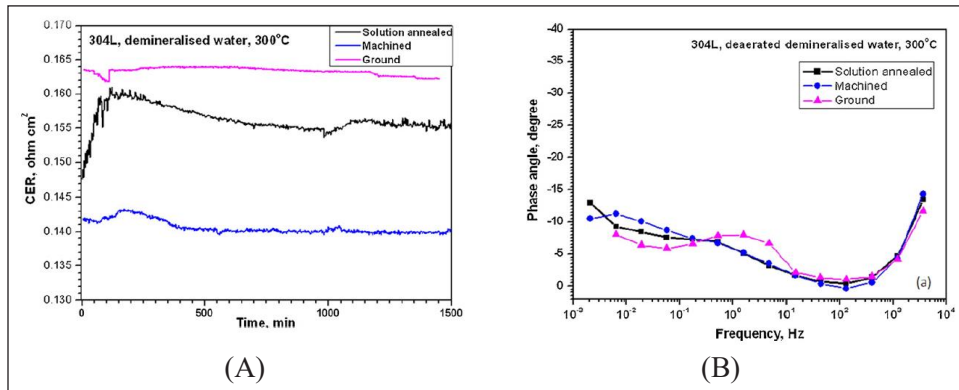


Figure 3. In-situ (A) CER and (B) EIS for SS304L in Annealed, machined and ground state exposed to 300 °C, 10 MPa deaerated DM water [12].

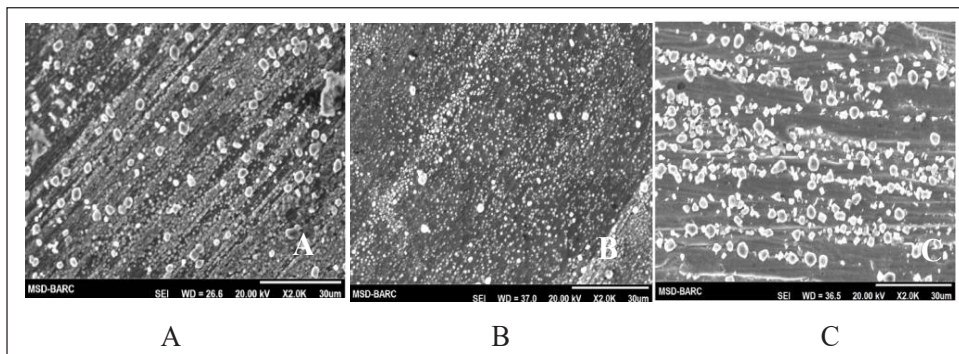


Figure 4. Oxide morphology on (A) annealed, (B) machined and (C) ground SS304L after exposure to 300 °C, 10 MPa deaerated water for 360 h [12].

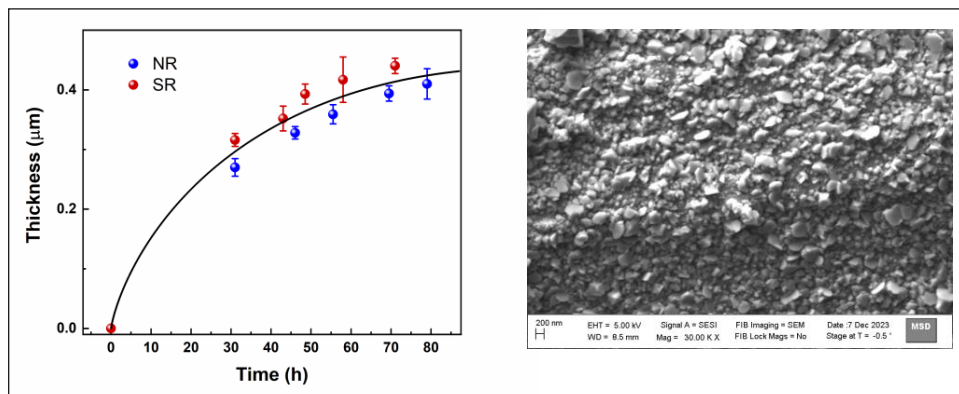


Figure 5. (A) Saturation of magnetite layer thickness on carbon steel during hot conditioning, (B) duplex morphology of completely covered magnetite layer [13].

applications of BWR is a concern and the surface oxidation characteristics play an important role [9] in this regard. This in turn is dictated by the nature of surface exposed [11] to the environment. In this study, SS304L subjected to different surface finishing operations (machined and ground) was exposed to HTHP water and oxidation was followed in-situ using CDE-EIS and CER. The results are shown in Fig.3. The differences in the DC electric resistance of the surface oxide films (Fig. 3A) and response from the electronic/ionic transport processes (Fig. 3B) do show interesting differences with the ground specimen showing an additional time constant at intermediate frequencies. The morphology of oxides (Fig. 4) on all three surfaces showed a duplex structure. It consisted of a compact inner layer in all cases while the outer layer showed distinct differences in size and distribution.

Carbon Steel- Hot conditioning of PHT system of PHWRs

Hot conditioning of primary heat transport (PHT) systems of Pressurised Heavy-Water Reactors (PHWRs) has been an important feature as a first step towards commissioning of a nuclear power plant. In this process, the PHT system is pre-conditioned in a light/heavy water environment

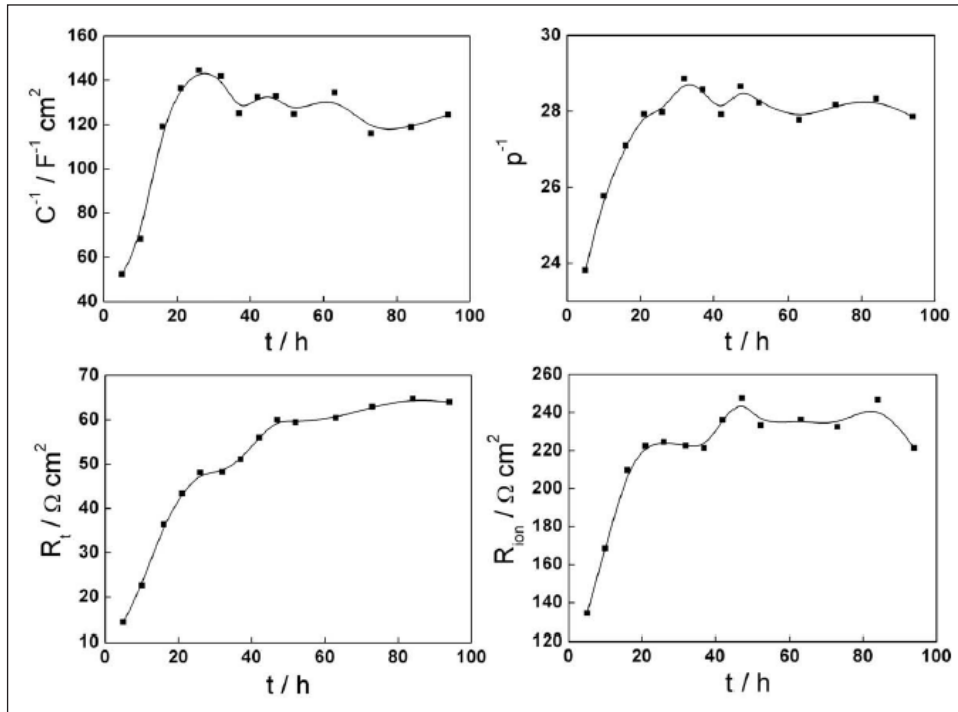


Figure 6. Parameters determined by fitting of the equations of the mixed conduction model to the in-situ EIS data as a function of exposure duration [14].

[13-15] under controlled conditions of temperature, pressure and water chemistry. The main objective of hot conditioning is to form an adherent, protective, impervious magnetite (Fe_3O_4 , inverse spinel) oxide layer on carbon steel surfaces and reduce the crud release rate thereby minimizing activity transport during subsequent operation. The oxide layer formed during hot conditioning are characterized by ex-situ methods like gravimetry after regular intervals of exposure in an autoclave connected in series to the PHT system. A saturation magnetite thickness is assessed by the saturation in thickness of the layer (Figure 5A) and a complete coverage (Figure 5B) of the carbon steel by magnetite. In addition to the assessment of oxide thickness, EIS can be a useful tool to arrive at saturation of derived kinetic parameters. In this study, the electric and electrochemical properties of the oxide layer was followed in-situ during oxidation in an autoclave attached to a recirculation loop. Kinetic parameters such as reciprocal of semiconductor layer capacitance, ionic transport resistance, etc. were derived from electrochemical impedance spectroscopy data and are shown in Figure 6. It can be seen clearly that most kinetic parameters implied saturation at about 40 hours of exposure and complements well with the thickness saturation at a similar duration.

Zirconium alloys

Zr based alloys used in the nuclear reactors undergo waterside oxidation and hydrogen pick-up. Oxidation type

and kinetics in high temperature high pressure water / steam and consequent hydrogen pick up is dictated by several material and environmental parameters [1-3, 10]. Some of the important parameters to be considered are chemical composition, microstructure in terms of phase composition and phase morphology, cold working, etc. [1-3, 10]. In order to assess the role such parameters play in the oxidation behaviour, accelerated autoclave oxidation is performed followed by gravimetry (weight gain) technique. However, due to the inherent gross statistical nature of weight gain technique, subtle or minute differences in the oxidation behaviour become difficult to capture at times. However, EIS is a sensitive technique and gives insights

into the mechanistic aspects of oxidation. Thus, it can be a complementary technique to weight gain. With the advent of CDE, it has been possible to perform such electrochemical measurements on Zr alloys in reactor simulated DM water environment. Some such parametric effects are illustrated in this section.

Role of fabrication route

A comparative assessment of oxidation behavior was carried out between Zr-2.5Nb pressure tube material fabricated through two different route (conventional cold worked stress relieved (CWSR) [16] and heat treated (HT)) as well as Zircaloy-4 clad. The HT tube with aged microstructure having globular β_{Zr} did show a better oxidation resistance than the CWSR tubes in the EIS spectra as shown in figure 7; although the same behavior could not be captured through gravimetry. On the other hand, the expected lower oxidation rate of Zircaloy-4 over Zr-Nb alloys in the initial stages is also clear from the EIS results. This is based on the impedance (Z) values at the low frequency range, higher impedance implying better oxidation resistance and a lower oxidation rate.

Effect of cold work

The pressure tubes of pressurized heavy water reactors (PHWRs) are fabricated from Zr-2.5%Nb alloy and are in a state of 20% cold work (through cold pilgering) [16]. They

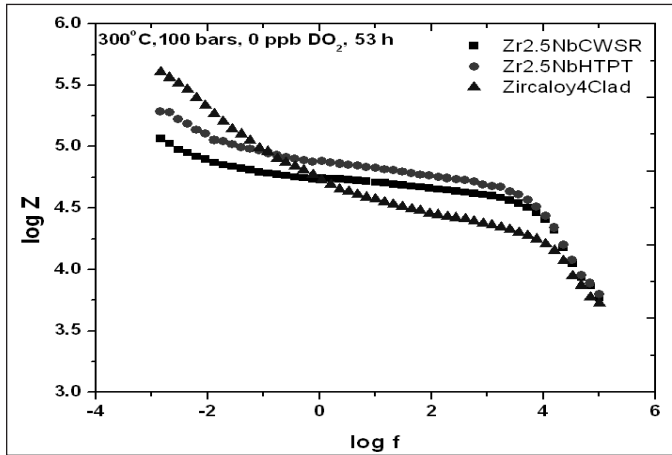


Figure 7. Impedance spectra for Zr-2.5Nb pressure tube (fabricated through CWSR and HT routes) and Zircaloy-4 cladding material exposed to 300°C, 10 MPa deaerated DM water for 53 h.

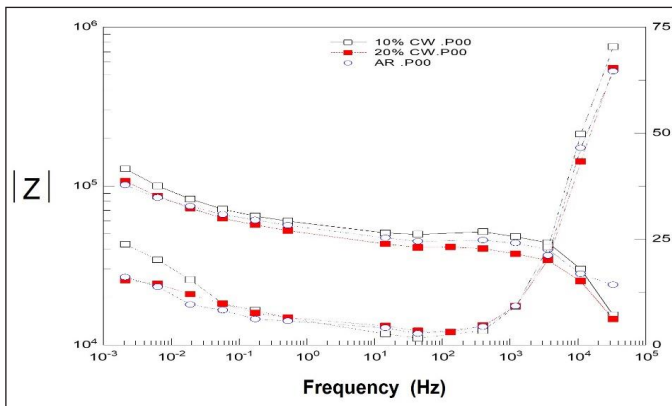


Figure 8. Effect of cold working on Zr-2.5Nb pressure tube material - CDE-EIS in 300°C, 10 MPa deaerated water for 100 h.

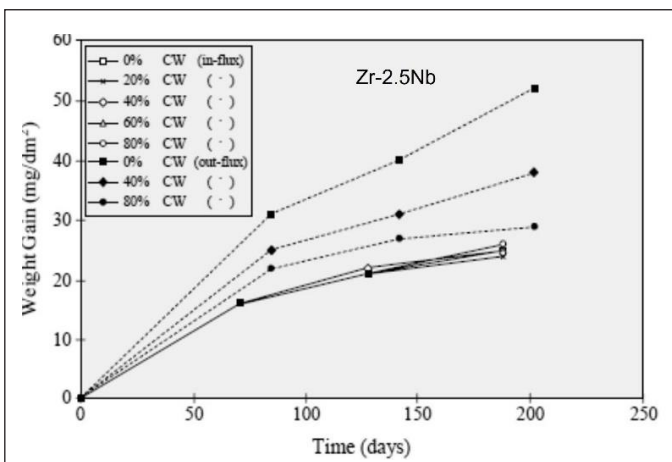


Figure 9. Effect of cold working on Zr-2.5Nb pressure tube material gravimetric measurement data after exposure to water at 300°C, both in-flux and out of flux [17].

undergo further deformation post fabrication, such as during rolled joining with end fittings, etc [3]. The effect of cold working on the oxidation behavior was studied using both in-situ CDE-EIS measurements (Fig.8) and accelerated steam tests in static autoclaves (Fig.9). The beneficial effect of cold working on the oxidation behavior of Zr-2.5Nb is clearly seen (Fig.8) through enhanced low frequency Warburg impedance, a measure of rate limiting ionic diffusion through the oxide and correlates well with the gravimetric observations in static autoclaves (Fig.9) [17].

Conclusion

The present paper discussed the unique capability of CDE technique as an effective tool for electrochemical measurements in electrolytes of very low conductivity such as DM water. This has been demonstrated by the in-situ CDE-EIS and CER studies on carbon steel (hot conditioning), stainless steel and Zr alloys in reactor simulated environments. The paper brought out the efficacy of CDE-EIS technique to capture minute differences in oxidation behaviour which are otherwise difficult through conventional weight gain technique.

References

1. V. Kain and M. Kiran Kumar, *Peacefulatom 2009*, Proceedings of the international conference on peaceful uses of atomic energy 2009, Eds A K Suri, C S Viswanadham and R N Singh, published by Department of Atomic Energy 2011, 215.
2. M. Bojinov, L. Hansson-Lyyra, P. Kinnunen, K. Makela, T. Saario and P. Sirkia; *J. ASTM Int.* 2 (2005), 183-198.
3. IAEA TECDOC-996, *Waterside corrosion of zirconium alloys in nuclear power plants*, IAEA, Vienna, Austria, 1998.
4. T. Saario, T. Laitinen, J. Piippo, *Materials Science Forum*, 1998, 289-292,193.
5. B. Beverskog, M. Bojinov, A. Englund, P. Kinnunen, T. Laitinen, K. Mäkelä, T. Saario and P. Sirkiä, *Corrosion Science*, 2002, 44,1901.
6. L. Charny, T. Saario, V.A. Marichev, *Surface Science* 312 (1994) 422-428.
7. R. K. Sinha, A. Kakodkar, *Nuclear Engineering and Design*; Volume 236, Issues 7-8, April 2006, Pages 683-700.
8. P. L. Andresen, M. M. Morra, *Journal of Nuclear Materials*, 2008, 383,97.
9. E.P. Simonen, L.E. Thomas, and S.M. Bruemmer, In: *Proc. 11th Int. Conf. Environmental Degradation of Materials in Nuclear Power Systems-Water Reactors*, ed. Nelson, J. L., G. S.Was, American Nuclear Society, 2004, 1062.
10. M. Kiran Kumar, S. Aggarwal, V. Kain, T. Saario and M. Bojinov, *Nuclear Engineering and Design*, 2010, 240, 985.
11. S. Ghosh, V. Kain, *Journal of Nuclear Materials*, 2010, 403, 62.
12. Swati Ghosh, M. Kiran Kumar, Vivekanand Kain; *Applied Surface Science* 264 (2013) 312- 319.

13. Vivekanand Dubey, M Kiran Kumar and Supratik Roychowdhury; Detailed analysis results of hot-conditioning coupons from RAPP-7 BARC/MP&CED/Corr/P 127886 February 16, 2024, MP&CED, BARC.
14. Martin Bojinov, Krishna Gaonkar, Swati Ghosh, Vivekanand Kain, Kiran Kumar, Timo Saario; Corrosion Science 51 (2009) 1146-1156.
15. M. Kiran Kumar, Krishna Gaonkar, Swati Ghosh, Vivekanand Kain, Martin Bojinov, Timo Saario; Journal of Nuclear Materials 401 (2010) 46-54.
16. M. Kiran Kumar, C. Vanitha, I. Samajdar, G.K. Dey, R. Tewari, D. Srivastava and S. Banerjee, Journal of Nuclear Materials, 2004, 335, 48.
17. Urbanic V. F.: Materials Research in AECL, Report AECL-4842, 1974.

	<p>Dr Kiran Kumar is a researcher in the field of corrosion degradation of materials used in nuclear power plants and allied applications; especially, in high temperature and high-pressure oxidation behaviour of zirconium alloys. He has a PhD degree in Metallurgical Engineering and Materials Science from Indian Institute of Technology, Bombay. He joined Bhabha Atomic Research Centre in the year 2007 and has since been contributing to the understanding and mitigation of corrosion issues facing nuclear materials. Dr Kiran Kumar was a postdoctoral fellow at the University of Michigan where he has worked on several projects dealing with development of accident tolerant fuel (ATF) clad materials. He has been awarded 'Distinction in Corrosion Science and Technology' from NACE International, Gateway India section for his contribution. Dr Kiran Kumar has a number of publications in international journals and conference proceedings, has delivered Invited talks at international symposia and has a couple of book chapters to his credit.</p>
	<p>Dr. Supratik Roychowdhury is presently the Head, Corrosion Engineering Section, Materials Processing & Corrosion Engineering Division, BARC. He completed B.E. in 1997 (Metallurgical Engg.) from NIT, Rourkela, M.Tech. in 2005 (Materials Science) and PhD (Corrosion Science & Engineering) in 2011 from IIT Bombay. He was awarded the prestigious Marie Curie research grant (COFUND scheme) for pursuing post-doctoral research in Paul Scherrer institute (PSI), Switzerland (2013-2015).</p> <p>His primary research interest is corrosion/SCC of nuclear structural materials in simulated nuclear reactor water environment, hydrogen embrittlement, flow-accelerated corrosion, oxidation of zirconium alloys in simulated operating conditions and accident conditions, providing metallurgical support (failure analysis, material selection) and delivering lectures on corrosion related topics. In recognition to his work, he has received the "Fellow Award" from AMPP, USA in 2023, "Excellence in corrosion science and technology" from NACE International India Section (presently AMPP) in 2012, DAE individual and group awards and has a number of publications in peer reviewed journals.</p>

Electrochemical Impedance Spectroscopy to elucidate the mechanism of Stellite #3 corrosion in permanganate based decontaminating formulations

Veena Subramanian, Sinu Chandran, S.V. Narasimhan, and T.V. Krishnamohan

Water and Steam Chemistry Division, Chemistry Group, BARC Facilities, Kalpakkam 603102, Tamilnadu, India
Email: veena@igcar.gov.in

Abstract

Some of the Indian Pressurized Heavy Water Reactors were facing increased radiation fields, hotspots, due to the presence of ^{60}Co in the moderator circuit. Source of ^{60}Co was attributed to wear of the stellite#3 balls which are part of the 'ball and screw' in the adjustor rod drive mechanism. Extensive laboratory studies proved that stellite particulates causing these radioactive hotspots can be effectively dissolved using a three-step redox process with permanganic acid (HMnO_4) as the oxidizing agent. The susceptibility of stellite to dissolve was strongly dependent on its microstructure apart from the concentration of permanganate, temperature and pH of the process. Electrochemical Impedance spectroscopy (EIS) was used to elucidate the mechanism of corrosion of stellite#3 during the redox treatment. EIS was done at 90°C in HMnO_4 , nitric acid permanganate (NP), and Alkaline permanganate (AP). In HMnO_4 , uniform corrosion of the surface was observed. In NP, only the chromium depleted inter-phase boundary was attacked leaving chromium-rich carbide phases intact. The NO_3^- in NP promoted repassivation of the surface. In AP only the carbide phases lean in cobalt were attacked. AP was found to be the least and HMnO_4 the most efficient in dissolving cobalt from stellite and thus the latter was effective in reducing radioactivity due to stellite. Based on these studies decontamination was done for 10 adjustor rod drive assemblies which had ^{60}Co activity of 3 R h^{-1} to 20 R h^{-1} . A maximum decontamination factor (DF) of 11.7 with an average DF of 6.8 was achieved.

Introduction

Stellites are Co-Cr-W alloys, where in cobalt which is present to the extent of 50 – 60 wt%, forms the dominant matrix phase. Stellites are hard-face alloys having hardness numbers varying from 40 to 63 on HRC scale. They are designed to resist high temperature corrosion and wear. Therefore stellite coated surfaces or the alloys themselves are frequently used as the material of construction for the internals of valves, pumps etc., in water cooled nuclear reactor systems.^[1]

The design of PHWR in India is based on that of CANDU reactor. The unique design of PHWR allows a separate moderator circuit. Figure 1 shows the moderator system with its main circulating system.^[2] D_2O after its circulation through the core for the purpose of moderating the neutrons gets heated up. It is cooled by using a set of heat exchangers made up of cupronickel 70:30 tubes. Apart from this main circulation system also supplies heavy water to

- Absorber/adjustor, regulating and shim rods
- IX purification for removal of boron and other ionic impurities
- Automatic liquid poison addition system (ALPAS tank)

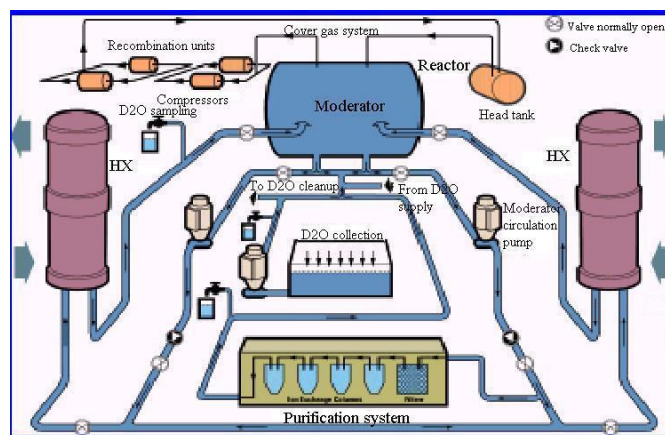


Figure 1: Moderator system of PHWR

Reactivity adjustments in PHWRs are done using three types of control rods viz. regulating rods, shim rods and absorber/adjustor rods. They are driven in groups of two so that the neutron flux shape is maintained as smooth as possible. They are driven into and out of the core by the driving mechanism. This mechanism is shown schematically in Figure 2a. It consists of a ball screw (Figure 2b) which rotates in its position, while the nut traverses vertically thus enabling the movement of drive rod.^[3] A driving assembly is placed out of the core in a low pressure, low temperature system and it consists of

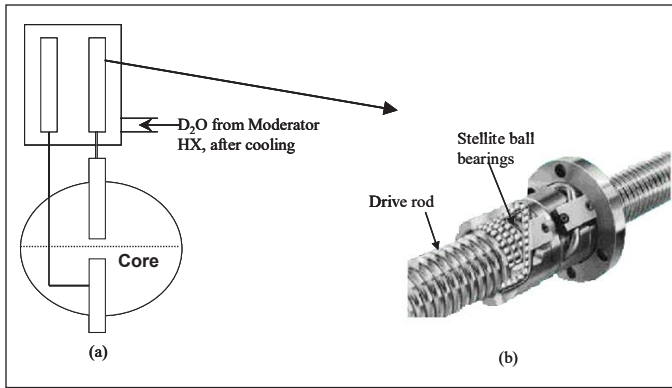


Figure 2: (a) Schematic of adjustor rod drive assembly and (b) Ball screw mechanism

two rods aiding the movements of both upper and lower absorbing elements. These assemblies become part of the moderator circuit as they are cooled by circulating a portion of the D₂O taken from downstream of the moderator heat exchangers.

The ball screw mechanism is made up of stellite #3 balls, whose erosion releases particles containing cobalt. These particles were carried along with the flowing moderator to various parts of the circuit. These particles got activated by the neutron flux with the dominant radionuclide formed being ⁶⁰Co (t_{1/2} 5.27 years) isotope which emits two high energy γ-rays (1.33 MeV and 1.17 MeV).

Except for heat exchangers, all other material of construction for moderator system is austenitic stainless steel (SS 304). At an operating temperature of 60 °C – 70 °C and with neutral water chemistry, the conditions are not conducive for oxidation and hence the oxide films formed on SS 304 under these conditions are extremely thin. The moderator carrying the fine powder of stellite allows deposition in low flow areas and crevices. Hence, two types of surface contamination can occur; particles giving raise to hotspots and soluble species getting incorporated on SS oxide films leading to uniform radiation buildup. In moderator system, radioactive hotspots were also found on straight portions of the heat exchanger (Cupronickel 70:30) tubes.

The oxide film formed on stellite even at high temperatures (≥ 250°C, i.e reactor operating temperatures) is extremely thin and is of the order of nanometers.^[4] Hence, at the lower temperatures prevailing in the moderator system no oxide film is expected on stellite particles. Thus, it is presumed that the stellite particles are present in the system mostly as metal particles embedded in the thin passive oxides of stainless steel systems. For this reason, in this study, emphasis was given on dissolution

of powdered stellite which is metallic in nature. Generally, decontaminating formulations are meant for dissolving the thermodynamically more stable oxide, keeping the base metal dissolution/corrosion low. But the aim of this study is to dissolve cobalt from the stellite particles, where the corrosion attack on stellite alloy is more important.

Pre-exposure Microstructure of stellite#3

Stellite #3 has bulk alloy composition as given in Table 1, all expressed in wt%. Stellite #3 has about 29 wt% carbides. Chromium has dual purpose of forming eutectic carbides of type M₇C₃ and M₂₃C₆ that gives the alloy its characteristic hardness and it also imparts corrosion resistance properties.^[5] The alloy typically consists of a cobalt rich solid solution (Phase A), in which chromium rich (phase B) and tungsten rich carbide precipitates (phase C) are present. Presence of tungsten helps in strengthening the solid solution by forming intermetallics with cobalt. However most of the chromium is consumed in the formation of these eutectic carbides leaving the adjacent regions Cr-depleted. This kind of microstructure is prone for aqueous corrosion due to the formation of micro-galvanic cells, with the chromium depleted zones acting as anodes and the Cr-rich surfaces acting as cathodes.^[6-8] Owing to its microstructure, stellite as an alloy could be attacked by decontaminating reagents, resulting in dissolution of fine particles of stellite. Thus the rate of dissolution of stellite in powdered form depends upon the alloy’s corrosion behaviour in the chosen chemical reagents. This factor is utilized in our study and it was shown that the radioactive hotspots due to stellite particles can be effectively eliminated by dissolving them by using suitable formulations.

Table 1: Bulk composition of Stellite #3

	Co	Cr	W	Fe	Ni	C	Si
Stellite#3	49	31	13	1.4	1.8	2.4	1

Pre-exposure microstructure of stellite #3 surface is presented in Figure 2. Table 2 gives the composition of each phase estimated by EDX.

Table 2: EDX data on composition of each phase in Stellite #3

Phase	Co (wt %)	Cr (wt%)	W (wt%)	Fe (wt%)
Matrix (A)	68.1	18.58	9.58	3.76
Carbide phase (B)	19.7	68	11.3	1.1
W-phase (C)	28.3	14.9	53	1.8

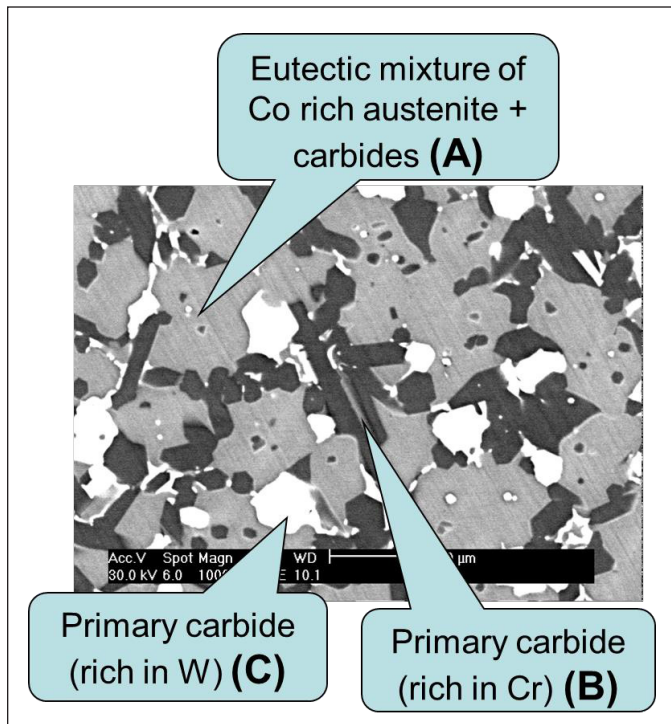


Figure 3: Pre-exposure microstructure of Stellite #3 showing different phases

The Process:

Since stellite contains significant amount of chromium, the inherent oxide present over it is Cr₂O₃, which is very similar to that on SS 304L.^[9-11] as a function of dissolved oxygen concentration and length of exposure time. The result surface films were analysed by X-ray photoelectron spectroscopy (XPS). Hence, well known decontaminating reagents based on potassium permanganate such as nitric acid permanganate (NP), alkaline permanganate (AP) and permanganic acid (HMnO₄) were chosen for the effective dissolution.

A three step three cycle oxidation-reduction process at 90 °C was proposed (Figure 4) based on extensive laboratory studies. It was shown that it was possible to dissolve stellite #3 in the form of metallic powder almost completely.^[12,13] pumps, etc. Due to either mechanical erosion or erosion coupled with corrosion under flow conditions (known as tribocorrosion). The acidified permanganate reagents were found to be more efficient in dissolving chromium and cobalt from stellite alloy as compared to alkaline permanganate (AP). From stellite#3 exposed to one oxidation step i.e. 24 h, chromium was found dissolve to the extent of 36%, 3% and ≤1% when HMnO₄, NP and AP was used as the oxidizing agents respectively. Citric acid and a mixture of EDTA, Ascorbic acid, Citric acid (called EAC)^[14] were used in the two

subsequent reduction steps for all the experiments and the duration of this step is 4h. During the reduction step, the cobalt dissolves and its concentration in the solution was found to be 50%, 5% and ≤3% subsequent to the oxidising pre-treatment with HMnO₄, NP and AP respectively. Hence, among the acidified permanganate reagents, HMnO₄ (used in the CORD process)^[15,16] had better dissolution capabilities as compared to NP of similar acidity. It was of interest to investigate this aspect as all the three types of permanganate reagents has been used for stainless steel decontamination worldwide and are known to have equal oxidizing powers.^[17,18] Understanding the corrosion behaviour of the alloy in these decontamination formulations would give an insight into the differences in mechanism of oxidation of Chromium hence their varying dissolution efficiency. For this purpose, it was a prerequisite to observe reactions occurring at metal/ film/ solution interface in-situ, as a function of time. This was best achieved by Electrochemical Impedance Spectroscopy (EIS). To augment EIS data surface analytical techniques like SEM/EDX was used.

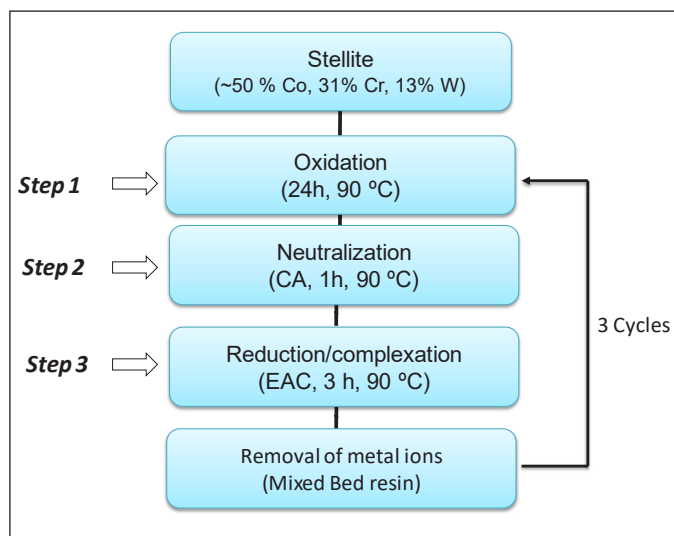


Figure 4: The proposed process for dissolution of radioactive hotspots due to Stellite particles

Surface after exposure:

Secondary electron images of stellite #3 after exposure to HMnO₄/CA/EAC, NP/CA/EAC and AP/CA/EAC are given in figure 5(a), figure 5(b) and figure 5(c) respectively. For HMnO₄/CA/EAC severe corrosion was observed especially in the inter-phase boundaries. The cobalt rich phase (A) had shallow pits, whereas no pits were seen on the rod like Cr-rich phase (B). After exposure to NP/CA/EAC stellite surface showed deep pits on cobalt phase and the inter-phase boundaries were corroded to a lesser

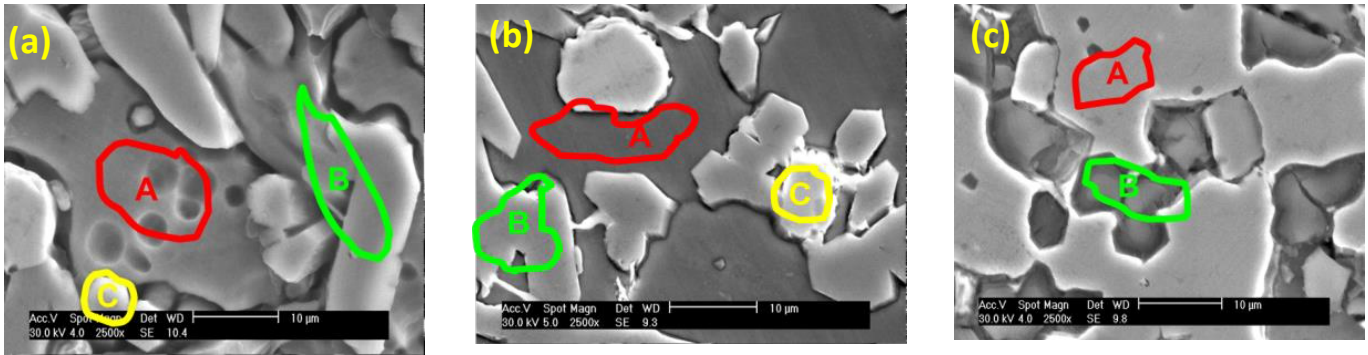


Figure 5: Stellite #3 after exposure to (a) HMnO₄/CA/EAC and (b) NP/CA/EAC (c) AP/CA/EAC

extent and chromium carbide phases appeared intact. In AP/CA/EAC the blocky carbide precipitates on stellite #3 were specifically attacked. From the SEM micrograph (figure 5(c)), it was clear that in AP, the attack is mainly on chromium rich carbide phases, which is quite in contrast to the corrosion behaviour in NP and HMnO₄ formulations where the attack was found to occur mainly at chromium-depleted inter-phase boundaries. In the image it was evident that in AP, the cobalt matrix was left unaffected in stellite #3, except for some pitting type of attack; the rest of the matrix phase was intact. This can be attributed to the increased corrosion resistance of cobalt metal at higher pH.^[19]

EIS measurements at 90°C with increase in exposure time:

A) In HMnO₄/CA/EAC

Impedance spectra (Nyquist plots) as a function of time for stellite #3 in HMnO₄ is presented in Figure 6.

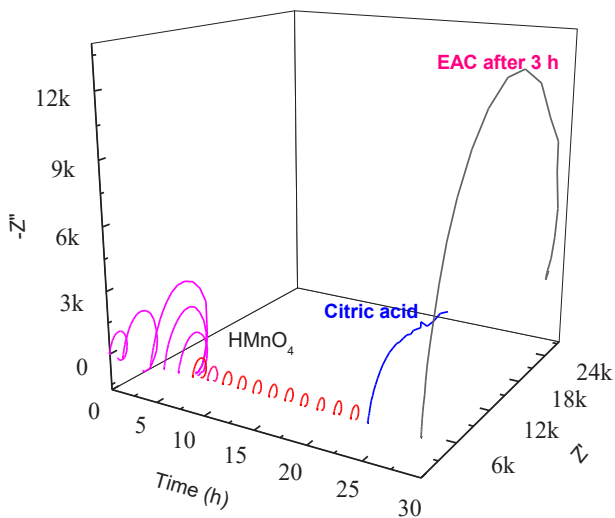


Figure 6: Impedance spectra with time for stellite #3 in one redox step using HMnO₄, CA and EAC

An inductive loop at low frequencies indicated a faradaic process occurring through an ‘adsorbed’ intermediate. The absolute impedance values were observed to gradually increase up to about 5 h, and then was found to decrease abruptly to remain almost constant till 24 h. Subsequent to the addition of citric acid, the response was found to change to that of a mixed control i.e. a charge transfer and diffusion process. Finally, with EAC addition (reduction step), the corrosion rate was observed to be rapidly increasing with

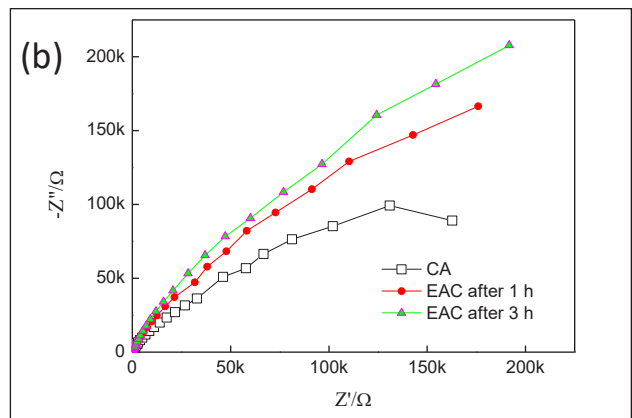
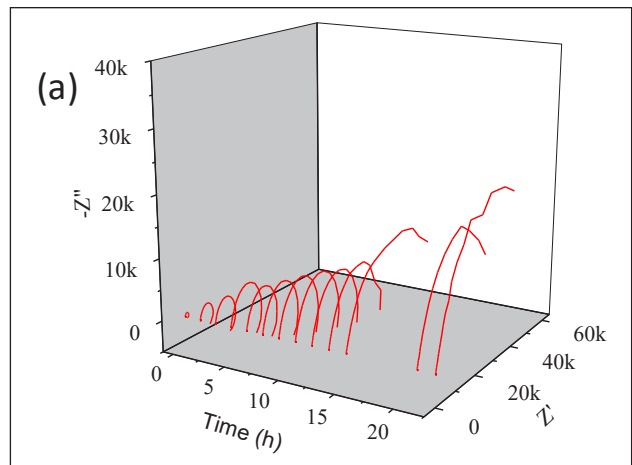


Figure 7: Impedance spectra with time for Stellite #3 in a) NP and b) CA and EAC at 90°C

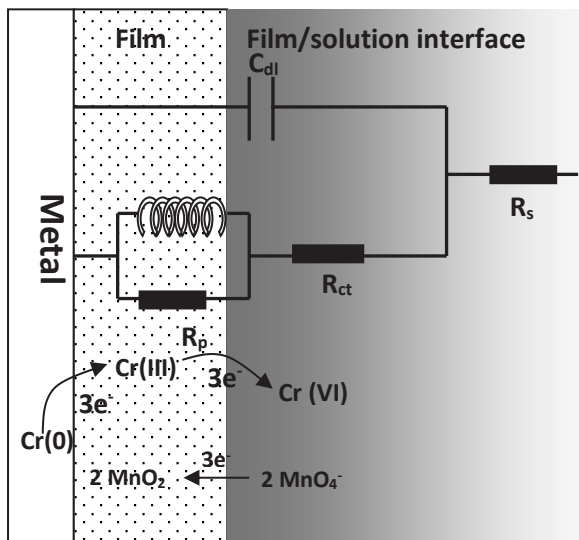


Figure 8: Physical model depicting reactions at the interfaces and corresponding equivalent circuit

time, as evident from the appearance of pseudo inductance at low frequencies.

(B) In NP/CA/EAC

In NP, the nyquist plot was quite similar to that in HMnO₄, as oxidation takes place through similar mechanism. However, the inductive loop completely disappeared after about 10 h of exposure (Figure 7(a)). The disappearance of inductive loop in NP suggests that at least one of the faradaic processes is hindered during the course of the reaction. In oxidation step, the absolute impedance values monotonously increased with time. In addition, very high values of 350-400 KΩ were also observed in the reduction step (Figure 7(b)). All the above factors indicated a highly inhibited dissolution from a passivated surface.

Oxidation of Stellite #3 in HMnO₄ and NP - Interpretation of EIS:

The oxidation of stellite#3 in acidified permanganates can be represented by the physical model as given in figure 8. Various interfacial reactions involved can be described as follows: The active reactant MnO₄⁻ gets adsorbed onto the surface film at the film / solution interface, and oxidizes Cr(III) to Cr(VI), its more soluble form. In this process MnO₄⁻ gets reduced to MnO₂. So, it involved a 3e⁻ transfer from the reactant. Subsequently, at the metal/film interface a Cr₂O₃ film grows in-situ as the underlying metal oxidizes. The kinetics of oxidation of Cr(0) to Cr(III) is relatively fast as compared to Cr(III) to Cr(VI) and hence the latter reaction occurring at the film / solution interface decides the overall rate of the reaction.

The uninhibited oxidative-dissolution process in these systems gave rise to an inductive loop at low frequencies, which was attributed to a multiple e⁻ transfer occurring through the soluble intermediate comprising of Cr(III) species. During the oxidation step, most of the cobalt tend to remain on the surface and hence it does not contribute significantly to the rate of the reactions.^[13] permanganic acid (HMnO₄) As the two-step oxidation processes of chromium are inter-dependent, the two resistances R_{ct} and R_p that represent them were kept in series in the electrical equivalent circuit (figure 8).

The observed redox potential vs. standard hydrogen electrode for HMnO₄ and NP are 1.231V and 1.204V respectively. These high potentials correspond to transpassive region in Pourbaix diagram of chromium where oxide of chromium is unstable and it dissolves by the formation of highly soluble Cr(VI).^[20] Thus both the reagents have equal oxidizing power. Figure 9(a) gives the 'change' in the open circuit potentials (OCP) for stellite

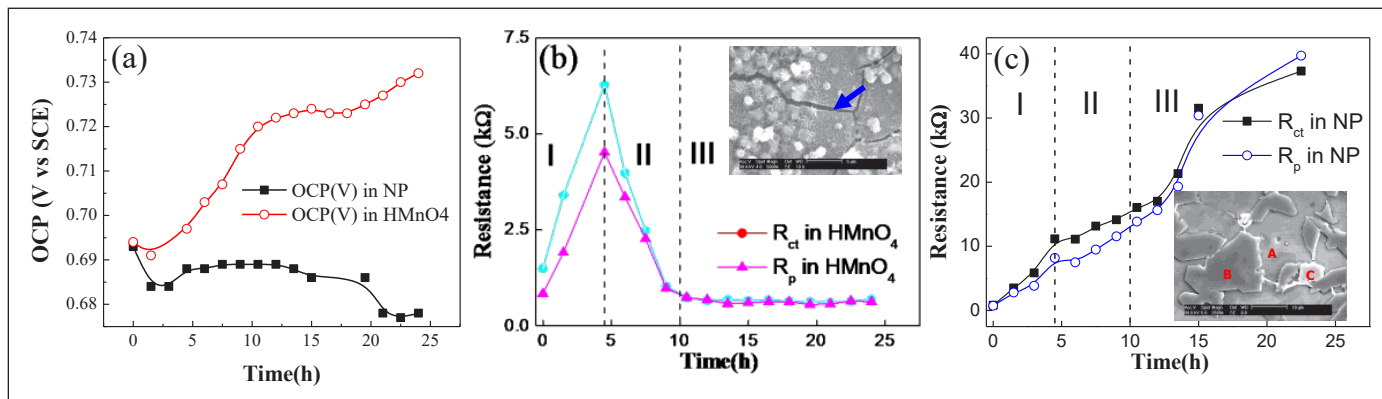


Figure 9: Variation of (a) open circuit potential and charge transfer and polarization resistance as a function of time (b) in HMnO₄ and (c) in NP for stellite #3

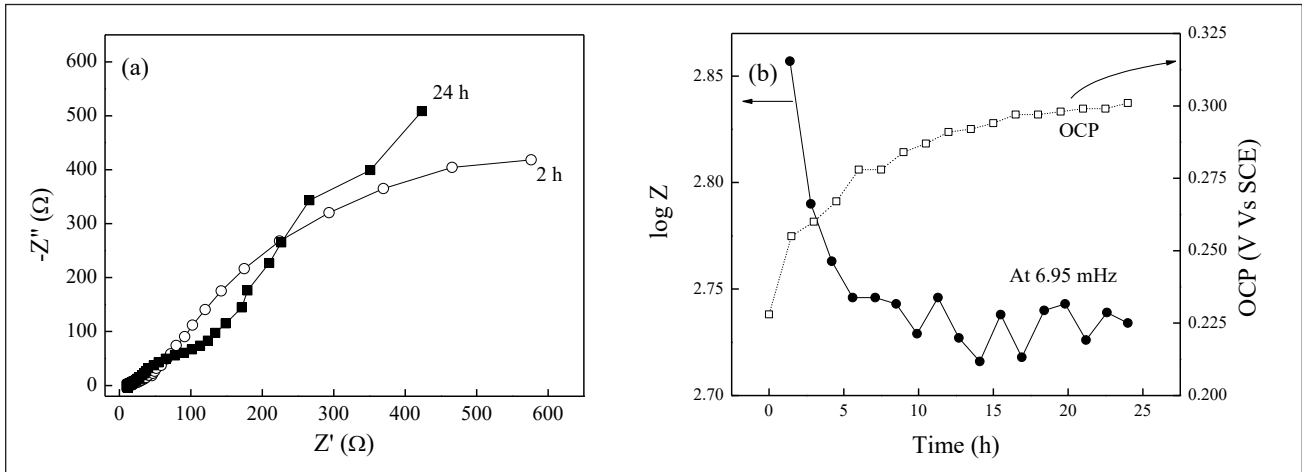


Figure 10: Stellite #3 in AP: (a) Impedance spectra (Nyquist plot) and (b) corresponding log Z values at 6.95 mHz

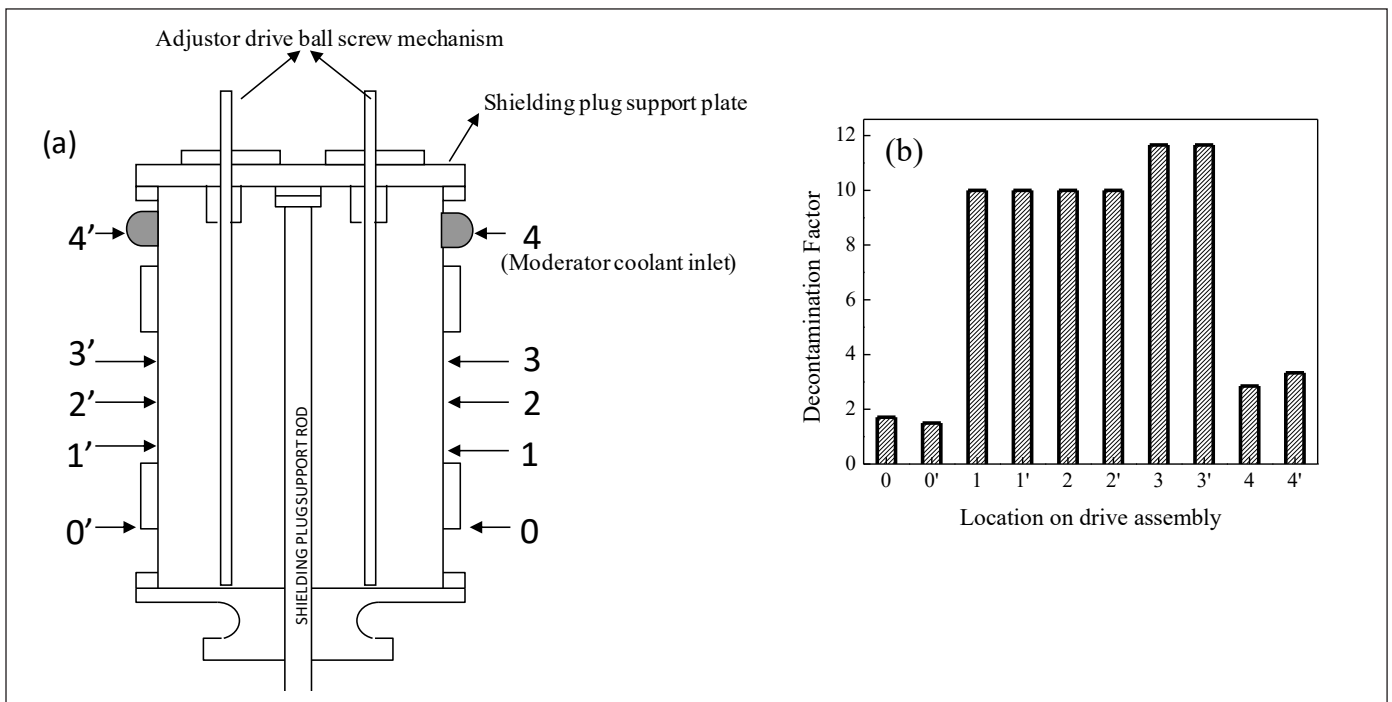


Figure 11: (a) Locations where dose measurements were done before and after decontamination of drive assembly and (b) DFs achieved at these locations

#3 in both the oxidants as measured Vs SCE during the oxidation.

The fitted R_{ct} and R_p values for stellite #3 in HMnO_4 and NP are given in figure 9(b) and figure 9(c) respectively. For stellite #/ HMnO_4 system, in figure 9(b) three regions I, II and III can be identified. Region I, where the film was intact, region B where the film started breaking leading to loss of passivity and region III, which corresponded to the constant uninhibited oxidation of Cr(0) to Cr(VI). The cracks in the passive film can be seen after shorter

duration exposure of stellite #3 to HMnO_4 (inset of figure 9(b)). This passivity breakdown may probably due to non-establishment of steady state between growth of a Cr(III)-film and its dissolution in the presence of highly oxidizing anions such as MnO_4^- . Since, the corrosion is associated with the change in valency of chromium, it has strong dependence on any change in potential of the system. Hence in the case of HMnO_4 , a small increase of ~ 30 mV in potential 'increased' the rate of transpassive dissolution of chromium.

In NP / stellite #3 system, OCP remained almost constant with a slight decreasing trend during initial times. In NP solution, a passivator such as NO_3^- ions along with the aggressive anions MnO_4^- are present. Hence, the oxidation is slow and inhibited and with time ends up in repassivation of the alloy surface. This was evident as both R_p and R_{ct} increased monotonously with time (Figure 9(c)). The values of resistances were also higher as compared to that in HMnO_4 , indicating slower electron / charge transfer at the stellite#3 /NP interface. The surface after short duration of exposure also reveals different phases of stellite #3 with chromium rich phase (B) almost intact. Reduced kinetics in the presence of NO_3^- resulted in the formation of a "stable" chromium oxide film that could not be dissolved at the same rate as that of its formation. Thus ultimately it resulted in repassivation of the surface.

(C) In AP/CA/EAC

The redox potential of alkaline permanganate solution was found to be 0.345 V vs. SCE (or 0.542 V vs. SHE) at 90°C. Here the log Z values at low frequencies (6.95 mHz) were used to understand the material's corrosion susceptibility. Initially as some specific Cr-carbides dissolve in AP, the EIS shows a charge transfer controlled reaction at ~2h, as shown in Figure 10(a). However, once the susceptible phases gets dissolved, the other remaining non-corrodible surface resists corrosion. This is evident in the EIS spectra at 10 h, which shows a mixed control i.e a combination of charge transfer and diffusion (Figure 10(a)). Figure 10(b) gives variation of both log Z and OCP of the system with time. Initially (< 5 h), the log Z values decreased or corrosion rate increased and this increase was coinciding with the increasing trend in OCP. However after 5 h, the log Z remained almost constant, as the reaction was controlled by a slow diffusion process. Since from the solution analysis and from the surface analysis it was evident that only non-cobalt phases dissolve in AP, its attack on stellite was not of much consequence.

Component decontamination of Adjustor rod drive assembly

The redox process (as in figure 4) with 2.5 mM HMnO_4 was applied for decontaminating adjustor rod drive assemblies removed from a reactor (Figure 11(a)). ^{60}Co activity on this component ranged from 3 R.h^{-1} to 20 R.h^{-1} . Decontamination was required before reinstallation of these drive assemblies. The detail of the experimental loop setup is described elsewhere.^[21] The results are given in figure 11(b) as decontamination factors.

Summary and Conclusions

Owing to its microstructure, stellite #3 as a metal was found to corrode in presence of strong oxidizing agents. In powdered form, stellite#3 could be dissolved by a redox process with HMnO_4 as the oxidizing agent. Monitoring the stellite/formulations interface in-situ by EIS helped in understanding the difference in mechanism of its corrosion in HMnO_4 , NP and AP.

With HMnO_4 , the dissolution rate is quite high as the initial Co-Cr-oxide film cracks and the attack was more or less uniform. In Sellite#3/NP, initially the corrosion occurs at Cr-depleted interface. However, once these sites are oxidized, the rest of the surface becomes Cr-rich and the oxidation of Cr slows down. In addition, the presence of nitrate ions in NP facilitates formation of a stable Cr-rich oxide that ultimately led to repassivation of the surface of the alloy.

In AP, the carbides were attacked and dissolved which are lean in cobalt and hence it is not useful for reducing radioactivity due to stellite.





Thus in the absence of passivating anions like nitrate ions, the HMnO_4 was found to be the more corrosive and hence more efficient in dissolving chromium and hence subsequently cobalt from stellite #3.

Based on these studies, a total of 10 adjustor rod drive assemblies removed from a PHWR were decontaminated and radioactive hotspots due to stellite were removed. In this component decontamination, an average DF of 6.8 with a maximum DF of 11.7 was achieved.

References:

1. T. R. Young, J. T. LaDuca, T. E. Quattrochi, M. Wiatrowski, **1982**.
2. *Heavy Water Reactors : Status and Projected Development*, International Atomic Energy Agency, **2002**.
3. N. P. C. Department of Atomic Energy, *Narora Atomic Power Station Safety Report - Design Description*, **n.d**.
4. N. K. Taylor, I. Armson, *Corrosion Product Release from Stellites and Stainless Steel in High Pressure, High Temperature Lithiated Water*, British Nuclear Energy Society, United Kingdom, **1983**.
5. P. Crook, W. L. Silence, in *Uhlig's Corros. Handb.*, John Wiley And Sons, New York, **2000**, pp. 717-728.
6. B. Schnyder, C. Stössel-Sittig, R. Kötz, S. Hochstrasser-Kurz, S. Virtanen, C. Jaeggi, N. Eichenberger, H. Siegenthaler, *Surf. Sci.* **2004**, 566-568, 1240-1245.
7. S. Hochstrasser-Kurz, *Berichte aus der Mater.* **2006**, DOI 10.3929/ETHZ-A-005164793.
8. M. Zhong, W. Liu, K. Yao, J.-C. Goussain, C. Mayer, A. Becker, *Surf. Coat. Technol.* **2002**, 157, 128-137.
9. N. S. McIntyre, D. Zetaruk, E. V. Murphy, *Surf. Interface Anal.* **1979**, 1, 105-110.

10. C. Maffiotte, M. Navas, M. L. Castaño, A. M. Lancha, *Surf. Interface Anal.* **2000**, 30, 161–166.
11. U. Malayoglu, A. Neville, G. Beamson, *Mater. Sci. Eng. A* **2005**, 393, 91–101.
12. V. Subramanian, P. Chandramohan, M. P. Srinivasan, A. A. Sukumar, V. S. Raju, S. Velmurugan, S. V. Narasimhan, *J. Nucl. Mater.* **2004**, 334, DOI 10.1016/j.jnucmat.2004.05.015.
13. V. Subramanian, S. Chandran, S. Velmurugan, S. Rangarajan, S. V. Narasimhan, *J. Appl. Electrochem.* **2009**, 39, DOI 10.1007/s10800-009-9850-1.
14. S. Velmurugan, S. V. Narasimhan, P. K. Mathur, K. S. Venkateshvaralu, *Nucl. Technol.* **1991**, 96, 248–258.
15. M. G. Segal, W. J. Williams, *J. Chem. Soc., Faraday Trans. 1* **1986**, 82, 3245–3254.
16. H. Wille, H. D. Bertholdt, in *Water Chem. Nucl. React. Syst. 6*, BNES, London, **1992**.
17. M. E. Pick, in *Water Chem. Nucl. React. Syst. 1(3)*, BNES, London, **1983**, pp. 61–66.
18. M. E. Pick, *Int. Jt. Top. Meet. Decontam. Nucl. Facil.* **1982**, 3–5.
19. J. Chivot, L. Mendoza, C. Mansour, T. Pauporté, M. Cassir, *Corros. Sci.* **2008**, 50, 62–69.
20. B. Beverskog, I. Puigdomenech, *Corros. Sci.* **1997**, 39, 43–57.
21. V. Subramanian, P. Chandramohan, S. Chandran, M. P. Srinivasan, S. Rangarajan, S. Velmurugan, S. V. Narasimhan, *Power Plant Chem.* **2011**, 13, 337–345.

	<p>Dr. Veena Subramanian is from 39th batch of BARC training school, Chemistry. She is presently working in Water and Steam Chemistry Division, BARC Facilities, Kalpakkam. Her areas of specialisation are Activity transport, Corrosion and Water Chemistry in Nuclear Reactors, Steam generator corrosion and its mitigation, Modeling radiolysis of water in reactor systems including that of AHWR, IPR and HFRR.</p>
	<p>Dr. Sinu Chandran, SO/E, working in Surface Characterisation and Mass Transport Studies Section, WSCD, BARC Facilities, Kalpakkam. He mainly works on electrochemical corrosion studies on reactor structural materials. He has got 14 journals, 40 conferences and 4 reports in his credit.</p>
	<p>Dr. S.V. Narasimhan is ex-Associate Director, Chemistry Group and also ex-Head Water and Steam Chemistry Division, BARC Facilities, Kalpakkam. He is from 14th batch of BARC training School. His areas of specialisation are Water chemistry of nuclear reactors, Dilute Chemical Decontamination, Thermal Ecology and Activity Transport.</p>
	<p>Dr. T.V. Krishna Mohan is Outstanding Scientist, Facility Director, BARC Facilities, Kalpakkam and Head, Water and Steam Chemistry Division, Chemistry Group, BARC. He completed his B.Tech (Chemical Engg.) in 1987 and MBA in 1989 from Osmania University, Hyderabad, before joining training school. He completed his Ph.D. (Eng. Sciences) in 2016 from HBNI. His field of specialization is Design, Procurement, Installation, Commissioning, and Operation of Simulated Engineering loops to carry out water chemistry, biology and heat transfer experiments. He had carried out studies related to Bioremediation, Flow Accelerated Corrosion, Biological Denitrification, Aerobic Granulation and Wastewater Engineering.</p>

Electrochemistry in Nuclear Fuel Cycle

Manoj Kumar Sharma

¹Fuel Chemistry Division, Bhabha Atomic Research Centre, Mumbai, INDIA

²Homi Bhabha National Institute, Mumbai, INDIA

E-mail: mkumars@barc.gov.in

Abstract

In recent years, environmentalists have raised the concern over the global warming and harsh climatic changes due to the increasing amount of green house gases (CO_2 , CH_4 , N_2O) in the atmosphere. The burning of fossil fuels (coal, gas, oil etc.) to generate electricity is the major contributor to the green house gas emission. Thus, there have been efforts to significantly decrease the green house emissions from fossil fuels in next few decades to save the planet earth. Nuclear power plants are perennial source of clean and environment friendly energy generated from controlled nuclear fission of fissile atoms like U^{235} , U^{233} and Pu^{239} . Nuclear science and technology involves multidisciplinary research in different branches of science and engineering to design & develop advanced reactors & associated technologies/processes for fuel material fabrication/production, chemical quality control, spent fuel reprocessing, etc. Nuclear fuel cycle begins with the mining of ore and ends with the safe disposal of radioactive waste generated during the reprocessing of the spent nuclear fuels. Nuclear fuel cycle consists of two stages: front-end & back-end. The electrochemical methods are used in many front-end and back-end processes viz. chemical quality control of nuclear fuel, spent-fuel reprocessing, pyroprocessing of spent nuclear fuel etc. In this article, the role of the “electrochemical science/electrochemistry” in a few imperative processes in nuclear fuel cycle is briefly presented.

Introduction:

India is one of the fastest growing economies in the world, and a large amount of electrical energy is required to sustain this rapid pace of the economic development. At present, the fossil fuel based thermal power stations are the major contributors (~54%) to electricity generation in India. The burning of fossil fuels (coal, gas, oil etc.) release the green house gases (CO_2 , CH_4 , N_2O) along with several other toxic gases and fly ash, therefore, the environmentalists have raised their concern over the global warming and harsh climatic changes that may also results in increasing sea level. The whole world is now gradually getting aware of the negative impacts of the combustion of fossil fuels over the future of our planet. Thus, there have been efforts to significantly decrease the green house emissions in next few decades to save the earth. The fossil fuels are non-renewable source of energy with limited availability in earth's crust as well; therefore, the growing demand of electricity cannot be met alone with the fossil fuel based thermal power plant for a very long duration. There is a need for environmentally friendly clean renewable source of energy and plenty of other means to generate clean & green electricity are available. The solar, wind, tidal, hydroelectricity etc. are clean renewable source of energy, but they suffer from some or the other disadvantages. Hydroelectric power plant requires construction of large water reservoirs leading to destruction of large forest and the bio-diversity available there. Solar and wind energy are

not perennial and their availability is season-dependent. Another source of clean and environment friendly energy is nuclear power plants based on nuclear fission of fissile atoms like U^{235} , U^{233} and Pu^{239} in nuclear fuels.¹ Nuclear power reactors may provide a long term sustainable clean energy, and account for approximately 13% electricity generation worldwide today without emitting greenhouse gases.² Fissile atoms like U^{235} are available in earth crust, whereas U^{233} and Pu^{239} are obtained from the reprocessing of spent nuclear fuels. Nuclear fuel cycle begins with the mining of ore, fuel fabrication, fuel utilisation in nuclear reactors, spent fuel reprocessing and finally ends with the safe disposal of radioactive waste generated during the spent fuel reprocessing.³ Nuclear fuel cycle consist of two stages: front end & back end. The electrochemical methods are used in front-end and back-end processes viz. chemical quality control of nuclear fuel, spent-fuel reprocessing, pyroprocessing of spent nuclear fuel etc. In this article, the role of the “electrochemical science/electrochemistry” in a few imperative processes in nuclear fuel cycle is briefly presented.

Electrochemistry:

Electrochemistry is a branch of chemical science that deals with the generation of electrical energy by chemical reactions, and the chemical reactions/changes caused by the passage of the electricity through the materials under study.⁴ The movement of electron at a polarised

electrode/electrolyte interface in an oxidation or reduction reaction along with the associated chemical reactions are studied. The redox analyte undergoes reduction or oxidation reaction at a specific potential, and the measured Faradaic current/charge is proportional to the quantity/concentration of the analyte leading to the qualitative or/and quantitative determination of the analytes. The experimental setup consists of a potentiostat-galvanostat, data acquisition system, and a two or three-electrode glass cell setup consisting of working, counter & reference electrodes dipped in an electrolyte solution containing redox analytes. Either the current or the voltage applied to the working electrode results in the redox reactions, thus causing the flow of electron across the electrode/electrolyte interface. Electrochemical methods can be easily coupled with various characterization techniques such as visible, IR, Raman, NMR, EPR, ellipsometry, AFM, XRD, EXAFS etc. for *in situ* characterization of the intermediate & final products during the electrochemical process. It involves different processes viz. electrochemical synthesis, corrosion, electrochemical sensors, electrochemical energy devices, etc., and plays a very crucial role in many industrial processes including nuclear industry.

Electroanalytical chemistry of uranium and plutonium in various supporting electrolytes (acidic, basic, and non-aqueous) at different electrodes (Hg, Pt, Ag, Au, graphite, and glassy carbon) is well documented in literature. Several publications dealing with the applications of carbon nanotubes, graphene, conducting polymers and metal nanoparticles modified electrodes for actinides electrochemistry are also available.⁵

Front End Nuclear Fuel Cycle:

Ore Mining and Milling

The mining and milling of U & Th have been a very safe operation, and all the necessary precautions are taken to prevent any radiation exposures to the public. The periodic monitoring of the site by the competent authority ensures that the radiation exposure, in any case, should remain within the permissible limits. The mining of U & Th removes hazardous radioactive constituents in the ore from their relatively safe underground location and converts them to a fine sand, then sludge, whereby the hazardous radioactive materials become more susceptible to dispersion in the environment. If this large quantity of waste is not managed properly, mining and mill tailings can have adverse impact on the environment leading to contamination of land, water, and air.⁶ It is a major health hazard concern among the inhabitants living in the surrounding of nuclear facilities like mining & ore-processing due to the radiochemical and biological toxicity

of these radioactive elements as they have long half-lives. Due to technical limitations, all of the uranium present in the ore cannot be extracted. Therefore, the sludge also contains 5% to 10% of the uranium initially present in the ore. The waste rocks produce during mining operation contains low grade U and it is not economical to process them in the mill. The waste rocks often contain elevated concentrations of radioisotopes compared to normal rock. The seepage from the waste rock piles must be monitored regularly.

Uranium mill tailings are normally dumped as sludge in special ponds. The amount of sludge produced is nearly the same as that of the ore milled. At a grade of 0.1% uranium, 99.9% of the material is left over. Apart from the portion of the uranium removed, the sludge contains all the constituents of the ore. As long lived decay products such as radium-226 are not removed, the sludge contains 85% of the initial radioactivity of the ore. In addition, the sludge contains heavy metals and other contaminants such as arsenic, as well as chemical reagents used during the milling process.

Electrochemical methods have limited applications in mining and milling operations in nuclear fuel cycle. But recently, a combined electrolysis and leaching process has been reported for rapid recovery of valuable Th & U from radioactive waste water making it suitable for final disposal.⁷ The recovery of the target metal ions by direct electrodeposition from waste streams in different electrolyte solutions are also being studied. The recovery of target metal ion through combined solvent extraction and electrochemical route is also studied.

Chemical Quality Control (CQC) of Nuclear Fuel

Uranium and plutonium are important actinides in view of their use as nuclear fuel in nuclear reactors. Trouble-free long term safe operation of nuclear reactors requires fabrication of high-quality nuclear fuels strictly adhering to the physical and chemical parameters (fissile content, isotopic ratio, metallic & non-metallic impurities etc.) laid down by the reactor and fuel designers, as these parameters will influence the chemical and physical properties of the fuel. The starting, intermediate, and final product of the fuel pass through a series of quality control checks before getting into the reactor core. Chemical quality control of nuclear fuel provides a means to ensure the quality of fuel to achieve the specified performance of the fuel inside the reactor.⁸ Each batch of the feed and the product and the intermediates at various stages of the fuel manufacturing process have to undergo chemical quality control checks for designed specifications. To meet the requirement of designed specification for the fissile

content very high accuracy and precision of the order of 0.2% is required. Therefore, stringent chemical quality assurance and control of nuclear fuel is very essential activity in front-end nuclear fuel cycle. Many reliable destructive and non-destructive analytical techniques are available in the arsenal of an analyst, but the preferred analytical method has to be highly precise and accurate over a large concentration range, involve simple and inexpensive instrumentation, simultaneous/sequential determination in a single aliquot solution if more than one analyte is present. Another important feature of the analytical method in case of radioactive sample is its capability of measurement from remote distance to reduce the radiation exposure to analyst. Though, the analysts are equipped with large number of destructive and non-destructive analytical techniques viz. spectrophotometry, x-ray fluorescence, mass spectrometry, neutron activation analysis, α -spectroscopy, and redox titrimetry, etc.⁹ Many of these techniques require expensive and complex instruments with high cost of operation and maintenance, which are hardly available in small laboratories as well as for the on-site environmental monitoring. Some techniques require the complete separation of the uranium and plutonium from the matrix components of the sample. The electrochemical techniques have played a very pivotal role in the chemical quality control of nuclear fuel, and are capable of sequentially or simultaneously determining U & Pu in submilligram to milligram amount with very high precision and accuracy of the order of 0.2%. Redox titrimetric methods with electrochemical end-point detection methods (potentiometry & biamperometry), controlled potential coulometry, and voltammetry (cyclic & pulse) are widely used techniques in quantitative determination of U & Pu in nuclear fuels, and offer several advantages over other techniques if cost, time, precision, accuracy, space, analysts' effort etc are all together taken into account.¹⁰ A brief description of different electroanalytical methods for quantification of U, Pu and Th is discussed herewith.

Biamperometry

Biamperometry is the most preferred redox titrimetric method for the quantitative determination of U, Pu and Th in nuclear fuel in laboratories because of inexpensive instrumentation requiring a current measuring device and simple titration cell setup consisting of twin identical Pt electrodes. Sequential determination of U and Pu in the same aliquot is also possible in a few cases.¹¹ A constant potential difference is maintained over the twin identical electrodes and current change is measured during the addition of chemical redox titrants. Conventional amperometric titration consist of three electrodes system

(working, counter, and reference electrode), whereas biamperometry consist of twin identical Pt electrode and advantageous over amperometric titration for end point determination. No standard reference electrode like saturated calomel electrode (SCE), which requires careful maintenance, is required. The progress and completion of all redox reactions taking place can be monitored by the current readings. The magnitude of the current prior to the titration is directly proportional to the concentration of the analyte and decreases linearly as the titration progresses. The end point corresponding to the current reaching a minimum that can be detected easily without plotting the titration curve. Analyst does not require any special training and the method is free from personnel bias. The method is competent enough to quantitatively determine U, Pu and Th in sub-milligram to milligram range with very high precision and accuracy.

U, Pu and Th content of fuel samples analysis using biamperometry involves three steps namely (i) dissolution of fuel sample in a suitable medium; (ii) aliquoting of the dissolved sample and (iii) U, Pu and Th determination by biamperometry. (U, Pu)O₂ or (U, Th)O₂ sample is quantitatively dissolved in concentrated nitric acid in presence of catalytic amount of HF by heating under reflux and (U, Pu)C carbide sample are dissolved in a mixture of conc. HNO₃ and conc. H₂SO₄ by heating under reflux.¹² A photograph of dissolution setup for carbide samples in FCD is shown in Figure 1. To obtain good precision and accuracy, redox titrimetry is performed on weight basis. Dissolved samples are aliquoted in triplicates on weight basis with the help of plastic weight burettes and are subjected to biamperometric titration. The aliquoting setup (weighing glove box) is shown in Figure 1.

U determination: Davies and Gray method is well known for U determination, but quantitative recovery of Pu from phosphoric acid (H₃PO₄) is very difficult. So this method is modified for U determination.¹³ In the modified method, U(VI) is at first reduced to U(IV) by excess Ti(III) in 6 M H₂SO₄ in absence of Pu or 9 M H₂SO₄ in presence of Pu. The unreacted Ti(III) is oxidized by nitric acid and the nitrous acid thus produced is destroyed by using sulphamic acid. Subsequently, U(IV) is oxidized to U(VI) by adding standard Fe(III) solution and the generated Fe(II) is titrated with standard K₂Cr₂O₇ solution using biamperometry to detect the end point. Pu, if present, will not interfere as Pu(IV, VI) will be reduced to Pu(III) by Ti(III) in the reduction step and Pu(III) will be oxidized back to Pu(IV) by HNO₂.

Pu determination: Modified Drummond and Grant method is used to determine Pu.¹⁴ In this method, Pu(III, IV)

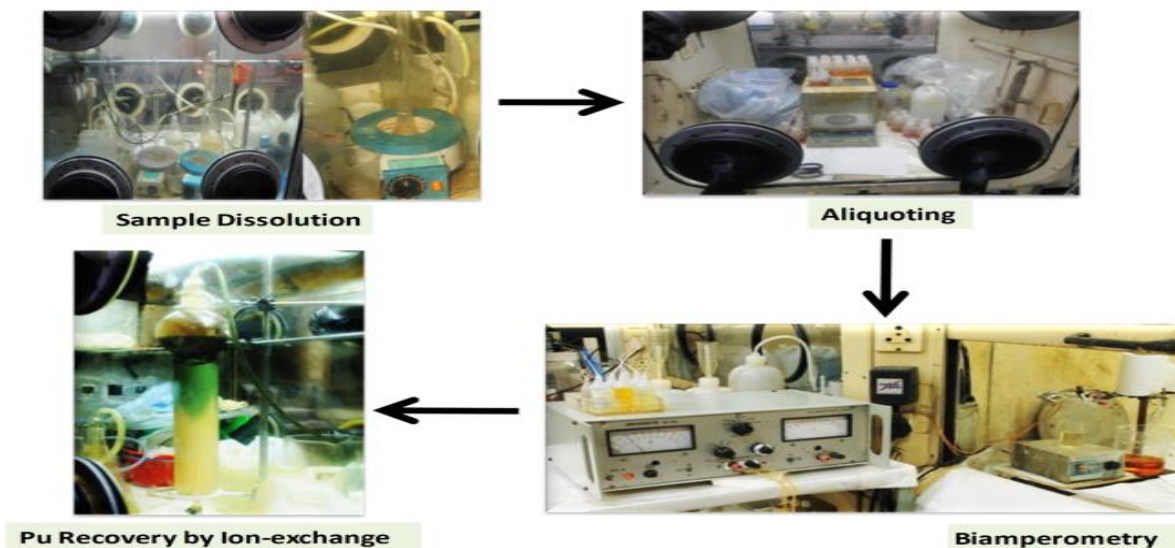


Figure 1. Photographs of experimental setup for fuel sample analysis.

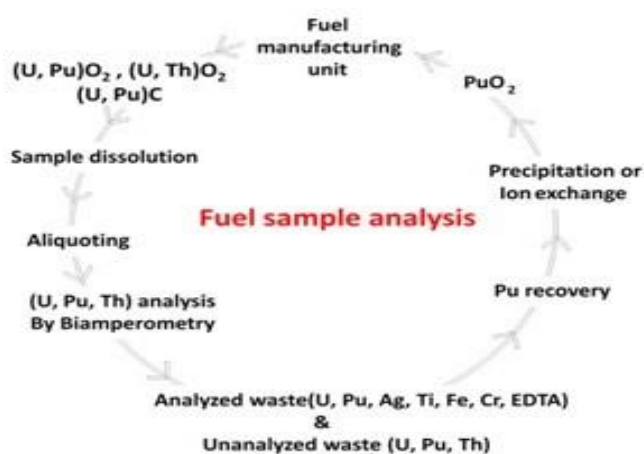


Figure 2. Schematic of routine nuclear fuel sample analyses cycle.

is first oxidized to Pu(VI) by adding excess argentic oxide (AgO) in 1 M H_2SO_4 . Then the excess AgO is selectively reduced with slight excess of sulphamic acid. The unreacted sulphamic acid does not interfere in the Pu determination. Then Pu(VI) is quantitatively reduced to Pu(IV) by adding excess of standard Fe(II) and the unreacted Fe(II) is titrated with standard potassium dichromate ($K_2Cr_2O_7$) solution. U, if present remains as U(VI) (most stable oxidation state) and does not interfere in Pu determination.

Th determination: Since, Th possesses single oxidation state (Th^{4+}), it cannot be determined using redox titrimetry like U and Pu. Complexometric titration using EDTA as a titrant is used for Th determination since EDTA forms stable complexes with Th^{4+} .¹⁵ EDTA is a hexadentate ligand

with four carboxyl groups and two amino N atoms, each having a lone pair of electrons. At lower pH, the amino group remains protonated and is thus unable to donate electrons to form coordinate covalent bonds. Disodium EDTA forms only tetradentate complexes with metal ions. Most of the metal ions react with EDTA in basic solutions ($pH \geq 10$) and only a few ions such as Th^{4+} , U^{4+} , Pu^{4+} , Bi^{3+} , Ga^{3+} , Fe^{3+} etc., quantitatively react at pH 2. The success of the titration depends upon the precise detection of the end point. Titrations using metal ion indicators are prone to personal bias in judging the colour change at the end point. Application of a biamperometric endpoint determination would eliminate the personal bias and, therefore, improve the accuracy, precision, and the detection limit. U(IV) and Pu(IV) will interfere in Th analysis and must be oxidized to U(VI) and Pu(VI) before titration. A picture of the biamperometric setup for U, Pu & Th is shown in Figure 1.

These methods lead to both unanalyzed waste (containing U, Pu and Th) and analyzed waste (containing U, Pu, Fe, Cr, Ag, Ti, EDTA) in acidic medium. Because of the strategic importance, and the hazardous & toxic nature of Pu, it must be recovered completely from these analytical waste solutions before their final disposal. It is desirable to recover Pu as pure PuO_2 powder and sent back to fuel fabricators for reuse. Oxalate precipitation or ion exchange is routinely employed for recovery of Pu from the solutions.¹⁶ A picture of Pu recovery setup (ion exchange setup) is also shown in Figure 1. Pu is recovered in the form of PuO_2 and sent back to the fuel manufacturer, thus completing the routine nuclear fuel sample analysis cycle, (shown in Figure 2).

Despite having several advantages compared with other techniques, biamperometry too suffers with the following disadvantages: (i) U, Pu and Th are mostly determined separately; (ii) recovery of U, Pu and Th from analyzed waste is cumbersome as it contains several metallic impurities like, Fe, Cr, Ag, Ti, EDTA etc. which are added during titration; (iii) requires standard reference material and (iv) analyst has to be present nearer to sample throughout the titration, thus, increasing the radiation exposure. Therefore, there is a need to develop another method which has all the merits of biamperometry as well as generates clean analytical waste devoid of metallic impurities and lesser radiation exposure to analyst.

To overcome these problems, other electroanalytical techniques like coulometry and voltammetry have been explored.

Coulometry

Coulometry means measurement of coulombs (unit of electrical charge named in honour of Charles-Augustin de Coulomb). Therefore, coulometry is the name given collectively to all those electrochemical techniques used for quantitative determination of analyte by measuring the charge consumed/produced when analyte undergoes reduction/oxidation during exhaustive electrolysis at large surface area electrode. It is necessary for precise and accurate determination that the current efficiency of the desired electrochemical reaction should be 100% i.e., no undesired interfering electrode reactions take place, e.g. hydrogen evolution etc. Faraday's first law of electrolysis is used for calculating the amount of analyte

$$m = \frac{M * Q}{n * F} = \frac{M * I * t}{n * F}$$

where, 'm' is the mass of analyte, 'M' is the molar mass of analyte, 'F' (= 96487 C) is the Faraday constant, 'n' is the number of electron change in redox process, 'Q' is the amount of electrical charge consumed/produced, 'I' is the current passing through the electrical circuit for time 't'.

Coulometry is an absolute measurement method (no standard reference material/calibration plot is required) since it is based on fundamental physical quantities. The coulometric techniques can be grouped into two basic categories: (1) Galvanostatic or constant-current coulometry and (2) Potentiostatic or controlled-potential coulometry (CPC).

Coulometry has been developed & used as an alternative bulk electrolysis method for CQC of nuclear fuels.¹⁷ The oxidation and reduction of the analytes (U & Pu) in solution is carried out by applying a suitable

redox potential on a very large dimension working electrode, therefore, CPC does not require chemical titrants for oxidation-reduction of analyte, and the chemical composition of the analyte solution remain unchanged even after the analysis. The generated clean analytical waste is free from the impurities coming from the redox titrants, thus, eases the recovery of U & Pu. Coulometer and attached input-output devices can be operated at remote distance from the sample cell, thus, resulting in lesser radiation exposure to analyst.

Controlled-Potential Coulometric Determination of Uranium: Prior to the development of controlled-potential coulometer, indirect coulometric titration methods were developed using electrolytically generated Ce(IV) or bromine which oxidized U(IV).¹⁸ These methods needed a preliminary reduction of U(VI) to U(IV) by chemical reductant, and absence of easily oxidisable species and nitrate ion. A direct constant-current coulometric procedure was developed for U(VI) determination by reduction of U(VI) to U(IV) using electrolytically generated titanous ion.¹⁹ The accuracy was good for high concentration of uranium but required a titration temperature of 85° C. The elevated temperature was required to increase the rate of reduction of U(V) with Ti(III), because at room-temperature the rate is impracticably low. Any easily reducible ion would be expected to cause bias in the uranium determination. Tanaka *et al* studied the current efficiency in the coulometric generation of Ti(III) as a function of electrolyte composition, current density and electrode (platinum, mercury and graphite) material.²⁰

The development of controlled-potential coulometer by Booman initiated the first study on coulometric determination of U(VI) at controlled potential in his group. The U(VI) was reduced to U(IV) at a controlled-potential mercury pool cathode in a potassium citrate-aluminium sulphate or a sulphuric acid electrolyte. Essentially complete reduction was accomplished in 5 to 10 minutes at room temperature by using a 5-mL capacity electrolysis cell. The method could tolerate Hg(II), Cu(II), Fe(III), and large amounts of nitric acid. Controlled-potential coulometric method showed excellent precision with results reliable to less than 0.1% standard deviation in the range from 75 to 0.75 mg uranium in sample and having sensitivity extending to a few micrograms of uranium.²¹ The mercury pool is used as the working electrode due to its large overpotential for hydrogen evolution reaction (HER) in acidic medium in cathodic potential region. Goode *et al* introduced differential controlled-potential coulometry technique for the determination of uranium in uranium standard by reducing U(VI) in 0.5 M H₂SO₄ at a mercury electrode. A higher precision was attainable than

controlled-potential coulometry.²² Analysis by controlled-potential coulometry takes relatively longer time compared to constant-current coulometric titration, Lingane introduced a new technique known as 'controlled-potential coulometric titration' for the determination of uranium.²³ Controlled-potential coulometric titration, combines the merits of both controlled-potential coulometry and constant-current coulometric titration.

The experimental setup consists of a controlled potential coulometer (potentiostat), data acquisition system, and a three-electrode glass cell setup consisting of working, counter & reference electrode dipped in an electrolyte solution containing redox analytes (U, Pu). Counter and reference electrodes are kept in separate compartments to avoid direct contact with the analyte solution. The reduction of UO_2^{2+} to U^{4+} is not a reversible process. Therefore, the selection of working electrode potential for irreversible redox couple ($\text{UO}_2^{2+}/\text{U}^{4+}$) is not as simple as in case of reversible redox couple ($\text{Fe}^{3+}/\text{Fe}^{2+}$ and $\text{Pu}^{4+}/\text{Pu}^{3+}$). The working electrode potential for UO_2^{2+} reduction is determined by plotting coulogram (charge or current vs. potential curve). The plot of charge or current against working electrode potential is S-shaped. The potential required for the attainment of maximum charge or current is chosen as the working electrode potential. From the coulogram for UO_2^{2+} reduction, pre-reduction at 0.085 V and reduction at -0.325 V (vs. SCE) were the most suitable potential to carry out precise and accurate determination of uranium in 1 M H_2SO_4 with 100 % current efficiency. Pre-reduction is carried out to reduce all the Pu (PuO_2^{2+} and Pu^{4+}) to Pu^{3+} along with other redox impurities present in the U-Pu mixed solution, and then finally UO_2^{2+} is reduced to U^{4+} . Vigorously stirred mercury pool was used as the working electrode because of electronegative potential of $\text{UO}_2^{2+}/\text{U}^{4+}$ redox couple. Iolar grade (N_2/Ar) gas of high purity was continuously purged over the electrolyte solution during electrolysis. The charge (in Coulombs) measured during the complete UO_2^{2+} reduction is used to calculate the amount of U using Faraday's laws of electrolysis. The pre-electrolysis step is important to avoid the interference caused by the chemical interaction between U(IV) and Pu(IV), and non-Faradaic current due to reduction of other redox impurities.²⁴

Controlled-potential coulometric determination of plutonium: In aqueous solution, plutonium can exist simultaneously in different oxidation states viz. Pu^{3+} , Pu^{4+} , PuO_2^+ and PuO_2^{2+} . The formal redox potentials of Pu(VI)/Pu(V) and Pu(IV)/Pu(III) couples are electropositive, and are electrochemically reversible in non-complexing solution. Several publications describe the use of coulometry

on routine basis for precise and accurate determination of Pu.²⁵ Prior to the development of controlled-potential coulometer, indirect coulometric titration methods were developed for plutonium determination. Furman *et al* studied the coulometric titration involving Pu(IV)/Pu(III) couples using the electrolytically generated Ce(IV) ions and determining end-point by potentiometric method.²⁶ The method was not suitable for determination of microgram quantity of Pu because of the significant interference from iron present in traces in reagents. Carson *et al* developed a coulometric titration method for a rapid and accurate determination of plutonium by reducing Pu(VI) to Pu(IV) using electrolytically generated ferrous ions.²⁷ The method can be used to determine very small quantity of plutonium (as low as 3 μg Pu) without any interference from iron. Controlled potential coulometric determination of Pu in nuclear fuel material is carried out in 1 M H_2SO_4 involving Pu(IV)/Pu(III) redox couple, by successive addition method. A bulk Pt wire gauge electrode with very large surface area is used as working electrode. All the Pu (PuO_2^{2+} and Pu^{4+}) in 1 M H_2SO_4 solution is first reduced to Pu^{3+} by applying a constant potential of 0.3 V vs. SCE, and then all Pu^{3+} is oxidized back to Pu^{4+} at 0.7 V vs. SCE using Pt gauze electrode in 1 M H_2SO_4 . The charge (in Coulombs) measured during the Pu^{3+} oxidation is equivalent to Pu content.²⁸ A photograph of experimental setup of coulometry for determination of U and Pu in nuclear fuel samples is shown in Figure 3.

The CPC too suffers from the following disadvantages (i) the formal redox potential for Pu(IV)/Pu(III) and U(VI)/U(IV) redox couples are wide apart, therefore, two different types of electrodes are used for determination of U (Hg pool electrode) and Pu (Pt wire gauge electrode) which makes the sequential determination of both U and Pu in a single aliquot difficult; (ii) the use of mercury as a working electrode is inconvenient while handling radioactive samples inside fume hood/glove-box and it is toxic too; (iii) Pt gets passivated in anodic potentials; and (iv) long analysis time. The controlled-potential coulometric determination of uranium by reduction of U(VI) has been studied at a silver, platinum, activated platinum and graphite working electrode.²⁹ Sequential determination of U and Pu at graphite electrode is reported using predictive coulometry, but the heterogeneous electron transfer kinetic is very slow at graphite electrode compared to that of Pt.³⁰

Voltammetry

Another important and widely used electrochemical method, known as voltammetry, has been evaluated for CQC of nuclear fuels. Like CPC, voltammetry does not require addition of chemical reagents. The cyclic and

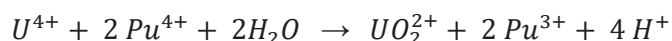


Figure 3. Coulometric setup employed for quantification of U and Pu in nuclear fuel samples.

pulse voltammetry techniques have been developed for simultaneous U & Pu determination in nuclear fuels, and are very accurate, precise, fast, require very small volume of solution and produce clean analytical waste.³¹ The low-cost portable instruments, simple experimental set up and capability to detect & determine sub-ppb level of actinides make the voltammetric techniques suitable for on-site environmental monitoring as well. The experimental setup consists of a potentiostat-galvanostat, data acquisition system, and a three-electrode glass cell setup consisting of working, counter & reference electrode dipped in an electrolyte solution containing redox analytes (U, Pu). The conventional working electrodes are Hg, metals (Pt, Au, Ag, Cu, Pd etc.), carbonaceous materials (graphite, glassy carbon etc.). Usually, the surface of conventional electrodes are chemically modified with metal (Pt, Au and Ru) nanoparticles, conducting polymers (PANI, PEDOT), carbonaceous nanoparticles (SWCNTs, graphene) to enhance the sensitivity, selectivity and heterogeneous electron transfer rate at the electrode/electrolyte interface. During the potential scan on the working electrode, the redox analytes are either reduced or oxidized at the working electrode/electrolyte interface resulting in the flow of the current through the working electrode. The peak current is directly proportional to the concentration of the redox analyte.

Simultaneous determination of U and Pu by differential pulse voltammetry on a single-walled carbon nanotubes (SWCNTs) modified gold electrode has been reported earlier.³² However, in another report on simultaneous determination of U and Pu on electrochemically reduced graphene oxide modified glassy carbon electrode, some inconsistency in U(VI) reduction peak current were

observed in presence of Pu(IV).³³ The inconsistency in U(VI) reduction peak current is explained in terms of coupled chemical reaction between U(IV) (formed at the electrode surface) and Pu(IV) (moves from bulk towards the electrode) that results in regeneration of U(VI) at the electrode-solution interface and thus leading to inconsistency in the U(VI) reduction peak-current measurement. Preliminary investigation revealed that due to the coupled chemical reaction between U(IV) and Pu(IV), the U(VI) to U(IV) reduction current is not constant and makes voltammetry unsuitable for U concentration determination.



Thus, the major hurdles before the development of a voltammetric method for simultaneous determination of U and Pu are: (i) the formal redox potential for Pu(IV)/Pu(III) and U(VI)/U(IV) redox couples are wide apart, therefore, two different types of electrodes are used for determination of U (Hg electrode) and Pu (Pt electrode). Pt and Au results in H₂ evolution in the negative potential region where U(VI) is reduced, but Pt & Au get passivated due to formation of surface oxide film in the positive potential region. The U(VI) reduction peak is very broad on graphite and glassy carbon working electrodes. Hg is toxic and very difficult to handle in radioactive fume hood. Hence, modification of conventional electrode surface is essential; (ii) coupled chemical reaction between U(IV) and Pu(IV) at the electrode solution interface resulting in inconsistent U(VI) reduction peak current; (iii) accuracy and precision of the method should match with well established biamperometry method. In this direction,

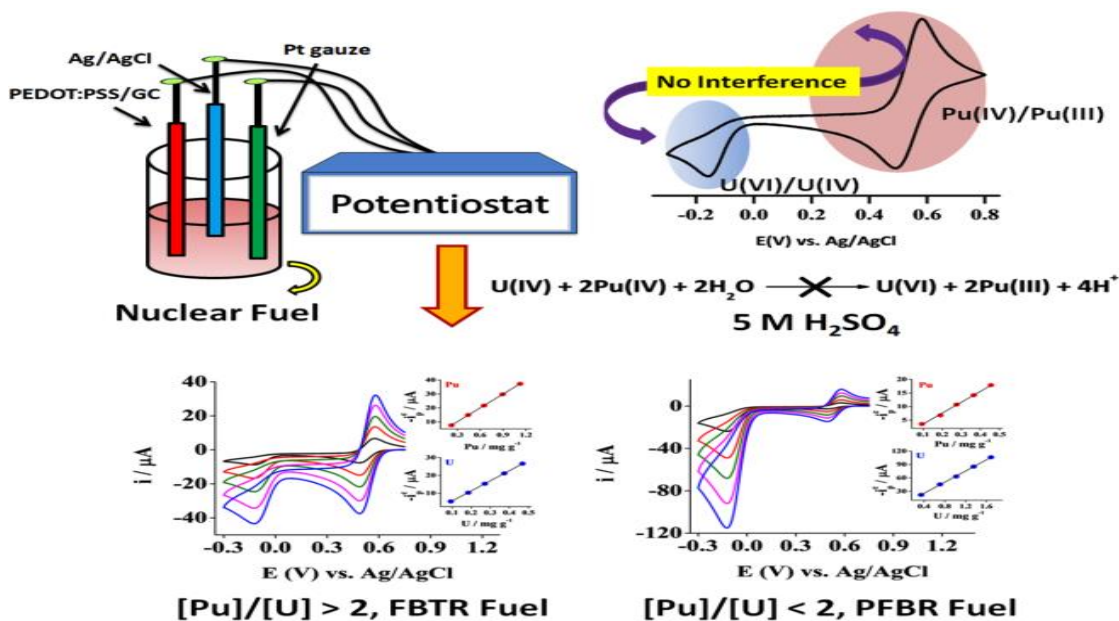


Figure 4. Schematic for simultaneous voltammetric determination of U and Pu in FBR samples.

a few studies were carried out in our laboratory to simultaneously determine U & Pu in nuclear fuel samples.

Simultaneous voltammetric determination of Uranium and Plutonium in Fast-breeder reactor (FBR) fuel: The surface of the glass carbon (GC) electrode has been coated by a thin film of the composite of (poly(3,4-ethylenedioxythiophene) poly(styrenesulfonate)) PEDOT:PSS to investigate the redox reaction of Pu(IV)/Pu(III) and U(VI)/U(IV) redox couples.³⁴ The high electrical conductivity, robustness, low cost, easy processability, large surface area and the low band gap of PEDOT-PSS enhances the heterogeneous electron transfer kinetics on PEDOT-PSS/GC electrode in compare to bare GC electrode which leads to distinct sharp redox peaks for U(VI)/U(IV) and Pu(IV)/Pu(III) couples and enables quantification.

The effect of acidity (H_2SO_4 concentration) on the coupled chemical reaction between U(IV) and Pu(IV) is examined and observed that an increase in acidity of H_2SO_4 minimize the coupled chemical reaction. In 5 M H_2SO_4 electrolyte, the value of U(VI) reduction peak current is independent of the Pu(IV) concentrations in sample solution. The coupled chemical reaction between U(IV) and Pu(IV) ceases at 5 M H_2SO_4 and hence, the simultaneous voltammetric determination of U and Pu is possible on PEDOT-PSS/GC, irrespective of [Pu]/[U] ratio in 5 M H_2SO_4 . The method is applied for both (U, Pu) O_2 (PFBR) and (U, Pu)C (FBTR) samples

No interference is observed from commonly encountered impurities present in FBR fuel samples.

It shows accuracy and precision comparable to that of biamperometry method. High robustness, fast analysis, simultaneous determination, less radiation exposure to analyst and ease of recovery of U and Pu from analytical waste, makes it suitable candidate to substitute the extensively used biamperometry titration method for CQC of nuclear fuel.

Back End Nuclear Fuel Cycle:

Spent Fuel Reprocessing:

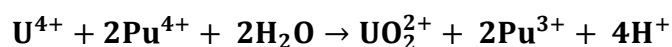
India has adopted a closed fuel cycle and reprocessing of spent nuclear fuel is done for the following reasons (1) recovery of valuable fissile materials (^{235}U , ^{239}Pu , ^{233}U) for subsequent reuse in next generation reactors; (2) to recover valuable radionuclide from high level waste (HLW) viz. ^{137}Cs , ^{90}Sr , ^{106}Ru etc.; (3) to significantly reduce the waste volume. Electrochemical methods have been developed and employed for aqueous reprocessing of spent nuclear fuel.³⁵

Plutonium, Uranium, Reduction, EXtraction (PUREX) Process

PUREX is a reprocessing method to recover U and Pu from the spent/irradiated nuclear fuel which contains actinides (U, Pu, Np & Am) and fission products (Cs, Ru, Mo, Tc, Ru, Rh, Pd etc.).³⁶ The spent fuel is dissolved in HNO_3 , and aqueous solution is separated from the solid by filtration. The U and Pu are separated from fission products and other actinides in aqueous solution by solvent extraction method using 30% tributyl phosphate

in kerosene as extractant. U and Pu are extracted in the organic phase, while fission products and other actinides remain in the aqueous phase. To separate U and Pu, the U/Pu loaded organic phase is contacted with aqueous nitric acid solution containing reductant (ferrous sulphamate, ferrous nitrate, hydroxylamine nitrate etc.) and stabilizer (hydrazine). Pu⁴⁺ is reduced to Pu³⁺, and Pu³⁺ is transferred to aqueous solution and U remains in organic phase. The U is stripped from the organic phase into the aqueous solution by contacting organic phase with 0.2 M HNO₃ solution.

Externally generated uranous (U⁴⁺) can be used to reduce Pu⁴⁺ to Pu³⁺ for separating U and Pu in the salt free reprocessing process.³⁷ The uranous (U⁴⁺) ions is generated by electrochemical reduction of uranyl UO₂²⁺ ions.



The external feed U(IV) method has a few drawbacks. A 6 to 10 times stoichiometric excess of uranous is required for effective separation of Pu from U, and hydrazine is required to stabilize uranous ion. Autocatalytic reoxidation of Pu(III) & U(IV) in the organic phase occurs sometimes.

The *in-situ* electrochemical reduction of UO₂²⁺ and Pu⁴⁺ to U⁴⁺ and Pu³⁺, respectively, can also be employed during partitioning to separate U and Pu. The *in-situ* electrochemical reduction offers several advantages, including all the advantages of the external feed U(IV) process without any of its drawbacks: non-requirement of chemical reductant, easy, simple, low cost, remote operation etc.³⁸ The reductant U⁴⁺ is homogeneously *in-situ* generated by electrochemically reducing UO₂²⁺. A

schematic of electrochemical mixer-settler for reductive separation of U and Pu is shown in Fig. 5. The 'e' in the schematic represents the electrochemical stage. The whole casing of the extraction section of the mixer-settler is made of titanium which acts as cathode. Platinum or platinized Ti, Ta is used as the anode. The plutonium is chemically and electrochemically reduced to lower valence state and is back-extracted into the aqueous phase. In an electrochemical mixer-settler, Pu³⁺ generation occurs via: (i) electroreduction of Pu⁴⁺ (ii) chemical reduction of Pu⁴⁺ by electrochemically generated uranous (U⁴⁺) (iii) chemical reduction of Pu⁴⁺ by hydrazine. Hydrazine prevents oxidation of Pu³⁺ by nitrous acid, which is produced during electrolysis. Electrochemically generated uranous rapidly reduces the majority of Pu⁴⁺ present in the feed, and reduction of Pu⁴⁺ by the hydrazine is comparatively much slower. The organic scrub (30% TBP in n-dodecane) re-extracts the uranium that leaves the feed stage and enters the aqueous phase. U contamination in Pu stream is in ppm level.

Many other applications of electrochemical methods to aqueous reprocessing of spent nuclear fuel includes stabilization of various oxidation state of actinides (U, Np, Pu) in aqueous solution, redox reaction in two-phase extraction system, electrochemically controlled extraction chromatography to carry out separation under laboratory conditions, dissolution of PuO₂ by electrochemically generated mediators who accelerates the dissolution by facilitating the transfer of electrons between anode and PuO₂, removal of organic compounds from liquid radioactive wastes prior to their disposal, recovery of platinum-group metals (Pd, Rh, Ru) and other precious radionuclides of societal benefits.³⁹

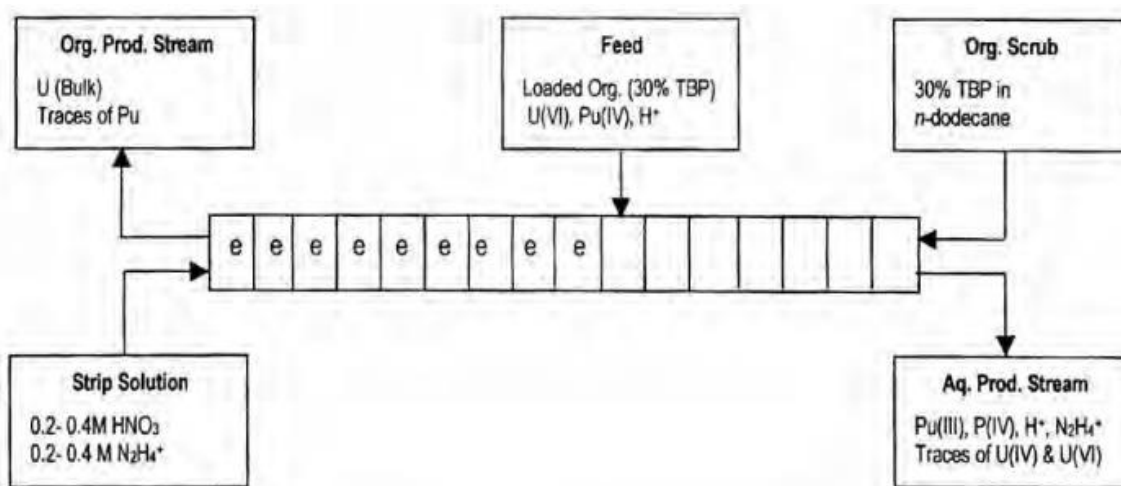


Figure 5. Schematic of electrochemical mixer-settler with electrochemical stage (e) for U and Pu separation. [Taken from Ref. 38a]

Pyroprocessing of Spent Nuclear Fuel

Pyrochemical processes or pyroprocessing are high temperature reprocessing/separation techniques that involve electrochemical reduction and oxidation processes in molten salt to recover metal fuels from spent metal oxide fuel.⁴⁰ The metal fuel produced from pyroprocessing can be used in nuclear fast reactors. The electrochemical processes comprise of electrochemical reduction, electro-refining and electro-winning. Many researchers have studied the viability of employing molten-salt based electrochemical methods for reprocessing of spent nuclear fuels and nuclear materials. The electrolysis cell for electrochemical reduction, also known as oxide reduction, consists of crucible, molten salt ($\text{Li}_2\text{O-LiCl}$) and electrodes (working cathode electrode, counter Pt anode electrode and reference electrode). The spent metal oxide fuel is loaded in the cathode basket and it is submerged in the molten $\text{Li}_2\text{O-LiCl}$ salt.

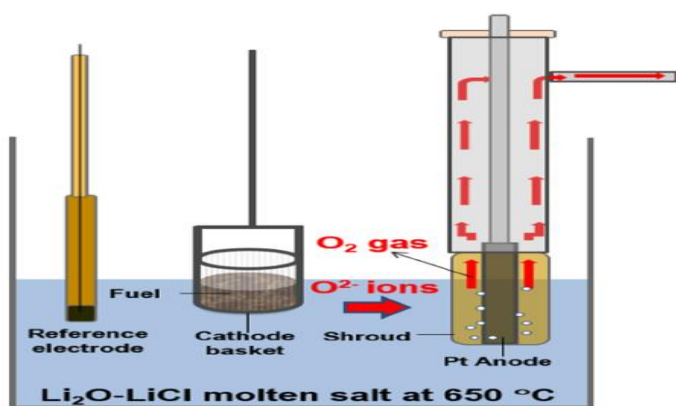


Figure 6. Schematic of electroreduction of spent oxide fuel [Taken from Ref. 40a]

At cathode, the spent metal oxide fuel feed is reduced to metal and fission products such as Cs, Sr and Ba get dissolved in molten $\text{Li}_2\text{O-LiCl}$ salt. The cathode reaction for the actinide oxide is as follows:



At Pt anode, oxygen evolution reaction occurs and anode reaction is as follow:



Electrorefining process is carried out to obtain pure U metal from the metal obtained at the cathode in the electrochemical reduction process. The metal is loaded into an anode basket and used as feed for the electrorefining process in molten LiCl-KCl eutectic salt. At anode the metal feed comprises of U, transuranium elements and other metallic impurities undergo anodic dissolution into the molten salt, and U metal is only deposited from the molten

salt at the cathode. The electrowinning process is used to recover the U and transuranium elements that remains in the molten salt after the electrorefining process.

Conclusion

Nuclear fuel cycle consists of two stages: front end & back end. The electrochemical methods are used in many front-end and back-end processes viz. chemical quality control of nuclear fuel, spent-fuel reprocessing, pyroprocessing of spent nuclear fuel etc. Recent publications have shown the applications of electrochemical methods in many of the unexplored area of nuclear fuel cycle viz. mining and milling, and improvement in the currently used electrochemical techniques.

References:

1. S. Banerjee, H. P. Gupta, *Prog. Nucl. Energy*, **2017**, *101*, 4; P. Puthiyavinayagam, P. Selvaraj, V. Balasubramanian, S. Raghupathy, K. Velusamy, K. Devan, B. K. Nashine, G. Padma Kumar, K. V. Suresh kumar, S. Varatharajan, P. Mohanakrishnan, G. Srinivasan, A. K. Bhaduri, *Prog. Nucl. Energy*, **2017**, *101*, 19.
2. T. Costas, *Nature Energy*, **2017**, *2*, 17007.
3. B. S. Tomar, P. R. Vasudeva Rao, S. B. Roy, Jose P. Panakkal, Kanwar Raj, A. N. Nandakumar, *Nuclear Fuel Cycle*, Springer Nature: Singapore, 2023, ISBN 978-981-99-0948-3 ISBN 978-981-99-0949-0 (eBook), <https://doi.org/10.1007/978-981-99-0949-0>
4. A. J. Bard, L. R. Faulkner, *Electrochemical Methods: Fundamentals and Applications*, 2nd Edition, Wiley: New York, 2001, ISBN: 978-0-471-04372-0.
5. P. D. Schumacher, J. L. Doyle, J. O. Schenk, S. B. Clark, *Rev. Anal. Chem.*, **2013**, *32*(2), 159; A. Rout, *J. Electrochem. Soc.*, **2022**, *169*, 126502.
6. K. T. Thomas, *IAEA Bulletin*, **1981**, *23*(2), 33.
7. J. Gao, J. Chen, H. Lv, X. Feng, S. Liao, Y. Yan, Y. Xue, F. Ma, *J. Cleaner Production*, **2023**, *427*, 139093.
8. *IANCAS Bulletin*, Guest Editors: A. Prakash, S. Jeyakumar, **2021**, *XVII* (2).
9. G. R. Relan, A. N. Dubey, S. Vaidyanathan, *J. Radioanal. Nucl. Chem.*, **1996**, *204*, 15; K. Suresh Kumar, P. Magesvaran, D. Sreejeya, T. Kumar, B. Shree Kumar, P. K. Dey, *J. Radioanal. Nucl. Chem.*, **2010**, *284*, 457; S. Dhara, S. Sanjay Kumar, K. Jayachandran, J. V. Kamat, A. Kumar, J. Radhakrishna, N. L. Misra, *Spectrochim. Acta Part B: Atomic Spectroscopy*, **2017**, *131*, 124; C. G. Lee, D. Suzuki, Y. Saito-Kokubu, F. Esaka, M. Magara, T. Kimura, *International Journal of Mass Spectrometry*, **2012**, *314*, 57; R. Kapsimalis, D. Glasgow, B. Anderson, S. Landsberger, S., *Journal of Radioanalytical and Nuclear Chemistry*, **2013**, *298*, 1721; T. Hashimoto, K. Taniguchi, H. Sugiyama, T. Sotobayashi, *Journal of Radioanalytical and Nuclear Chemistry*, **1979**, *52*, 133; J. V. Kamat, K. Jayachandran, P. Patil, D. M. Noronha, D. Alamelu, S. K. Aggarwal, *Journal of Radioanalytical and Nuclear Chemistry*, **2013**, *295*, 601; P. R. Nair, M. Xavier, S. K. Aggarwal, *Radiochimica Acta*, **2009**, *97*, 419; C. V. Karekar, K. Chander, G. M. Nair, P. R. Natarajan, *Journal of Radioanalytical*

- and Nuclear Chemistry, **1986**, 107, 297.
10. J. V. Kamat, K. Jayachandran, P. Patil, D. M. Noronha, D. Alamelu, S. K. Aggarwal, *Journal of Radioanalytical and Nuclear Chemistry*, **2013**, 295, 601; P. R. Nair, M. Xavier, S. K. Aggarwal, *Radiochimica Acta*, **2009**, 97, 419; Manoj K. Sharma, J. V. Kamat, A. S. Ambolikar, J. S. Pillai, S. K. Aggarwal, **2012**, BARC/2012IE/001; W. D. Shults, *Talanta*, **1963**, 10, 833; R. Agarwal, M. K. Sharma, K. Jayachandran, J. S. Gamare, D. M. Noronha, K. V. Lohithakshan, *Analytical Chemistry*, **2018**, 90, 10187; R. Agarwal, M. K. Sharma, D. M. Noronha, J. S. Gamare, K. Jayachandran, *Dalton Transactions*, **2019**, 48, 7875; R. Gupta, K. Jayachandran, S. K. Aggarwal, *RSC Advances*, **2013**, 3, 13491.
 11. P. R. Nair, K. V. Lohithakshan, M. Xavier, S. G. Marathe, H. C. Jain, *Journal of Radioanalytical and Nuclear Chemistry*, **1988**, 122, 19.
 12. K. Chander, B. N. Patil, J. V. Kamat, N. B. Khedekar, R. B. Manolkar, S. G. Marathe, *Nuclear Technology*, **1987**, 78, 69.
 13. A. R. Eberle, M. W. Lerner, C. G. Goldback, C. J. Rodden, *Report NBL 252*, **1972**; P. R. Nair, K. V. Lohithakshan, M. Xavier, S. G. Marathe, H. C. Jain, *Journal of Radioanalytical and Nuclear Chemistry*, **1988**, 122, 19.
 14. C. L. Rao, G. M. Nair, N. P. Singh, M. V. Ramaniah, N. Srinivasan, *Journal of Analytical Chemistry*, **1971**, 234, 126.
 15. K. Jayachandran, J. S. Gamare, P. R. Nair, M. Xavier, S. K. Aggarwal, *Radiochimica Acta*, **2012**, 100, 311.
 16. S. P. Hasilkar, N. B. Khedekar, K. Chander, H. C. Jain, *Journal of Radioanalytical and Nuclear Chemistry*, **1994**, 185, 119.
 17. G. L. Booman, *Analytical Chemistry*, **1957**, 29, 213; G. L. Booman, W. B. Holbrook, J. E. Rein, *Analytical Chemistry*, **1957**, 29, 219; J. E. Harrar, *Electroanalytical Chemistry*, **1975**, Vol. 8, edited by A. J. Bard, Marcel Dekker, Inc., NY; Manoj K. Sharma, J. V. Kamat, A. S. Ambolikar, J. S. Pillai, S. K. Aggarwal, **2012**, BARC/2012IE/001; W. D. Shults, *Talanta*, **1963**, 10, 833.
 18. N. Bett, W. Nock, C. Morris, *Analyst*, **1954**, 79, 607; W. D. Cooke, N. H. Furman: *Analytical Chemistry*, **1950**, 22, 896.
 19. W. D. Cooke, C. N. Reilley, N. H. Furman, *Analytical Chemistry*, **1951**, 23, 16; J. J. Lingane, R. T. Iwamoto, *Analytica Chimica Acta*, **1955**, 13, 465.
 20. T. Tanaka, G. Marinenko, W. F. Koch, *Talanta*, **1985**, 32, 525.
 21. G. L. Booman, *Analytical Chemistry*, **1957**, 29, 213; G. L. Booman, W. B. Holbrook, J. E. Rein, *Analytical Chemistry*, **1957**, 29, 219.
 22. G. C. Goode, J. Herrington, *Analytica Chimica Acta*, **1967**, 38, 369.
 23. J. J. Lingane, *Analytica Chimica Acta*, **1970**, 50, 1.
 24. N. Gopinath, J. V. Kamat, H. S. Sharma, S. G. Marathe, H. C. Jain, *Bulletin of Electrochemistry*, **1989**, 5, 805.
 25. F. A. Scott, R. M. Peekema, *Report, HW - 58491*, **1958**, U. S. Atomic Energy Commission; F. A. Scott, R. M. Peekema, *Proc. U. N. Intern. Conf. Peaceful Uses Atomic Energy, 2nd*, Geneva, **1958**, 28, 573; W. D. Shults, *Report, ORNL - 2921*, 1960, U. S. Atomic Energy Commission; G. W. C. Milner, J. W. Edwards, *Report, AERE - R 3772*, **1961**, U. K. Atomic Energy Authority; W. D. Shults, *Talanta*, **1963**, 10, 833.
 26. N. H. Furman, W. D. Cooke, C. N. Reilley, *Analytical Chemistry*, **1951**, 23, 945
 27. W. N. Carson, J. W. Vanderwater, H. S. Gile, *Analytical Chemistry*, **1957**, 29, 1417
 28. Manoj K. Sharma, J. V. Kamat, A. S. Ambolikar, J. S. Pillai, S. K. Aggarwal, **2012**, BARC/2012IE/001; H. S. Sharma, N. B. Khedekar, S. G. Marathe, H. C. Jain, *Nuclear Technology*, **1991**, 89(3), 399.
 29. G. W. C. Milner, J. W. Edwards, *Report, AERE - R 3951*, **1962**, U. K. Atomic Energy Authority; C. M. Boyd, O. Menis, *Analytical Chemistry*, **1961**, 33, 1016; W. Davies, W. Gray, K. C. McLeod, *Talanta*, **1970**, 17, 937; A. R. Joshi, U. M. Kasar, *Journal of Radioanalytical and Nuclear Chemistry*, **1991**, 150, 483; H. S. Sharma, R. B. Manolkar, J. V. Kamat, S. G. Marathe, *Fresenius Journal of Analytical Chemistry*, **1993**, 347, 486; N. Gopinath, N. N. Mirashi, K. Chander, S. K. Aggarwal, *Journal of Applied Electrochemistry*, **2004**, 34, 617.
 30. H. S. Sharma, R. B. Manolkar, J. V. Kamat, S. G. Marathe, *Fresenius Journal of Analytical Chemistry*, **1993**, 347, 486
 31. R. Agarwal, M. K. Sharma, K. Jayachandran, J. S. Gamare, D. M. Noronha, K. V. Lohithakshan, *Analytical Chemistry*, **2018**, 90, 10187; R. Agarwal, M. K. Sharma, D. M. Noronha, J. S. Gamare, K. Jayachandran, *Dalton Transactions*, **2019**, 48, 7875; R. Gupta, K. Jayachandran, S. K. Aggarwal, *RSC Advances*, **2013**, 3, 13491.
 32. R. Gupta, K. Jayachandran, S. K. Aggarwal, *RSC Advances*, **2013**, 3, 13491.
 33. S. K. Guin, A. S. Ambolikar, J. V. Kamat, *RSC Advances*, **2015**, 5, 59437.
 34. R. Agarwal, M. K. Sharma, K. Jayachandran, J. S. Gamare, D. M. Noronha, K. V. Lohithakshan, *Analytical Chemistry*, **2018**, 90, 10187; R. Agarwal, M. K. Sharma, D. M. Noronha, J. S. Gamare, K. Jayachandran, *Dalton Transactions*, **2019**, 48, 7875.
 35. R. Natarajan, *Progress in Nuclear Energy*, **2017**, 101, 118; R. T. Jubin, *Spent Fuel Reprocessing*, ORNL, 2009; V. N. Kosyakov, V. I. Marchenko, *Radiochemistry*, **2008**, 50(4), 289-300.
 36. A. Ramanujam, *IANCAS Bulletin*, **1998**, 14(2), 11; W. B. Lanham, T. C. Runion, *Purex Process for Pu and U Recovery*, USAEC, ORNL-479
 37. H. A. C McKay, R. J. W. Streeton, A. G. Wain, **1963**, UKAEA Report, AERE-R 4381.
 38. (a) N. K. Pandey, S. B. Koganti, *Indian J. Chem. Technol.*, **2004**, 11, 535; (b) H. Schmieder, U. Galla, *Journal of Applied electrochemistry*, **2000**, 30, 201-207;
 39. V. N. Kosyakov, V. I. Marchenko, *Radiochemistry*, **2008**, 50(4), 289-300.
 40. (a) E-Y Choi, S. M. Jeong, *Prog. Nat. Sci.: Mater. Int.*, **2015**, 25, 572-582; (b) M. Mirza et al, *Energy & Environmental Science*, **2023**, 16, 952.



Dr. Manoj Kumar Sharma, SO(G), joined Fuel Chemistry Division, BARC in 2003 after completing M.Sc. (Chemistry) from Indian Institute of Technology, Delhi in 2002 and graduating from the OCES-46th batch of BARC Training School. He obtained Ph.D. (Chemical Sciences) from the Homi Bhabha National Institute (HBNI) in the year 2013. Since 2003, he has been actively involved in electrochemical studies of actinides in aqueous/non-aqueous solutions, and development of electroanalytical methods for analysis of nuclear fuels. His areas of interest are applications of electrochemical techniques for advanced materials synthesis, material characterization, separation; development of chemically modified electrodes for electrocatalysis & electroanalysis; development of electrochemical energy devices, ion-selective membranes etc

Rapid and sensitive redox speciation method for vanadium during electro-synthesis of V(II) formate

K. K. Bairwa and V. S. Tripathi

Radiation and Photochemistry Division, Bhabha Atomic Research Centre, Mumbai, India 400085

Email: vst_apcd@barc.gov.in

Abstract

Electrochemical synthesis of aqueous vanadous formulation using material compatible precursors is the preferred route for its nuclear power plant application. A methodology for in-situ monitoring of the electrolytic synthesis of vanadous formate with minimum intervention has been developed. This is based on continuous solution potential monitoring with a redox electrode impressed with a high frequency alternating voltage to overcome polarization of the electrode.

The redox speciation method for periodic batch samples has also been evolved which is based on simple, rapid and sensitive indirect spectrophotometric measurement. V(V) in solution is evaluated by adding Fe(II) and estimating the Fe(III) formed by the spectrophotometric determination of the sulfosalicylic acid complex where neither V(IV) nor Mn(II) has shown any interference over a wide range of concentration. The redox speciation involves evaluating the V(V) reducing strength of the sample. Total vanadium concentration in the sample is separately evaluated by completely oxidizing it to V(V) with acidic permanganate. The composition of the redox mixture in the sample is thence calculated by analyzing V(V).

Introduction

Vanadium ions exist in aqueous solution as V(II), V(III), V(IV), or V(V), or as a mixture of any two contiguous valence states [1]. The lower oxidation states are air sensitive and hence the synthesis of lower oxidation state vanadium compounds in aqueous solution require continuous monitoring to ensure inert atmosphere in the experimental setup. Thus redox speciation of aqueous vanadium is an essential prerequisite for efficient synthesis of lower oxidation state aqueous vanadium compounds in aqueous solutions.

Synthesis of vanadous formulation through electrolytic reduction is a viable option for the purpose of its use in the decontamination formulation as electrolysis provides the advantage of selecting a non corrosive medium while avoiding any spare ionic species in the final product [2]. These are primary objectives for nuclear power plant application owing to structural integrity and active waste volume generation concerns. The prevalent oxidation states of vanadium compounds are (V) and (IV) and preparation of V(II) from these states require proper monitoring of the process. V(II) and even V(III) formulations are air sensitive and hence a stringent inert atmosphere has to be maintained throughout the preparation process. Thus, a reliable on-line vanadium redox species measurement based on minimum intervention and fast response is required to monitor the progress of electrolysis. Redox potential monitoring has been explored for on-line measurement during electrolytic preparation of lower oxidation state aqueous vanadium

compounds. Solution potential monitoring with a redox electrode impressed with a high frequency of 1.13 kHz, 10 mV alternating voltage to overcome polarization of the electrode has been evolved for evaluating the progress of electrolysis.

Spectrophotometric determination of aqueous vanadium is the method of choice when rapid redox speciation is required [3]. However, direct spectrophotometric determination of vanadium suffers from poor sensitivity and selectivity. Extraction to organic phase followed by spectrophotometric determination using suitable chromophores is normally practiced to improve sensitivity and selectivity [4, 5]. Catalytic spectrophotometric methods are also used for sensitive spectrophotometric determination of V(V) [6]. However, these methods require extensive processing of the sample, maintaining specific concentration ratio of reagents and providing specific reaction conditions for good results. A modified method used by King and Garner [7] has been used for spectrophotometric redox speciation. The vanadium samples are initially analysed for total V(V) reducing strength. This is done by converting the sample to V(V)/V(IV) mixture by adding known excess of V(V) solution. Also, another aliquot of the sample is completely oxidized to V(V) by acidic KMnO_4 [8]. Redox interaction of V(V) with Fe(II) is known to be instantaneous in acidic aqueous medium and has been used to evaluate the V(V) concentration [9]. The same route but with the estimation of Fe(III) by the established spectrophotometric Fe(III)-

sulfosalicylate complex method [10] has been followed. The figures of merit has already been evaluated for the method [11]. The interference of V(IV) and Mn(II) on the method has been evaluated as these ions will be a part of the sample matrix. Direct spectrophotometric method for V(III)/(II) speciation based on thiocyanate complex formation is also explored.

Experimental

125 mM sodium metavanadate was electrolyzed in 750 mM formic acid medium using a two compartment electrolysis cell. Graphite felt was used as the cathode while stainless steel AISI 304 was used as the anode and the compartments were separated by a commercial anion exchange membrane. Constant current electrolysis with a current density of around 55 mA/cm² across the anion exchange membrane was used to electrolyze 550 ml of the solution. One of the two plates of the conductivity probe of the conductivity meter (TH-2300, El-Hamma Instruments) has been used to measure solution potential with respect to a Ag/AgCl, sat. KCl reference electrode with the help of a digital multimeter (81K-TRMS, MECO) connected to PC. The conductivity meter applies a high frequency of 1.13 kHz, 10 mV alternating voltage signal on the redox probe.

0.5 ml of sample was periodically collected at an interval of 30 minutes with a 5 ml liquid syringe and was mixed with an aliquot of stock V(V) solution (125 mM NaVO₃ in 750 mM HCOOH). The ratio of the mixture was varied from 1:1 to 1:3 and finally to 1:4 for the sample volume to initial stock volume respectively with the progressing stages of electrolysis. These variations in the composition were done when V(V) concentration in the mixture came down to 62.5 mM for the first two stages of electrolysis (as per the analysis). The mixture was initially diluted to 41.6 times with deaerated water in a 25 ml volumetric flask (0.6 ml of mixture taken) under inert atmosphere and then finally to another 25 times in a 1 cm path length spectrophotometric quartz cuvette of 12.5 ml volume (0.5 ml of diluted mixture taken) again under the inert atmosphere. 1 ml of 3 mM FeSO₄ stock solution in 50 mM H₂SO₄ was added to the cuvette. Finally, 5 ml of 2 M CH₃COOH and 1.1 M CH₃COONa buffer solution was added before adding 5 ml of 40 mM sulfosalicylic acid solution to the cuvette and making up the solution to 12.5 ml by adding water. The absorbance was measured at 465 nm.

Total vanadium concentration was separately determined by using 10 ml of 41.6 times diluted V(V)/V(IV) mixture. The mixture was converted to pure V(V) solution by drop wise addition of acidified KMnO₄ (5 mM KMnO₄ in

40 mM H₂SO₄ solution) at 80 °C until a stable purple color solution is obtained. The solution was made up to 20 ml after cooling and was analysed by ferric sulfosalicylic acid method as described above.

V(IV) formate was prepared by reducing NaVO₃ by hydrazine in formic acid medium [12]. It was mixed with initial stock V(V) solution (125 mM NaVO₃ in 750 mM HCOOH) in a molar ratio of 0.1 to 30. The resulting mixture was analysed by the above mentioned procedure to evaluate the V(IV) interference in the analysis. MnSO₄ was also mixed with stock V(V) solution in 0.1 to 30 molar ratio and the solution was analysed for the Mn²⁺ interference in the analysis process.

Direct spectrophotometric determination of V(III) and V(II) solutions has also been evaluated. This is explored to further simplify the analysis of these solutions. The V(III)/V(II) solution formed during the electrolysis was added to a solution of 0.5 M KSCN in 1 M HCl and the UV-visible spectra was recorded.

Results and discussion

(A) Evaluation of progress of electrolysis

The redox potential variation using the platinum electrode impressed with an alternating potential is shown in **Fig 1**. Segment I of the curve represents V(V)/V(IV) redox couple, segment II represents the V(IV)/V(III) redox couple while the segment III indicates the V(III)/V(II) redox couple. The redox potential measurement by the conventional setup has been unsuccessful as the polarization of the platinum redox electrode led to a non responsive readout after some time. The polarization of redox electrode could be ascertained by the receipt of proper response from the electrode upon its cleaning using aqua regia solution. Redox potential measurement using one of the two plates of the conductivity meter against a Ag/AgCl, sat. KCl has been explored to overcome the polarization of the redox probe. The application of high frequency alternating voltage on the electrode by the conductivity meter during the measurement could effectively overcome the polarization and hence the response for the entire range of electrolysis has been proper. The two pole conductivity meter applies frequency as per the conductivity of solution to avoid polarization. Combining the expression for concentration variation for flow cell under limiting current condition and Nernst equation, the variation in potential with respect to time can be given as:

$$E_{sol.} = E^{o'} - \frac{RT}{nF} \ln [e^{pt} - 1] \quad (1)$$

Where, E_{sol} is the redox potential of the solution, E° is the formal potential of the solution; R , T , n and F are the usual constants of the Nernst equation; t is the time of electrolysis and p is the cell factor which depends upon mass transfer rate, specific area and porosity of the electrode [13]. The redox potential variation has been fitted to

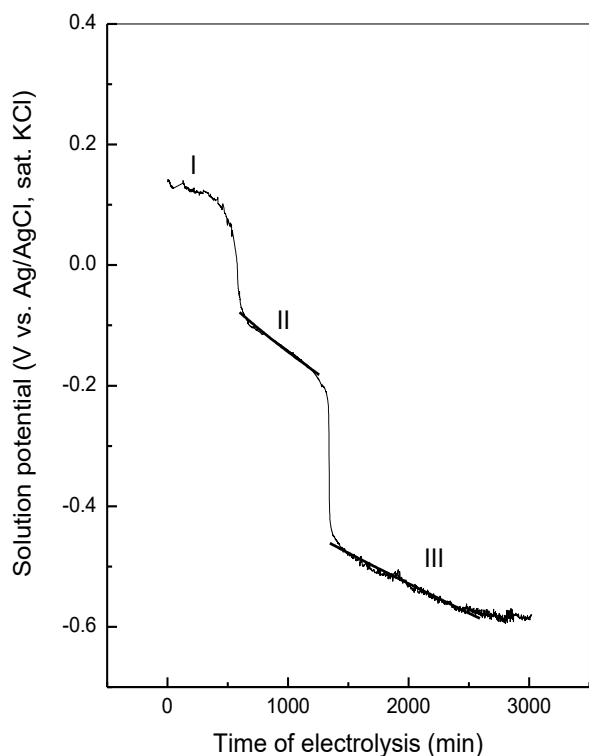


Fig 1: Redox potential variation of vanadium formate solution during electroreduction

equation (1) in three segments and a good fitting could be observed for all the three segments.

The cell factor value obtained by fitting the solution potential variation to equation (1) has been similar for the three segments with the values of 0.00162, 0.00207 and 0.00223 min^{-1} for segment I, II, and III respectively. The similar cell factor values indicate the proper progress of the controlled current electrolysis for the entire run.

(B) Spectrophotometric method for redox speciation of aqueous vanadium ions

The indirect spectrophotometric method for redox speciation of aqueous vanadium ions has been evolved on the basis of rapid redox reaction of V(V) with Fe(II) [9]. The resulting mixture has been analysed by the spectrophotometric determination of the resulting Fe(III) formed by the redox interaction of V(V) with Fe(II). The UV-visible spectrum of the Fe(III) sulfosalicylic acid

complex at pH 4.5 is shown in **Fig 2**. The absorption maximum (λ_{max}) for the complex was observed at 465 nm. The molar extinction coefficient obtained under the experimental conditions was determined to be $3740 \text{ dm}^3 \text{ mol}^{-1} \text{ cm}^{-1}$. This method has been selected for determination of iron as the known standard method of analyzing iron by using o-phenanthroline as the chromogenic agent could not be used in the present system. The Fe(III)/Fe(II)-o-phenanthroline complex has the standard reduction potential of +1.06 V vs. SHE which is higher than the redox potential of V(V)/V(IV) (1.0 V vs. SHE) system. Thus if o-phenanthroline is used for the analyzing the residual Fe(II), erroneous results will be obtained due to the oxidation of V(IV) by Fe(III)-o-phenanthroline in the solution. Such an interaction between Fe(III)-sulfosalicylic acid complex and V(V)/V(IV) solution is not observed.

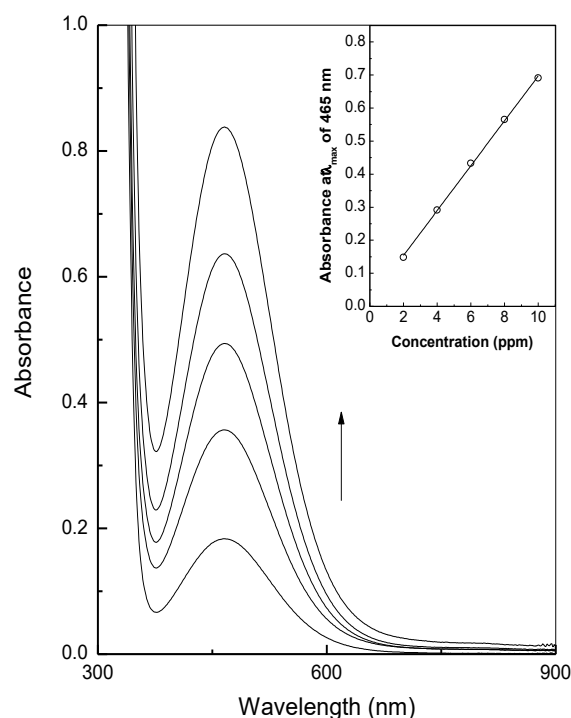


Fig 2: UV-visible spectrum of the ferric sulfosalicylic acid complex at pH 4.5

The analysis procedure was developed in a way where other chemicals are added to minimum extent in the system to avoid large matrix variations. Hence initial V(V) solution alone was used for oxidation of all vanadium solutions having different oxidation states which were formed during the course of electrolysis. The procedure was verified by the triplicate analysis of the known redox mixtures of vanadium formate which were prepared by mixing V(II) formate and V(V) formate. The results of the analysis are given in **Tables 1 and 2**.

Table 1: Results of analysis of V(III)-V(IV) mixture (triplicate analysis)

Mixture Taken V(III) + V(IV) (mM)	V(III) analysed (mM)	V(IV) analysed (mM)
5 + 5	4.9 ± 0.13	4.9 ± 0.11
10 + 10	10.01 ± 0.13	9.9 ± 0.06
5 + 10	4.95 ± 0.15	10.1 ± 0.05
10 + 5	9.9 ± 0.07	5.1 ± 0.14

Table 2: Results of analysis of V(II)-V(III) mixture (triplicate analysis)

Mixture Taken V(II) + V(III) (mM)	V(II) analysed (mM)	V(III) analysed (mM)
5 + 5	5.52 ± 0.29	5.1 ± 0.18
10 + 10	9.74 ± 0.04	10.2 ± 0.09
5 + 10	4.94 ± 0.38	10.1 ± 0.08
10 + 5	10.3 ± 0.02	5.1 ± 0.11

This method has been found to have no interference from the excess V(IV) in solution. Any change in absorbance values could not be seen even upon adding 10 mM concentration of V(IV) in the analysis solution which is about 50 times the concentration of the V(IV) normally expected in the analysis solution. Also, the interference from manganese (Mn²⁺) has also been checked. Any interference of Mn²⁺ in the Fe(III) sulfosalicylic acid spectrophotometric determination could not be observed.

Thus, this method could be used to assess the progress of electrolysis during the preparation of V(II) formate. The variation in concentration of the various aqueous vanadium redox species during the electrolysis of V(V) formate solution is shown in Fig 3. The change in concentration could be seen to closely follow the redox potential variation as shown in Fig 1. Thus, this indirect spectrophotometric method is a useful and rapid method of analyzing various redox mixtures of vanadium species in an aqueous medium.

(C) Direct spectrophotometric determination of aqueous V(III)/V(II) redox couple

Aqueous V(III) and V(II) ions have relatively sharp absorbance peaks as compared to V(IV) or V(V) and hence the direct spectrophotometric determination of these species has been evaluated. The spectral behaviour of V(II) and V(III) formate is shown in Fig 4. V(II) formate has shown two peaks, one at 562 nm and other at 843 nm

while V(III) formate has shown a peak at 591 nm and a hump around 420 nm. The calibration plot for these peak absorbance values is shown in Fig 5. The absorbance values have shown a good linear fitting with the slope of 0.00727 and 0.0854 for V(II) at 562 and 842 nm respectively while a slope of 0.03225 was obtained for V(III) at 591 nm. However, the peak positions for the two species are severely interfering at the peak of 562 nm for V(II) and the absorbance for the peak at 843 nm is too low. Thus, the

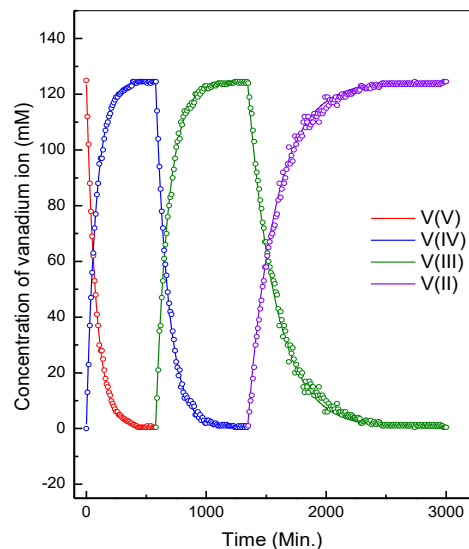


Fig 3: Variation in the concentration of various vanadium redox species during controlled current electroreduction of V(V)

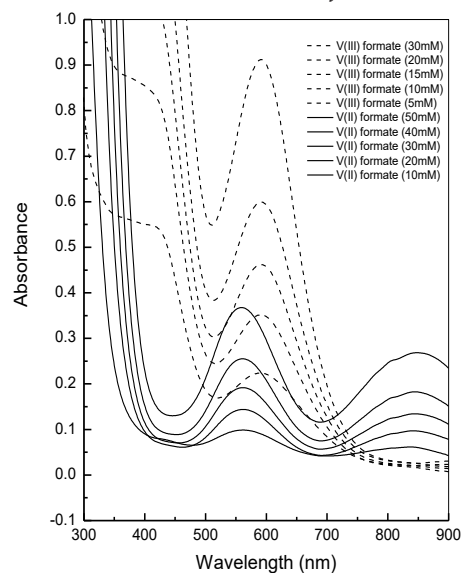


Fig 4: UV-visible spectra of V(II) and V(III) formate

determination of V(II) and V(III) as formate is not suitable for this concentration range. The spectral behaviour of V(II) and V(III) in thiocyanate medium is shown in Fig 6. The spectra was obtained in a high acidic medium wherein vanadium aliquot was added to the conc. HCl solution followed by KSCN addition to eliminate any

possibility of hydroxylation of V(III). Well separated peaks for V(II) and V(III) were obtained with V(II) SCN having a maxima at 724 nm while V(III) SCN having a maxima at 595 nm. A good linear behaviour was obtained for the two peaks as shown in Fig 5 for V(II) SCN at 595 nm and 724 nm respectively and at 595 nm and 724 nm for V(III) SCN respectively. The results of the analysis of known mixtures of V(II) and V(III) are given in Table 3. The requirement of maintaining an acidic condition leads to slight error in the determination of V(II) by this method as V(II) is partly oxidized in the high acidic medium.

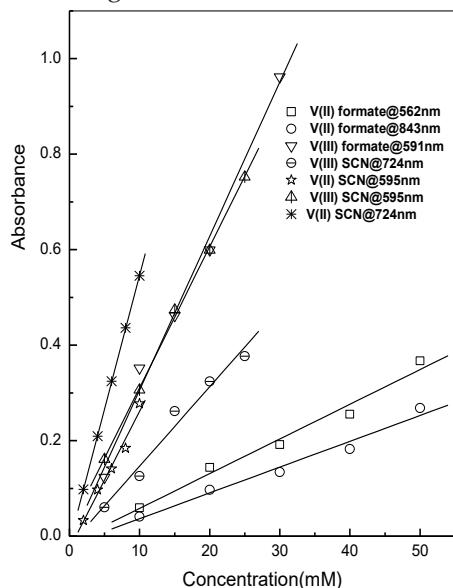


Fig 5: Calibration plots of various V(II) and V(III) species

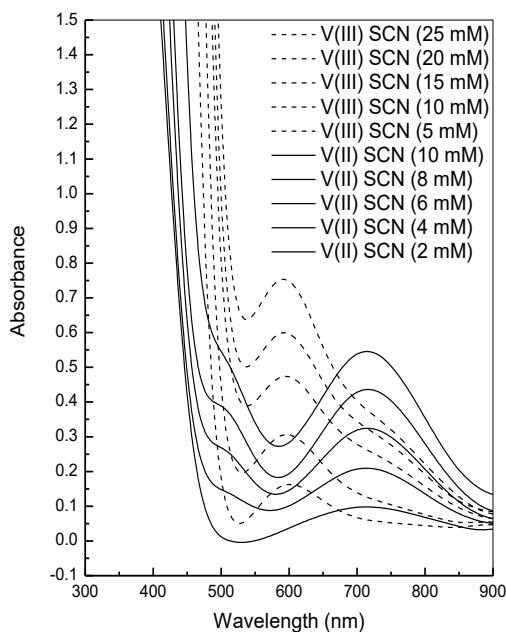


Fig 6: UV-visible spectra of V(II) and V(III) thiocyanate

Table 3: Results of analysis of V(II)-V(III) mixture (triplicate analysis)

Mixture Taken V(II) + V(III) (mM)	V(II) analysed (mM)	V(III) analysed (mM)
5 + 5	4.43 ± 0.59	5.51 ± 0.58
10 + 10	9.17 ± 1.04	10.14 ± 1.09
5 + 10	4.05 ± 1.49	10.61 ± 0.81
10 + 5	9.35 ± 1.02	5.43 ± 0.92

Conclusion

The on line monitoring methodology for electrolytic synthesis of low oxidation state of vanadium by solution potential monitoring with AC impressed probe has been developed. A simple and rapid redox speciation methodology for aqueous vanadium ions solutions of all possible oxidation states has been developed. It is an indirect spectrophotometric method based on the redox interaction of ferrous with V(V) and the subsequent analysis of the ferric sulfosalicylic acid complex. A direct spectrophotometric method for evaluating V(III)/V(II) mixture based on analyzing the thiocyanate complex has also been studied.

References

1. E. L. Martin and K. E. Bentley, *Anal. Chem.*, 34 (1962) 354.
2. C. J. Wood, *Progress in Nuclear Energy*, 23 (1990) 35.
3. M. J. C. Taylor and J. F. van Staden, *Analyst*, 119 (1994) 1263.
4. C. Agarwal, M. K. Deb, R. K. Mishra, *Analytical Letters*, 23 (1990) 2063.
5. S. A. Abbasi, *Analytical Letters*, 9 (1976) 113.
6. M. R. Shishehbore and R. Jokar, *Anal. Methods*, 3 (2011) 2815.
7. W. R. King, and C. S. Garner, *J. Phys. Chem.*, 58 (1954) 29.
8. C. L. Rulfs, J. J. Lagowski, and R. E. Bahor, *Anal. Chem.*, 28 (1956) 84.
9. H. Willard and P. Young, *Ind. Eng. Chem.*, 6 (1934) 48.
10. K. Ogawa and N. Tobe, *Bull. Chem. Soc. Japan*, 39 (1966) 223.
11. D. G. Karamanev, L. N. Nikolov, V. Mamatarikova, *Minerals Engineering*, 15 (2002) 341.
12. V. S. Tripathi, J. Manjanna, G. Venkateswaran, B. K. Gokhale and V. Balaji, *Ind. Eng. Chem. Res.*, 43 (2004) 5989.
13. A. J. Bard and L. R. Faulkner, *Electrochemical Methods Fundamentals and Applications: Second Edition*, John Wiley & Sons, Inc., 2001, pp 445.



Shri Kamalesh K. Bairwa, TO/C has joined the chemistry group, BARC after completion of CAT-1 training. He is working in the field of reactor chemistry. He is involved in the studies related with Pulsed electrodeposition of cobalt and nickel over aluminum brass surfaces separately, electrochemical synthesis of low oxidation state metal ion (LOMI), dissolution of frozen LiF-ThF₄ molten salt in various formulations and electrochemical corrosion evaluation of relevant structural materials in molten fluoride medium.



Dr. V. S. Tripathi has joined the chemistry group, BARC after graduating from the 45th batch of BARC training school. He is working in the field of reactor chemistry and radiation chemistry. He is involved in the field of development of decontamination formulations, evaluation of corrosion rates of relevant structural materials in the molten fluoride medium, evaluation of electrocatalytic hydrogen generation and radiolytic degradation of paints under different environments.

Advancing Green Hydrogen Revolution: A Comprehensive Review of Bifunctional Electrocatalysts and Hybrid Materials for Water Electrolysis

Naseem Kousar, Gouthami Patil, Lokesh Koodlur Sannegowda*

Department of Studies in Chemistry, Vijayanagara Sri Krishnadevaraya University, Vinayakanagara, Ballari-583105, Karnataka, India.

*Corresponding author E-mail: kslokesh@vskub.ac.in

Abstract:

As the world shifts towards sustainable energy solutions, hydrogen fuel has gained immense importance due to its high energy density and environmental benefits. However, the current production methods for hydrogen, including grey and blue hydrogen, are either carbon-intensive or rely on fossil fuels, while green hydrogen, produced via water electrolysis using renewable energy, is the most sustainable approach but faces efficiency and cost challenges. Electrochemical water splitting, involving the Oxygen Evolution Reaction (OER) and Hydrogen Evolution Reaction (HER), is a key method for green hydrogen production. Yet, the high energy barriers and requirement of expensive noble metal catalysts limit its scalability. To address these issues, research is focused on alternative catalyst materials such as alloys, oxides, phosphides, nanoparticles, polymers, and metal-organic frameworks (MOF), which can offer improved properties like high surface area, enhanced stability, and tuneable characteristics. This review examines recent progress in these advanced materials, their role in enhancing electrocatalytic performance, and their potential to overcome the limitations of traditional catalysts. It also explores future directions for developing efficient, cost-effective, and durable bifunctional catalysts, crucial for advancing hydrogen production and contributing to the broader goals of clean energy and sustainability.

Keywords: Water electrolysis; Nanoparticles; Polymers; Metal Organic Frameworks; Cell voltage; Tafel Slope; Overpotential.

1. Introduction

The global attempts to reduce the dependency on fossil fuels to eliminate the adverse impacts of increasing carbon emission has shifted the focus towards the sustainable energy systems¹. Hydrogen has emerged as an essential component in this shift due to its substantial energy density, abundance, and potential as a clean energy source. Due to its versatility in wide range of electrochemical applications, it can be used in an array of energy systems, from industrial processes to powering fuel cells². However, the key obstacle lies in producing hydrogen in an economically and ecologically friendly approach. Basically, hydrogen production methods are divided into three categories based on their environmental impact i.e., grey, blue, and green hydrogen. The most common method which is currently in use for the production of grey hydrogen is via steam reforming of natural gas, which not only uses an enormous amount of energy but discharges plenty of carbon dioxide. Blue hydrogen, which uses a similar method of production but offers carbon capture and storage, hence reduces emissions while continuing to depend on fossil fuels. Green hydrogen, on the other hand, is the most sustainable and promising option for

accelerating the transition to a carbon-neutral future. It is produced from splitting of water powered by renewable energy sources and it emits zero greenhouse gases³.

Considering the adverse ecological consequences of grey and blue hydrogen, there exist an urgent need to develop more sustainable methods to produce green hydrogen. In this regard, a number of cutting-edge methods, such as biological, thermochemical, photocatalytic, and electrochemical water splitting, have been investigated for the production of sustainable hydrogen. Enzymes or microbes are used as catalysts during biological operations like photosynthetic water splitting and microbial electrolysis. Even though these approaches are promising, but have negative aspects with respect to scalability, complexity of system, and reaction kinetics⁴. Thermochemical water splitting employs extreme temperatures from nuclear power plants or concentrators of solar energy to produce hydrogen, but it often requires costly large-scale tools and advanced materials that are capable of resisting harsh environments⁵. Due to its simplicity, the photocatalytic water splitting which utilises materials that absorb light and convert radiation directly into chemical energy, this approach holds tremendous

potential. It encounters difficulties related to charge separation, light absorption, optimised performance, inefficiency, and the photo-catalytic stability⁶. By taking into account the drawbacks of other green hydrogen production techniques, electrochemical water splitting which includes the Oxygen Evolution Reaction (OER) and the Hydrogen Evolution Reaction (HER) becomes the most viable and scalable approach. This method presents a direct route for the production of high-purity hydrogen by splitting water into hydrogen (H_2) and oxygen (O_2) molecules using a voltage source (Figure 1)⁷. Depending on the pH of electrolyte, HER and OER follow different reaction routes i.e., in acidic media, the HER involves the direct reduction of protons (H^+) to form H_2 gas, whereas in alkaline media, water molecule provide H^+ 's, releasing hydroxide ions (OH^-) alongside H_2 gas⁸. Similarly, the OER in acidic media involves the oxidation of water molecules to generate O_2 gas and H^+ 's, while in alkaline media, OH^- ions are oxidized to produce O_2 and water⁹. With its ability to store intermittent renewable energy as hydrogen fuel, while functioning with mild operating conditions without releasing greenhouse gases, the electrochemical water splitting is an attractive and efficient path for renewable energy schemes.

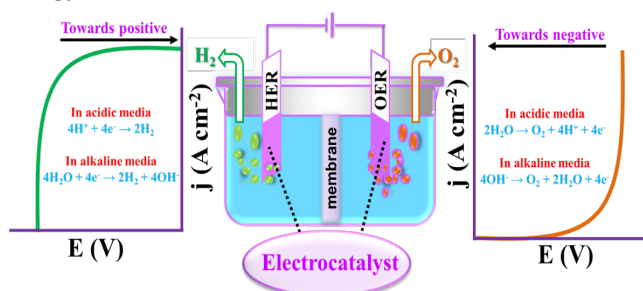


Figure 1. Graphical representation of water electrolysis.

Despite its benefits, the efficiency of electrochemical water splitting is severely limited by the high energy barrier because of the efficient configuration and hybridisation of water molecules. Therefore, the catalysts which have the ability to reduce the activation energy barrier and improve the efficiency and functionality of the water electrolyzer to attain effective HER and OER are crucial¹⁰. Currently, traditional noble metal catalysts, such as platinum for HER and iridium/ ruthenium oxide for OER, are effective but these catalysts face limitations in their large-scale production due to their high price, scarce supply, uni-functionality and limited stability over time¹¹. This has driven the research towards the development of alternative materials that are capable of addressing the challenges accompanied with the traditional catalysts. In the pursuit of efficient bifunctional electrocatalysts for electrochemical water splitting, researchers have explored

a range of alternatives, including nanoparticles, polymers, and Metal-Organic Frameworks (MOFs). Nanoparticles are known for their high surface areas and tuneable conductive properties, which enhance their catalytic performance¹². Polymers, on the other hand, offer cost-effectiveness and flexibility, making them suitable for electrochemical applications¹³. Similarly, MOFs are distinguished by their exceptionally adjustable porosity, high surface areas, and customizable metal centers, which contribute potentially towards electrocatalysis¹⁴. To highlight the potential of these alternative catalysts for sustainable water electrolysis, this review aims to comprehensively overview the recent advancements in bifunctional electrocatalysis. It focuses on the performance and potential of nanoparticles, polymers, and MOFs, with particular attention to MOF hybrids. By examining the state-of-the-art developments in these areas, this review offers valuable insights into the future directions for creating efficient, stable, and cost-effective electrocatalysts for sustainable hydrogen production.

2. Important parameters involved in the measurement of catalytic efficiency of electrocatalyst towards water electrolysis:

A number of important factors are taken into account when assessing the effectiveness and performance of electrocatalysts in water electrolysis. For the purpose of optimising the catalyst's design and use in hydrogen and oxygen evolution reactions, these parameters offer insights into the catalyst's catalytic activity, reaction kinetics, and long-term stability. The following are the primary parameters that are frequently used to evaluate the catalytic efficiency of electrocatalysts:

- Onset Potential: The potential at which the HER or OER is initiated by the catalyst.
- Overpotential: The excess potential needed to propel water electrolysis above and beyond the thermodynamic threshold. A more effective electrocatalyst is indicated by a lower overpotential.
- Tafel slope: The Tafel Slope indicates the rate-determining step by reflecting the reaction kinetics. Efficient catalysis and quicker reaction kinetics are indicated by a smaller Tafel slope.
- Current density: It is the measurement of current per unit area (A/cm^2) of the electrode. It is desirable to have higher current densities by taking into account the overpotential and mass transport constraints.
- Cell Voltage (also known as cell potential or applied potential): It is one of the crucial factors in water electrolysis, which represents the total energy

needed to split water into H_2 and O_2 . It represents the potential difference between the electrolyser's anode and cathode, which is usually greater than the thermodynamic minimum voltage required for water splitting (1.23 V under standard conditions) due to real-world inefficiencies.

- **Mass Transport:** This describes the flow of products (H_2 and O_2) and reactants (water, protons, etc.) to and from the electrode surface. Inadequate mass transport can lead to concentration gradients and bubble formation, which can impede performance, especially at high current densities.
- **Electrochemical Surface Area (ECSA):** It refers to the total active surface area of the catalyst available for the reaction. A larger ECSA results to the improved catalytic performance.

3. Advanced Electrocatalytic Materials for Electrochemical Water Splitting:

Researchers are increasingly focussing on advanced materials such as nanoparticles, polymers, and metal-organic frameworks (MOFs) in their quest to develop more efficient, stable, and cost-effective water splitting catalysts (Figure 2). Electrocatalysts that are capable of driving both OER and HER in a single system are needed for efficient bifunctional water splitting reactions. Nanoparticles, polymeric materials, and MOFs, along with their hybrid composites are optimised for catalytic activity, stability, and energy efficiency, opening the way for sustainable hydrogen production - a critical component of future energy solutions. This section discusses the latest developments in these materials and emphasises the way they could be used as dual-purpose electrocatalysts to produce hydrogen as well as oxygen.

3.1 Nanoparticles

Nanoparticles are prominent in electrocatalytic research due to their inherently high surface area-to-volume ratio, versatile electronic properties, and ability to enhance catalytic performance. Current investigations focus on mono-metallic, bi-metallic, and multi-metallic nanoparticles to develop efficient bifunctional electrocatalysts that exhibit superior activity, efficiency, and stability under demanding conditions. For instance, Wang et al. demonstrated that lithium-induced ultra-small $NiFeO_x$ nanoparticles are highly effective as bifunctional catalysts for overall water splitting in basic media. These nanoparticles achieved a cell potential of 1.51 V at 10 mA/cm² and found to be stable even after 200 hours of stability studies without degradation in a two-electrode configuration with 1.0 M KOH electrolyte

and, outperformed the benchmark iridium and platinum catalysts. The study explored the conversion reaction mechanism between lithium (Li) and transition metal oxides (TMOs), showing that the reaction ($MO + 2 Li^+ + 2 e^- \rightleftharpoons M + Li_2O$) involves the breaking of metal-oxygen (M-O) bonds and forming metal-metal (M-M) and lithium-oxygen (Li-O) bonds. Lithium extraction and reforming of MO resulted in significantly smaller particles with nanometer diameters which greatly increased the surface area of TMOs¹⁵. In a similar vein, Wang and colleagues presented 2D nano-meshes and 3D microflower structures of Mo_2CT_x , created through the design of novel Mo/Zn bimetal imidazole frameworks (Mo/Zn BIFs) and subsequent pyrolysis. These electrocatalysts exhibited outstanding performance for HER, OER, and overall hydrolysis processes. The 2D Mo_2CT_x nano-mesh achieved high efficiency for OER with a current density of 10 mA/cm² at a low overpotential of 180 mV, while the 3D microflower Mo_2CT_x demonstrated superior activity for HER, reaching 10 mA/cm² at an overpotential of 140 mV. Furthermore, the Mo_2CT_x microflower catalyzed overall water splitting, achieving a current density of 10 mA/cm² at a low voltage of 1.7 V in a two-electrode test system. Mo LIII-edge X-ray near-edge absorption (XANES) studies and theoretical calculations indicate that surface-terminated oxygen enhances OER performance, while the positioning of Mo atoms on the surface is crucial for optimizing HER performance, suggesting that surface chemical modifications and multiscale structure design are effective strategies for advanced catalyst engineering¹⁶.

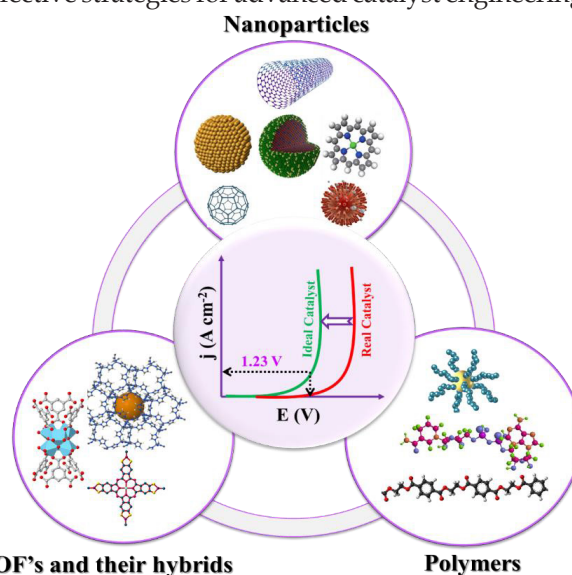


Figure 2. Graphical representation of various innovative materials for water electrolysis.

Additionally, Xie et al. introduced a novel N-anion-decorated Ni_3S_2 material, synthesized via a straightforward

one-step calcination process, showing exceptional performance as a bifunctional electrocatalyst for both OER and HER. The incorporation of N anions improved the morphology, electronic structure, and surface activity of Ni_3S_2 , leading to enhanced electrical conductivity, optimal HER Gibbs free energy, and better water adsorption energy. The N- Ni_3S_2 /NF 3D electrode achieved low overpotentials of 330 mV for OER and 110 mV for HER, with current densities of 100 and 10 mA/cm², respectively, in 1.0 M KOH. Additionally, a water-splitting device using this electrode achieved 10 mA/cm² at a low cell voltage of 1.48 V, indicating promising approach in the development of advanced bifunctional catalysts for water splitting¹⁷. Likewise, Shu-Hong Yu utilized carbon fiber paper (CFP) as a catalyst substrate, for the electrodeposition followed by annealing to produce ternary $\text{Ni}_{0.1}\text{Co}_{0.9}\text{P}$ nanosheets with a highly porous structure. These nanosheets exhibited remarkable activity and stability for both HER and OER in neutral water under mild conditions. The CFP-supported $\text{Ni}_{0.1}\text{Co}_{0.9}\text{P}$ catalyst in neutral-pH water electrolysis cell enabled the device to achieve a current density of 10 mA/cm² with a voltage of just 1.81 V, making it one of the most efficient noble-metal-free neutral pH electrolyzers to date¹⁸. Despite the benefits of nanoparticles, they face several challenges in bifunctional water electrocatalysis, including issues such as aggregation, instability under harsh conditions, and limited interaction with electrolytes. These challenges are compounded by the tendency of nanoparticles to lose their active surface area over time.

3.2 Polymeric Materials

Polymeric materials offer significant advantages over nanoparticles in addressing common challenges in electrocatalysis, such as aggregation and instability. Their tuneable properties, ease of processing, and potential for scalability make them a promising platform for advancing water splitting technologies. Ongoing research focuses on optimizing these materials to enhance their performance and stability in practical applications. Transition metal nitrides have emerged as highly effective bifunctional electrocatalysts for both HER and OER. The integration of nitrogen-containing conductive polymers, such as polyaniline (PANI), facilitates the formation of transition metal nitrides without the need for hazardous ammonia gas. For instance, Song et al. developed a cobalt nitride-vanadium oxynitride nanohybrid derived from PANI on carbon cloth (CVN/CC). This catalyst exhibited remarkable bifunctional activity with overpotentials of -118 mV for HER and 263 mV for OER at a current density of 10 mA/cm². The CVN/CC catalyst-based device achieves a cell voltage of 1.64 V for water splitting, comparable to commercial $\text{RuO}_2/\text{CC}/\text{Pt-C}/\text{CC}$ electrolyzers,

and maintains about 90% of its initial activity after 100 hours. The N-doped carbon layers, resulting from PANI, enhanced the electron and charge transport throughout the catalyst system¹⁹.

Likewise, Xu et al. synthesized a hydrogel by polymerizing pyrrole and tetrakis(4-carboxyphenyl) porphyrin iron ($\text{Fe}^{\text{III}}\text{TCP}$) to form PPy/ FeT CP. Co^{2+} ions were adsorbed onto this hydrogel and pyrolyzed to yield PPy/ FeT CP/Co. This catalyst achieved an OER current density of 10 mA/cm² at 1.61 V versus RHE, which is competitive with RuO_2 nanoparticles, and demonstrated superior HER activity with an overpotential of 0.24 V at 10 mA/cm². Tafel slope measurements indicated that the HER followed the Volmer-Heyrovsky mechanism. The self-powered system efficiently decomposed water at room temperature with H_2 and O_2 production rates of 280 and 140 $\mu\text{mol h}^{-1}$, respectively²⁰. Similarly, Jun et al. developed nickel-cobalt nitride heterostructures on carbon cloth (NCN/CC) through a three-step synthetic approach. This catalyst showed low overpotentials of 68 mV for HER and 247 mV for OER at a current density of 10 mA/cm² in 1 M KOH. It delivered a cell voltage of 1.56 V for overall water splitting, surpassing the performance of Pt-C/CC// RuO_2 /CC electrolyzers, and retained nearly 93% of its initial current density after 240 hours. The NCN/CC catalyst also demonstrated excellent activity in acidic media. The incorporation of PANI in the synthesis aids in the environmental friendly production of nitrides, while N-doped carbon improved conductivity and stability. The large surface area of the one-dimensional nanoglass structures facilitated efficient electron and charge transport, and the bimetallic nitrides enhance water splitting efficiency²¹.

Jin-Tao Ren et al. developed 3D hybrid structures comprising FeNi nanoalloys embedded in N-doped bamboo-like carbon nanotubes and 2D N-doped carbon nanosheets ($\text{FeNi@N-CNT}/\text{NCSs}$). This material, derived from a polyaniline layer with $\text{Fe}^{3+}/\text{Ni}^{2+}$ salts-coated graphitic carbon nitride, exhibited high bifunctional activity with low overpotentials of 310 mV for OER and 203 mV for HER. It achieved a current density of 10 mA/cm² for overall water splitting at cell voltage of 1.72 V and, maintained stability during extended operation. The N-doped carbon-coated FeNi nanoalloys enhanced mass diffusion and electron conductivity, demonstrating performance comparable to noble-metal-based standards²². Despite their numerous benefits, polymeric materials have some drawbacks in electrocatalysis. One of the main obstacles is that many polymers are less electrically conductive than metals or metal oxides, which can reduce their effectiveness as electrocatalysts. Concerns about

stability also surface because the polymers may deteriorate in severe electrochemical environments, resulting in decreased functionality and shortened lifetimes. Polymeric materials synthesis and processing can also be expensive and complex, requiring exact control for achieving ideal results and scalability. Additionally, the total catalytic activity of these materials may be reduced by the lack of or restricted access to active sites. Finally, it can be difficult to achieve reproducibility across batches due to differences in polymer characteristics or synthesis techniques, which could result in inconsistent performance.

3.3 Metal Organic Frameworks and their hybrids

Metal-organic frameworks (MOFs) have emerged as promising alternatives to polymeric materials in the realm of water electrolysis, effectively addressing several of the limitations arising with nanoparticles and polymeric materials. MOFs offer distinct advantages due to their highly tuneable porosity, large surface area, and versatile composition, which enable the engineering of porous frameworks tailored for catalytic applications. These frameworks are constructed from metal ions or clusters coordinated by organic ligands, resulting in a crystalline network that facilitates effective reactant and product interactions, crucial for efficient catalysis. However, despite their structural benefits, MOFs often exhibit limited electrical conductivity, a critical drawback that impedes their performance as standalone electrocatalysts. The low conductivity stems from the insulating nature of the organic linkers and the lack of efficient electron transport pathways within the MOF structure. This intrinsic limitation reduces the overall catalytic activity of MOFs. To overcome these issues, researchers have developed hybrid composites that integrate MOFs with various conductive materials. These hybrids combine the advantageous structural features of MOFs with the enhanced electrical conductivity provided by substances such as carbon-based materials, metals, or conductive polymers.

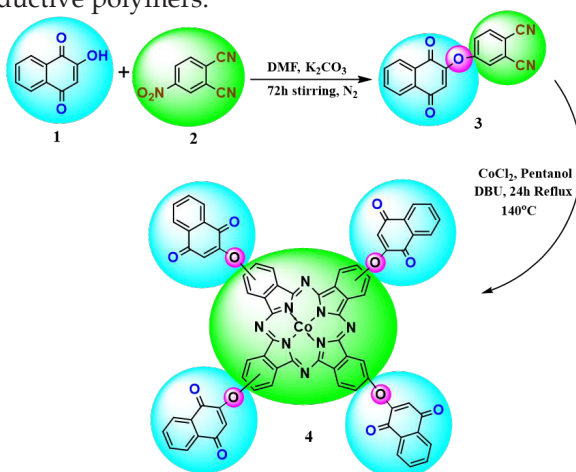


Figure 3. Synthetic route for the preparation of quinone substituted cobalt (II) phthalocyanine (HQCoPc) complex.

For instance, Giddaerappa et al. synthesized cobalt (II) phthalocyanine electrocatalyst bearing quinone groups at the periphery (HQCoPc) (Figure 3). To enhance its catalytic properties, they developed a hybrid composite by integrating HQCoPc with conductive Ketjen Black (KB). The resulting HQCoPc+KB material exhibited outstanding electrocatalytic activity for both HER and OER. It achieved an onset potential of -76 mV for HER and overpotentials of -234 mV and 360 mV at a current density of 10 mA/cm² for HER (0.5 M H_2SO_4) and OER (1.0 M KOH), respectively, with lower Tafel slopes, higher ECSA and exceptional stability, maintaining performance over $40,000$ seconds at varying current densities (Figure 4). The hybrid's high activity for HER and OER is attributed to the electroactive cobalt ions and the conductive carbon nanoparticles in KB, which promote both inter- and intra-molecular transitions, resulting in an increased number of electroactive sites. The porous structure of KB supports the HQCoPc framework by preventing aggregation, which helps to preserve the availability of active sites. Additionally, the synergy between KB and HQCoPc enhances the catalyst's stability on the electrode surface. KB also modulates the electronic properties of HQCoPc, potentially altering its electronic structure, leading to faster charge transfer and more favorable energetics. The quinone groups attached to HQCoPc contribute to these effects by serving as redox-active centers that facilitate electron transfer during catalysis. When integrated into the CoPc structure, these quinone groups provide extra sites for redox activity, boosting electron transfer at the electrode-electrolyte interface and enhancing overall catalytic efficiency. Moreover, these quinone groups increase the number of available active sites for reactions like HER and OER by improving the adsorption and activation of reactant molecules, such as protons for HER and water molecules for OER, ultimately leading to superior catalytic performance in both the processes²³.

Similarly, Ye and colleagues developed a bifunctional electrocatalyst by coating Fe- H_2 BDC MOF nanosheets over Pt quantum dot cores on nickel foam (NF). This Pt QDs @Fe-MOF hybrid exhibited outstanding HER and OER performance in 1.0 M KOH, with overpotentials of 33 mV and 144 mV, respectively, and a total water-splitting voltage of 1.47 V at 10 mA/cm², maintaining stability for over 100 hours²⁴. Jahan et al. prepared a Cu-MOF hybrid composite with graphene oxide (GO), achieving notable catalytic activity with overpotentials of -0.209 V for HER and 1.34 V for OER in 0.5 M H_2SO_4 , benefiting from the enhanced charge transfer facilitated by GO²⁵. Furthermore, the Jeong

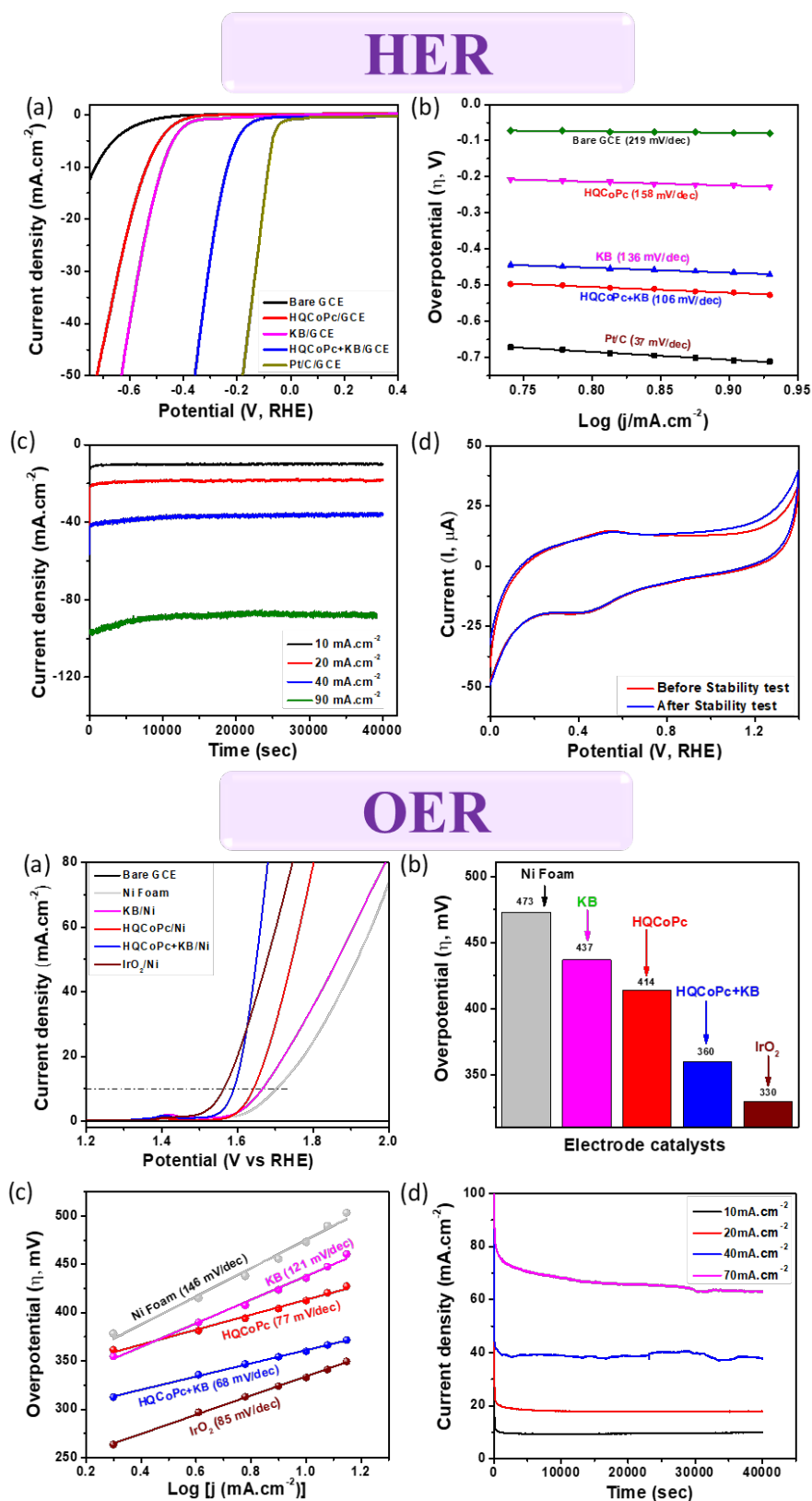


Figure 4. Electrocatalytic activity performance of HQCoPc and its hybrid with KB towards HER and OER.

group developed a NiCoP nanoneedle array on Ti₃C₂T_x MXene-coated Ni foam (NCP-MX/NF), which showed low overpotentials of -72 mV for HER and 303 mV for OER, and superior overall water-splitting performance with a cell voltage of 1.54 V at 10 mA/cm² in alkaline media. The integration of MXene significantly improved electron transfer and stability, demonstrating the effective synergy between MOFs and conducting materials in advancing water splitting technologies²⁶. Table 1 summarizes different bifunctional electrocatalysts towards water electrolysis.

4. Conclusion and Future Perspective

With an emphasis on nanoparticles, polymers, and metal-organic frameworks (MOFs) as viable substitutes for conventional noble metal catalysts, this review outlines the developments in bifunctional electrocatalysis for the production of sustainable hydrogen. Even though traditional catalysts like platinum and iridium oxide have high efficiencies, their high prices, scarcity, single function, and short-term stability make the development of more affordable and sustainable alternatives necessary. The challenges associated with traditional catalysts can be potentially addressed by MOFs with metal centres and adjustable porosity, polymers with scalable and customisable structures, and nanoparticles with high surface area and tuneable electronic properties. Significant advancements in improving the stability, efficiency, and bifunctionality of electrocatalysts for electrochemical water splitting have been shown by the investigation of these materials. These cutting-edge materials do, however, still have issues with aggregation, structural instability, and limited catalytic durability in challenging operating

Table 1: Summary of various bifunctional electrocatalysts towards water electrolysis

Catalyst	Electrolyte	η of HER (mV) @ 10 (mA/cm ²)	η of OER (mV) @ 10 (mA/cm ²)	Voltage (V)@ 10 (mA/cm ²)	Ref
Co ₃ O ₄ nanorods	1.0 mol/L KOH	260	275	1.72	27
Cu-CoP	1.0 mol/L PBS	81	411	1.72	28
Ni ₃ S ₂ /NF	1.0 mol/L NaOH	223	260	1.76	29
CoMoNiS-NF	1.0 mol/L KOH	113	166	1.54	30
	0.5 mol/L H ₂ SO ₄	105	2555	1.45	
	1 mol/L PBS	117	405	1.80	
UTBrImPc+MWCNT	0.5 mol/L H ₂ SO ₄	15	202	--	31
	1.0 mol/L KOH				
V-CoP@a- CeO ₂	1.0 mol/L KOH	68	225	1.56	32
CoMnCH/NF	1.0 mol/L KOH	180	294 (30mAcm ⁻²)	1.68	33
Mo-Co ₉ S ₈	0.5 mol/L H ₂ SO ₄	98	370	1.68	34
	1.0 mol/L KOH	113	200	1.56	

environments. In order to move these materials from laboratory-scale research to real-world, large-scale applications, these issues must be resolved.

In order to progress the development of bifunctional electrocatalysts for sustainable hydrogen production, a number of important areas should be given priority. Initially, more investigation is required to maximise the longevity and stability of catalysts based on MOFs, polymers, and nanoparticles, particularly when operating for extended periods of time. The development of hybrid materials, doping schemes, and sophisticated surface modification techniques could help get around the present constraints caused by structural instability and aggregation. Secondly, by predicting ideal compositions and structures and eliminating the need for complicated trial-and-error testing, combining computational modelling and machine learning techniques could accelerate the discovery of new materials. Thirdly, the emphasis should be on increasing the synthesis of these innovative substances while preserving their affordability and environmental sustainability. Lastly, investigating the synergistic effects between various materials, for example, mixing conductive polymers and nanoparticles or adding MOFs to hybrid composites may result in the development of novel catalysts with improved performance. By focussing on these areas, future research can help create electrocatalysts that are stable, effective, and economically feasible. This

will facilitate the global shift towards sustainable energy and open doors for the widespread adoption of green hydrogen production technologies.




Acknowledgements

Authors would like to acknowledge DST-SERB, Govt. of India grant no. DST-FIST (SR/FST/CSI-003/2016), India-Uzbekistan Collaborative Grant (no. INT/Uzbek/P-21), VGST-KFIST grant no. KSTePS/VGST-KFIST (L1)/2017/267 (GRD no.555). N.K. is indebted to KSTePS, DST, Govt. of Karnataka for the financial assistance. G.P. acknowledges DST, Govt. of India for the Inspire fellowship.

References:

1. N. Healy, Jessica Debski, *Local Environment*, **2017**, 22(6), 699-724. DOI: <https://doi.org/10.1080/13549839.2016.1256382>
2. N. Sazali, *International Journal of Hydrogen Energy*, **2020**, 45(38), 18753-18771. DOI: <https://doi.org/10.1016/j.ijhydene.2020.05.021>.
3. M.Newborough, G. Cooley, *Fuel Cells Bulletin*, **2020**, 2020(11), 16-22. DOI: [https://doi.org/10.1016/S1464-2859\(20\)30546-0](https://doi.org/10.1016/S1464-2859(20)30546-0)
4. G. Mahidhara, H.Burrow, C.Sasikala, C. V. Ramana, *World Journal of Microbiology and Biotechnology*, 2019, 35(8), 116. DOI: <https://doi.org/10.1007/s11274-019-2692-z>
5. S.Abanades, P.Charvin, G.Flamant, P. Neveu, *Energy*, **2006**, 31(14), 2805-2822. DOI: <https://doi.org/10.1016/j.energy.2005.11.002>
6. S.Nishioka, F. E.Osterloh, X.Wang, T. E.Mallouk, K.Maeda,

- Nature Reviews Methods Primers*, **2023**, 3(1), 42. DOI: <https://doi.org/10.1038/s43586-023-00226-x>
7. N.Kousar, L. K. Sannegowda, *International Journal of Hydrogen Energy*, **2024**, 50, 37-47. DOI: <https://doi.org/10.1016/j.ijhydene.2023.06.296>
 8. H.Tan, B.Tang, Y.Lu, Q.Ji, L.Lv, H.Duan, W. Yan, *Nature Communications*, **2022**, 13(1), 2024. DOI: <https://doi.org/10.1038/s41467-022-29710-w>
 9. G.Patil, S.Daniel, L. K. Sannegowda, *Chemistry–A European Journal*, **2024**, 30(51), e202401759. DOI: <https://doi.org/10.1002/chem.202401759>
 10. H.Sun, X.Xu, H.Kim, W.Jung, W.Zhou, Z.Shao, *Energy & Environmental Materials*, **2023**, 6(5), e12441. DOI: <https://doi.org/10.1002/eem2.12441>
 11. N.Kousar, S.Kumar, M.Hojamberdiev, L. K. Sannegowda, *Electrochimica Acta*, **2024**, 475, 143575. DOI: <https://doi.org/10.1016/j.electacta.2023.143575>
 12. N.Narayan, A.Meiyazhagan, R. Vajtai, *Materials*, **2019**, 12(21), 3602. DOI: <https://doi.org/10.3390/ma12213602>
 13. Q.Zhou, G. Shi, *Journal of the American Chemical Society*, **2016**, 138(9), 2868-2876. DOI: <https://doi.org/10.1021/jacs.5b12474>
 14. C.Li, H.Zhang, M.Liu, F. F.Lang, J.Pang, X. H.Bu, *Industrial Chemistry & Materials*, **2023**, 1(1), 9-38. DOI: <https://doi.org/10.1039/D2IM00063F>
 15. H.Wang, H. W.Lee, Y.Deng, Z.Lu, P. C.Hsu, Y.Liu, Y.Cui, *Nature communications*, **2015**, 6(1), 7261. DOI: <https://doi.org/10.1038/ncomms8261>
 16. Z. Kou, L. Zhang, Y. Ma, X. Liu, W. Zang, J. Zhang, S. Huang, Y. Du, A. K. Cheetham and J. Wang, *Applied Catalysis B Environment and Energy*, **2019**, 243, 678–685. DOI: <https://doi.org/10.1016/j.apcatb.2018.11.008>
 17. P.Chen, T.Zhou, M.Zhang, Y.Tong, C.Zhong, N.Zhang, Y. Xie, *Advanced Materials*, **2017**, 29(30), 1701584. DOI: <https://doi.org/10.1002/adma.201701584>
 18. R.Wu, B.Xiao, Q.Gao, Y. R.Zheng, X. S.Zheng, J. F.Zhu, S. H.Yu, *Angewandte Chemie*, **2018**, 130(47), 15671-15675. DOI: <https://doi.org/10.1002/ange.201808929>
 19. S.Dutta, A.Indra, Y.Feng, H.Han, T. Song, *Applied Catalysis B: Environmental*, **2019**, 241, 521-527. DOI: <https://doi.org/10.1016/j.apcatb.2018.09.061>
 20. J.Yang, X.Wang, B.Li, L. Ma, L. Shi, Y. Xiong, H. Xu, *Advanced Functional Materials*, **2017**, 27(17), 1606497. DOI: <https://doi.org/10.1002/adfm.201606497>
 21. C.Ray, S. C.Lee, B.Jin, A.Kundu, J. H.Park, S. C. Jun, *Journal of Materials Chemistry A*, **2018**, 6(10), 4466-4476. DOI: <https://doi.org/10.1039/C7TA10933D>
 22. J. T.Ren, L.Chen, Y. S.Wang, W. W.Tian, L. J.Gao, Z. Y. Yuan, *ACS Sustainable Chemistry & Engineering*, **2019**, 8(1), 223-237. DOI: <https://doi.org/10.1021/acssuschemeng.9b05238>
 23. Giddaerappa, N. Kousar, U. Deshpande, L. K. Sannegowda, *Energy & Fuels*, **2024**, 38(9), 8249-8261. DOI: <https://doi.org/10.1021/acs.energyfuels.4c00037>
 24. B.Ye, R.Jiang, Z.Yu, Y.Hou, J.Huang, B.Zhang, R. Zhang, *Journal of Catalysis*, **2019**, 380, 307-317. DOI: <https://doi.org/10.1016/j.jcat.2019.09.038>
 25. M. Jahan, Z. Liu, K. P. Loh, *Advanced Functional Materials*, **2013**, 23(43), 5363–5372. DOI: <https://doi.org/10.1002/adfm.201300510>
 26. M. Jeong, S. Park, T. Kwon, M. Kwon, S. Yuk, S. Kim, C. Yeon, C.-W. Lee, D. Lee, *ACS Applied Materials & Interfaces*, **2024**, 16(27), 34798–34808. DOI: <https://doi.org/10.1021/acsaami.4c00798>
 27. G. Cheng, T. Kou, J. Zhang, C. Si, H. Gao, Z. Zhang, *Nano Energy*, **2017**, 38, 155–166. DOI: <https://doi.org/10.1016/j.nanoen.2017.05.043>
 28. L. Yan, B. Zhang, J. Zhu, Y. Li, P. Tsiakaras, P. K. Shen, *Applied Catalysis B Environment and Energy*, **2020**, 265, 118555. DOI: <https://doi.org/10.1016/j.apcatb.2019.118555>
 29. L.-L. Feng, G. Yu, Y. Wu, G.-D. Li, H. Li, Y. Sun, T. Asefa, W. Chen, X. Zou, *Journal of the American Chemical Society*, **2015**, 137(44), 14023–14026. DOI: <https://doi.org/10.1021/jacs.5b08186>
 30. Q. Liang, H. Jin, Z. Wang, Y. Xiong, S. Yuan, X. Zeng, D. He, S. Mu, *Nano Energy*, **2019**, 57, 746–752. DOI: <https://doi.org/10.1016/j.nanoen.2018.12.060>
 31. Giddaerappa, K. P. C. H. Puttaningaiah, S. Aralekallu, Shantharaja, N. Kousar, A. C. Kumbara, L. K. Sannegowda, *ACS Applied Nano Materials*, **2023**, 6(10), 8880–8893. DOI: <https://doi.org/10.1021/acsanm.3c01328>
 32. L.Yang, R.Liu, L.Jiao, *Advanced Functional Materials*, **2020**, 30(14), 1909618. DOI: <https://doi.org/10.1002/adfm.201909618>
 33. T. Tang, W.-J. Jiang, S. Niu, N. Liu, H. Luo, Y.-Y. Chen, S.-F. Jin, F. Gao, L.-J. Wan, J.-S. Hu, *Journal of the American Chemical Society*, **2017**, 139(24), 8320–8328. DOI: <https://doi.org/10.1021/jacs.7b03507>
 34. L.Wang, X.Duan, X.Liu, J.Gu, R.Si, Y.Qiu, J.Sun, *Advanced Energy Materials*, **2020**, 10(4), 1903137. DOI: <https://doi.org/10.1002/aenm.201903137>
- Authors Biographies:

	<p>Naseem Kousar completed her Master's degree in Chemistry at the University of Mysore. Currently, she is a Ph.D. candidate at Vijayanagara Sri Krishnadevaraya University, Ballari, under the guidance of Prof. K. S. Lokesh. Her doctoral research is focused on the design and development of macrocyclic redox-active molecules, with an emphasis on their applications in sustainable and clean energy technologies. Her work aims to address critical challenges in energy storage and conversion, contributing to advancements in the field. She has received several awards, including the DST Fellowship from the Government of Karnataka, the Young Scientist Award from the Indian Academy of Physical Sciences in Prayagraj, and the Research Award of Excellence from VOICE, India.</p>
	<p>Gouthami Patil completed her Master's degree in Chemistry at the Vijayanagara Sri Krishnadevaraya University, Ballari, graduating with first rank. Currently, she is advancing her research as a Ph.D. candidate at the same university, under the supervision of Prof. K. S. Lokesh. Her doctoral research is concentrated on the design and development of bio-inspired redox-active molecules, focusing particularly on their electrochemical applications. Her work aims to innovate within the field by exploring new avenues for redox chemistry. Gouthami has been awarded the DST Inspire Fellowship award.</p>
	<p>Lokesh Koodlur Sannegowda completed his Masters degree with First Rank and Ph.D degree from University of Mysore, Mysore. His research interest includes novel N4 macrocycles for electrochemical applications like sensing, water electrolyser, fuel cell, batteries and supercapacitors. He worked as Postdoctoral fellow at IISc, Bangalore; University Joseph Fourier, France; Ghent University, Belgium; Shinshu University, Japan. He joined Vijayanagara Sri Krishnadevaraya University as Associate Professor in Chemistry in 2012 and was promoted as Professor in 2015. He has been awarded with TWAS Visiting Fellow to visit China, Sir C.V. Raman Young Scientist award and Best Publication award from Karnataka Govt, India. He has also been adjudged as best faculty of VSK university in 2015 and 2017. He has received research grants from DST, CSIR, UGC-DAE, VGST (Karnataka Govt), KSTA (Karnataka Govt) of worth more than Rs, 200 lakhs. He was awarded the Indo-Uzbekistan joint project in the field of hydrogen energy by DST. He has published more than 110 publications and has 02 patents to his credit. He has guided 11 students for PhD and 6 are working. His h-index is 31 and i10 index is 72.</p>

Fabrication of a voltammetrically effective Vanillin sensor at a ZnO-modified carbon paste electrode: A cyclic voltammetric study

G.S. Sumanth, B.E. Kumara Swamy*, K. Chetankumar

Department of P.G Studies and Research in Industrial Chemistry, Kuvempu University,
Jnanasahyadri, Shankaraghatta -577451, Shivamogga (D), Karnataka, India

Abstract

Vanilla is widely used, yet this has detrimental effects on health. The use of vanillin (VAN) in infant food is restricted by the Federal Office of Public Health. Therefore, the goal was to develop a sensor that would enable the rapid identification of VAN in food essence, non-alcoholic drinks, and medication formulations. By combining zinc oxide nanoparticles (ZnO Nps) with carbon paste, a modified electrode was created and tested using cyclic voltammetry methods. At a physiological pH of 7.4, to analyse vanillin (VAN), a zinc oxide modified carbon paste electrode (ZnO/MCPE) was used. The ZnO nanoparticle was fabricated by simple coprecipitation method. Utilising SEM and X-ray diffraction (XRD), the surface topography and particle size of ZnO Nps were evaluated. ZnO/MCPE had a superior electrochemical response as compared to bare carbon paste electrode BCPE as determined by the cyclic voltammetry (CV) method for the individual and simultaneous detection of VAN and mycophenolate mofetil (MMF). The VAN's limit of detection (LOD) was observed to be 0.49 μM under optimised conditions. ZnO/MCPE also exhibits excellent selectivity and an efficient method for studying VAN in practical samples with sustainable recovery of 97.4-99.2%.

Keywords: Cyclic voltammetry, Electrochemical sensor, Chemical coprecipitation, ZnO Nanoparticle, Carbon paste electrode, Vanillin

Introduction

Naturally derived from vanilla beans, vanillin (VAN) (4-hydroxy-3-methoxybenzaldehyde) is amongst the most commonly recognised scent/flavouring ingredients [1,2]. Most often it is used as an aromatic in air fresheners, candles, scents, makeup, and incense [3-5]. The human brain demonstrates a high level of VAN receptivity. It is also frequently used to flavour cuisine, drinks, candies, and medications [4,6]. Additionally, One of VAN's health advantages is that it lowers the chance of dying from heart disease and sickle cell anemia as it acts as an antisickling agent [7]. Application of VAN as an anticarcinogenic agent are also being investigated by mainstream scientific research to address various malignant tumours [8]. According to a study conducted on MRI patients, the smell of vanilla helps patients feel less anxious by almost 68% subjects. VAN is well recognized to arouse our senses, induce excitement, and improve our mood [9].

On the other hand, excessive consumption of VAN can harm the kidneys and liver and result in negative health effects such nausea, headaches, skin irritation, and vomiting [10-12]. As a result, the FDA established a regulation stating that edible goods should contain no more than 70 mg/kg of VAN [13]. Premium natural vanillin is becoming more and more in demand as worries about food safety emerge, even though synthetic VAN is widely available and reasonably priced. As a result, it is crucial

to develop and promote a possible method for the quick, accurate, and cost-effective determination of VAN quantity in food products in order to ensure food safety and quality.

The quantification of VAN has been done using a variety of analytical techniques such as capillary electrophoresis [2], chemiluminescence [14], liquid chromatography-mass spectrometry [15], High performance liquid chromatography [16]. Though several assay methods have been evaluated, as there are multiple steps involved in the complex pretreatment processes, these operations are usually time-consuming and require higher level of skill thus making the analysis a costly one. Electrochemical sensors provide benefits over alternative techniques and because VAN is electroactive, it can be detected by suitable electrochemical sensor.

The electrochemical sensor's applications and attention have expanded recently due to the link between biology and nanoscience. Among these, ZnO nanoparticles (Nps) are widely used in several industries from electronics to cosmetics [17-21]. ZnO NPs are regarded as a suitable material for a wide range of devices, including semiconductor diodes, transistors, and UV photodetectors, because of their high exciton binding energy of 60 meV and broad direct bandgap of 3.37 eV [22,23]. ZnO NPs are a wonderful option for biomedical applications because of their broad range of morphological shapes and forms and overall biosafety. ZnO nanoparticles (Nps) are employed

as carbon paste electrode modifiers (CPEs), which are more widely used because they are easier to obtain and are less costly. In order to produce an electrode material with improved preset properties, blending with admixtures of various compounds is a commonly followed route. Highly selective electrodes that handle organic and inorganic electrochemistry are made with this technique of electrode production.

2. Experimental

2.1 Investigation techniques and chemicals

The CHI-660c, a three-electrode electrochemical workstation, was used to conduct cyclic voltammetric experiments. The working, reference, and auxiliary electrodes are the ZnO/MCPE or BCPE, saturated calomel electrode, and platinum electrodes, respectively. The Hitachi S-3400N was utilised for the SEM and EDAX experiments, and the Rigaku Smart Lab system was used for the XRD investigations. Sigma Aldrich make Vanillin (VAN), sodium dihydrogen phosphate, $K_4[Fe(CN)_6]$, potassium chloride and Nice chemicals make disodium hydrogen phosphate and methanol were used in the study.

2.2 Synthesis of ZnO Nps

The 0.1M $Zn(CH_3COOH)_2$ solution was hydrolysed by blending it dropwise with the 0.2M NaOH solution for almost an hour while being agitated by using a magnetic stirrer. Following three or four distilled ethanol washes, the precipitate was dried for an hour at 90 °C in an oven. The dry precipitate was subsequently annealed for four hours at a temperature more than 450 °C to create the ZnO Nps powder[24].

2.3 Fabrication of BCPE and ZnO/MCPE

For about 45 minutes, 0.04 ml silica oil and 0.24 g of graphite powder in a 70:30 ratio was mixed into an agate mortar. To fabricate an electrode made of bare carbon paste (BCPE), the resultant powder was carefully poured into a Teflon chamber and polished it with tissue paper[25]. ZnO/MCPE was prepared using 4mg of ZnO Nps, and repeating the above process.

3 Results and Discussion

3.1 Investigation of surface topography and elemental study

ZnO characterisation has been discussed in details in the previously published paper given as the reference number [26].

3.2 Electrochemical behaviour of ZnO/MCPE

This is the continuation of the work on the analyte Mycophenolate mofetil as in [26], and the fabricated

electrode has higher active surface area (to 0.0378 cm²) than BCPE (0.0285 cm²).

3.3 Electrochemical behaviour of VAN at ZnO/MCPE

As shown in Fig. 2, the manufactured electrode was utilised to investigate the VAN (10 μM) at a sweep rate of 50 mVs⁻¹ using a supporting electrolyte of (0.2M, pH 7.4) PBS solution. The manufactured electrode (Green solid line) exhibited greater electroactive reactivity of VAN and a much larger peak current as compared to BCPE (Black dotted line) [27,28].

3.4 Concentration and sweep rate studies.

Concentration variation (10-50 μM) of VAN at ZnO/MCPE with a sweep rate of 50 mVs⁻¹ (0.2M PBS, pH 7.4) is shown in Fig. 3(A). The Ipa progressively increases with increasing concentration levels. As per the regression equation $Ipa(A) = 4.71 \times 10^{-5} \mu M - 8.43 \times 10^{-6}$ ($R^2=0.9918$) [29], the Ipa vs. VAN graph in Figure 3(B) exhibits remarkable linearity. The LOD and LOQ values were estimated using equations (3) and (4) [30,31], and were found to be 0.49 and 1.649 μM, respectively.

$$LOD = \frac{3S}{m} \text{ -----(3)}$$

$$LOQ = \frac{10S}{m} \text{ -----(4)}$$

Where, S is standard deviation, m refers to slope value.

Table 1. Comparing the LOD and LOQ values acquired using various electrochemical methods.

Electrode Type	Modifier	Technique	LOD (in μM)	LOQ (in μM)	Reference
CPE	Organic solvents	SWV	4.20	13.86	[32]
PVC/graphite electrode	Liquid membranes	Amperometry	290.00	965.6	[33]
GCE	n.a	Sono-SWV	16.00	53.29	[34]
CPE	Lysine	DPV	2.88	9.585	[35]
CPE	Poly Niacin	CV	1.01	3.356	[36]
CPE	ZnO Nps	CV	0.49	1.649	Present work

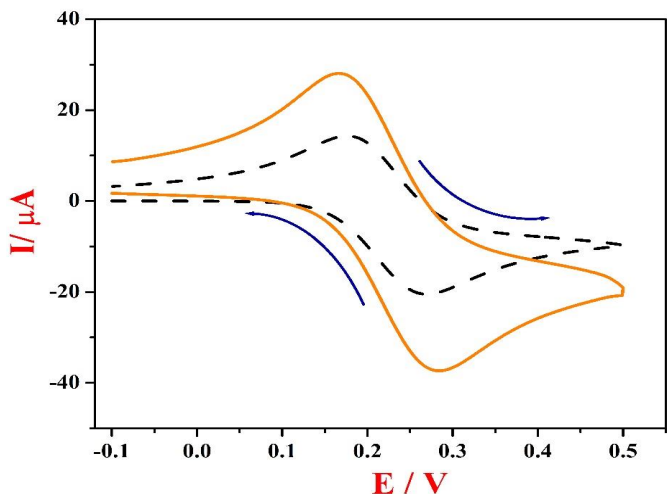


Fig. 1 CVs recorded at 1 mM K₄[Fe(CN)₆] at sweep rate 50 mVs⁻¹, BCPE (Black dashed line) and ZnO/MCPE (Red line)

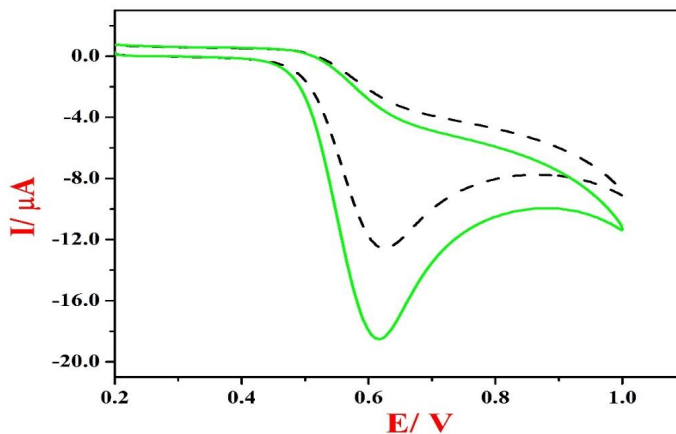


Fig. 2 CVs recorded at 10 μM VAN at sweep rate 50 mVs⁻¹, BCPE (Black dashed line) and ZnO/MCPE (Green solid line)

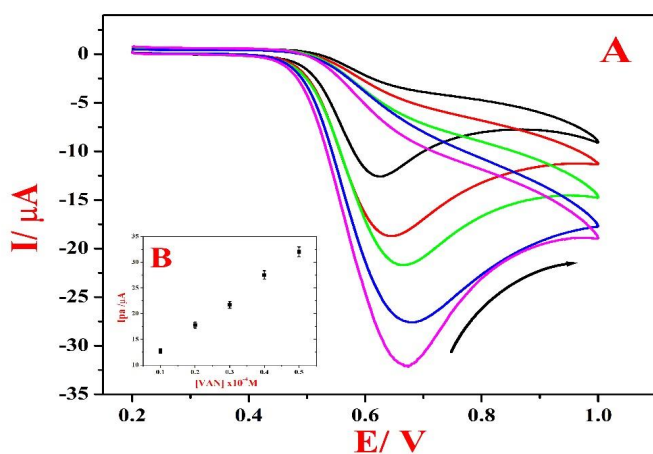


Fig. 3(A) CV's of VAN at ZnO/MCPE with varied concentrations (10-50 μM) using 0.2M PBS(pH=7.4) with sweep rate of 50mVs⁻¹. (B) Graph of I_{pa} vs concentrations of VAN.

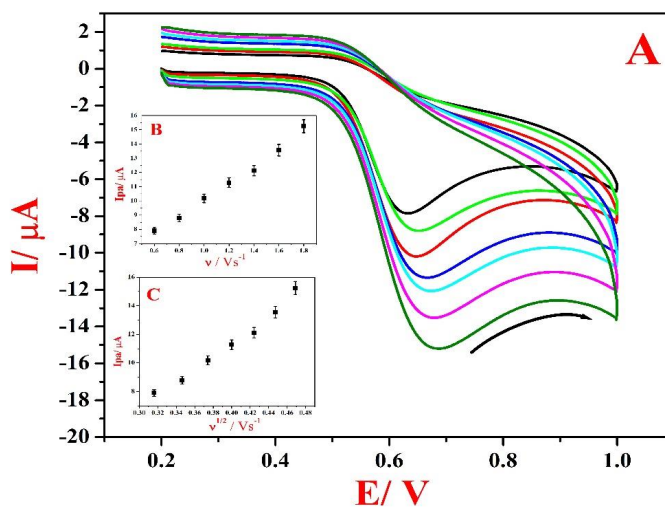


Fig. 4(A) CV's of VAN at ZnO/MCPE with varied sweep rates (50-400 mVs⁻¹). (B) Graph of I_{pa} versus sweep rate (v) (C) Graph of I_{pa} versus square root of sweep rate (v^{1/2}).

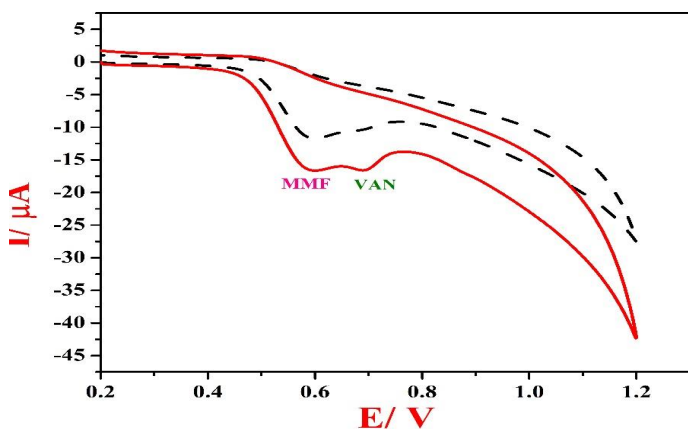


Fig. 5 CV's for simultaneous study of VAN and MMF (10μM each) at BCPE (Black dashed line) and ZnO/MCPE (Red solid line).
Table. (1) Data from the electrodes that were previously reported for the voltametric measurement of VAN

Compared to the LOD values gathered from earlier published studies for a range of detection approaches, the LOD value obtained in this work is significantly low. The present upgraded sensor is therefore more sensitive than the ones given in Table 1.

As illustrated in Fig. 4(A), 10 μM VAN in (0.2M, pH 7.4) PBS solution was used at ZnO/MCPE (200-500 mVs⁻¹) to modify the sweep rate. Peak potential shifts slightly with the sweep rate, but the peak current increases steadily. The I_{pa} vs sweep rate (v) graph in Figure 4(B) shows enhanced linearity with an R² value of 0.9928. Furthermore, as seen in Fig. 4(C), the I_{pa} vs v^{1/2} graph also showed improved linearity [37]. These findings imply that the ZnO/MCPE exhibits diffusion controlled faradic process for VAN reduction [38].

3.5 Simultaneous study of Vanillin

The experiment involved the use of mycophenolate mofetil (MMF). The cyclic voltammograms of MMF and VAN (10 μM concentration range) in PBS (0.2M PBS, pH 7.4) solution are shown in Fig. 5 at a sweep rate of 50 mVs^{-1} [39]. The results indicate that ZnO/MCPE demonstrated significant sensitivity with clearly distinct reduction peak separations, while BCPE (dashed line) demonstrated relatively low current sensitivity and selectivity. These results imply that the designed electrode is suitable for taking multiple measurements simultaneously.

3.6 Interference Study at ZnO/MCPE

A (0.2 M, 7.4 pH) PBS solution containing a range of chemical analytes (10 μM each) such as adenine, Na^+ , K^+ , dopamine, folic acid, and uric acid is tested together with MMF (10 μM)[40]. No interference was found during the research, indicating that any possibly interfering ions or compounds in the electrolytic solution had no effect on the potential peak of VAN. This demonstrates the exceptional selectivity of ZnO/MCPE electrode.

3.7 Practical analysis.

Commercial vanilla flavour was acquired from the local market and Histafree raspberry syrup, which was acquired from a nearby pharmacy, was put through a CV procedure to assess the practicality of the developed electrode. The analysis was done in accordance with the amount of VAN in that sample. We computed the sample's recovery using the data we had obtained, which are included in Table 2. The acquired recovery results (97.4-99.2%) indicate that VAN can be detected in real food samples using the currently constructed electrode[6].

Table. 2

Sample	Added (in μM)	Founded (in μM)	% Recovery
Vanilla essence	5	4.89 ± 0.12	97.8
	10	9.76 ± 0.13	97.6
	15	14.89 ± 0.1	99.2
Histafree Syrup	5	4.87 ± 0.1	97.4
	10	9.85 ± 0.12	98.5
	15	14.7 ± 0.1	98

4 Conclusion.

To produce the suggested sensor for measuring VAN at physiological pH, the ZnO/MCPE electrode is employed. The enlarged surface area exhibited exceptional catalytic activity as a result of the outstanding synergy


between the carbon paste and the adsorbed surface. The ZnO/MCPE displayed a larger active surface area than the BCPE, resulting in a significant current response. In addition, the study showed reduced LOD and LOQ when compared to previous published electrodes. There was a linear response observed when the concentration of the analyte and sweep rate of the electrode were varied. Simultaneous and interference testing verify the electrode's outstanding selectivity. Further stability testing indicates remarkable stability of modified electrodes with superior VAN recovery with good outcomes. The procedure was used in analysis of essences and medicinal formulations. Therefore, the study indicates that it is possible to consider the suggested sensor as a viable and promising alternative for the rapid and precise identification of VAN in pharmaceutically and physiologically viable materials.

References

- N.J. Walton, M.J. Mayer, A. Narbad, Vanillin, *Phytochemistry* 63 (2003) 505-515.
- M. Ohashi, H. Omae, M. Hashida, Y. Sowa, S. Imai, Determination of vanillin and related flavor compounds in cocoa drink by capillary electrophoresis, *J Chromatogr A* 1138 (2007) 262-267. <https://doi.org/https://doi.org/10.1016/j.chroma.2006.10.031>.
- L. Shang, F. Zhao, B. Zeng, Sensitive voltammetric determination of vanillin with an AuPd nanoparticles-graphene composite modified electrode, *Food Chem* 151 (2014) 53-57. <https://doi.org/https://doi.org/10.1016/j.foodchem.2013.11.044>.
- M. Luque, E. Luque-Pérez, A. Ríos, M. Valcárcel, Supported liquid membranes for the determination of vanillin in food samples with amperometric detection, *Anal Chim Acta* 410 (2000) 127-134. [https://doi.org/https://doi.org/10.1016/S0003-2670\(00\)00737-6](https://doi.org/https://doi.org/10.1016/S0003-2670(00)00737-6).
- P. Deng, Z. Xu, R. Zeng, C. Ding, Electrochemical behavior and voltammetric determination of vanillin based on an acetylene black paste electrode modified with graphene-polyvinylpyrrolidone composite film, *Food Chem* 180 (2015) 156-163.
- V. Erady, R.J. Mascarenhas, A.K. Satpati, Highly efficient and selective quantification of vanillin in food, beverages and pharmaceuticals using surfactant modified carbon paste sensor, *Sensors International* 1 (2020) 100023. <https://doi.org/https://doi.org/10.1016/j.sintl.2020.100023>.
- D.J. Abraham, A.S. Mehanna, F.C. Wireko, J. Whitney, R.P. Thomas, E.P. Orringer, Vanillin, a Potential Agent for the Treatment of Sickle Cell Anemia, *Blood* 77 (1991) 1334-1341. <https://doi.org/https://doi.org/10.1182/blood.V77.6.1334.1334>.
- Y. Cai, Q. Luo, M. Sun, H. Corke, Antioxidant activity and phenolic compounds of 112 traditional Chinese medicinal plants associated with anticancer, *Life Sci* 74 (2004) 2157-2184. <https://doi.org/https://doi.org/10.1016/j.lfs.2003.09.047>.
- J.D. Bythrow, Vanilla as a Medicinal Plant, *Seminars in*

- Integrative Medicine 3 (2005) 129–131. <https://doi.org/https://doi.org/10.1016/j.sigm.2006.03.001>.
- 10 P. Deng, Z. Xu, R. Zeng, C. Ding, Electrochemical behavior and voltammetric determination of vanillin based on an acetylene black paste electrode modified with graphene-polyvinylpyrrolidone composite film, *Food Chem* 180 (2015) 156–163. <https://doi.org/https://doi.org/10.1016/j.foodchem.2015.02.035>.
 - 11 C. Li, C.-L. Zhao, Determination of Vanillin in Milk Powder by Rapid Column High Performance Liquid Chromatography., *Asian Journal of Chemistry* 26 (2014).
 - 12 A. Yiğit, N. Alpar, Y. Yardım, M. Celebi, Z. Şentürk, A graphene-based electrochemical sensor for the individual, selective and simultaneous determination of total chlorogenic acids, vanillin and caffeine in food and beverage samples, *Electroanalysis* 30 (2018) 2011–2020.
 - 13 J. Zhao, H. Xia, T. Yu, L. Jin, X. Li, Y. Zhang, L. Shu, L. Zeng, Z. He, A colorimetric assay for vanillin detection by determination of the luminescence of o-toluidine condensates, *PLoS One* 13 (2018) e0194010.
 - 14 M. Timotheou-Potamia, A.C. Calokerinos, Chemiluminometric determination of vanillin in commercial vanillin products, *Talanta* 71 (2007) 208–212.
 - 15 Y. Shen, C. Han, B. Liu, Z. Lin, X. Zhou, C. Wang, Z. Zhu, Determination of vanillin, ethyl vanillin, and coumarin in infant formula by liquid chromatography-quadrupole linear ion trap mass spectrometry, *J Dairy Sci* 97 (2014) 679–686. <https://doi.org/https://doi.org/10.3168/jds.2013-7308>.
 - 16 Y.-H. Li, Z.-H. Sun, P. Zheng, Determination of vanillin, eugenol and isoeugenol by RP-HPLC, *Chromatographia* 60 (2004) 709–713.
 - 17 M.M. Foroughi, S. Jahani, Z. Aramesh-Boroujeni, M. Vakili Fathabadi, H. Hashemipour Rafsanjani, M. Rostaminasab Dolatabad, Template-free synthesis of ZnO/Fe₃O₄/Carbon magnetic nanocomposite: Nanotubes with hexagonal cross sections and their electrocatalytic property for simultaneous determination of oxymorphone and heroin, *Microchemical Journal* 170 (2021) 106679. <https://doi.org/https://doi.org/10.1016/j.microc.2021.106679>.
 - 18 S.B. Khan, M. Faisal, M.M. Rahman, A. Jamal, Low-temperature growth of ZnO nanoparticles: photocatalyst and acetone sensor, *Talanta* 85 (2011) 943–949.
 - 19 Y. Wang, G. Zhu, M. Li, R. Singh, C. Marques, R. Min, B.K. Kaushik, B. Zhang, R. Jha, S. Kumar, Water pollutants p-cresol detection based on Au-ZnO nanoparticles modified tapered optical fiber, *IEEE Trans Nanobioscience* 20 (2021) 377–384.
 - 20 P.-J. Lu, S.-C. Huang, Y.-P. Chen, L.-C. Chiueh, D.Y.-C. Shih, Analysis of titanium dioxide and zinc oxide nanoparticles in cosmetics, *J Food Drug Anal* 23 (2015) 587–594.
 - 21 T. Mocan, C.T. Matea, T. Pop, O. Mosteanu, A.D. Buzoianu, C. Puia, C. Iancu, L. Mocan, Development of nanoparticle-based optical sensors for pathogenic bacterial detection, *J Nanobiotechnology* 15 (2017) 25. <https://doi.org/10.1186/s12951-017-0260-y>.
 - 22 S. Venkatramanan, S.Y. Chung, T. Ramkumar, S. Selvam, Environmental monitoring and assessment of heavy metals in surface sediments at Coleroon River Estuary in Tamil Nadu, India, *Environ Monit Assess* 187 (2015) 505. <https://doi.org/10.1007/s10661-015-4709-x>.
 - 23 W. Muhammad, N. Ullah, M. Haroon, B.H. Abbasi, Optical, morphological and biological analysis of zinc oxide nanoparticles (ZnO NPs) using *Papaver somniferum* L., *RSC Adv* 9 (2019) 29541–29548.
 - 24 Z.M. Khoshhesab, M. Sarfaraz, M.A. Asadabad, Preparation of ZnO nanostructures by chemical precipitation method, Synthesis and Reactivity in Inorganic, Metal-Organic, and Nano-Metal Chemistry 41 (2011) 814–819.
 - 25 C.B.A. Hassine, H. Kahri, H. Barhoumi, Simultaneous Determination of Catechol and Hydroquinone Using Nickel Nanoparticles\Poly-4-Nitroaniline Nanocomposite Modified Glassy Carbon Electrode, *IEEE Sens J* 21 (2021) 18864–18870. <https://doi.org/10.1109/JSEN.2021.3089249>.
 - 26 G.S. Sumanth, B.E. Kumara Swamy, K. Chetankumar, S.C. Sharma, An enhanced electrochemical sensor using ZnO nanoparticles to measure mycophenolate mofetil: A cyclic voltammetric investigation, *Inorg Chem Commun* 169 (2024) 113050. <https://doi.org/https://doi.org/10.1016/j.inoche.2024.113050>.
 - 27 M. Sivakumar, M. Sakthivel, S.-M. Chen, Simple synthesis of cobalt sulfide nanorods for efficient electrocatalytic oxidation of vanillin in food samples, *J Colloid Interface Sci* 490 (2017) 719–726. <https://doi.org/https://doi.org/10.1016/j.jcis.2016.11.094>.
 - 28 P. A Pushpanjali, J. G Manjunatha, G. Tigari, S. Fattepur, Poly (niacin) based carbon nanotube sensor for the sensitive and selective voltammetric detection of vanillin with caffeine, *Analytical and Bioanalytical Electrochemistry* 12 (2020) 553–568.
 - 29 S. Reddy, B.E.K. Swamy, U. Chandra, B.S. Sherigara, H. Jayadevappa, Synthesis of CdO Nanoparticles and their Modified Carbon Paste Electrode for Determination of Dopamine and Ascorbic acid by using Cyclic Voltammetry Technique, *Int J Electrochem Sci* 5 (2010) 10–17. [https://doi.org/https://doi.org/10.1016/S1452-3981\(23\)15262-X](https://doi.org/https://doi.org/10.1016/S1452-3981(23)15262-X).
 - 30 K. Chetankumar, B.E.K. Swamy, T.S.S.K. Naik, Electrochemical sensing of catechol in presence of hydroquinone using a carbon paste electrode amplified with poly (vanillin), *Chemical Data Collections* 28 (2020) 100392. <https://doi.org/https://doi.org/10.1016/j.cdc.2020.100392>.
 - 31 K. Chetankumar, B.E.K. Swamy, T.S.S.K. Naik, A reliable electrochemical sensor for detection of catechol and hydroquinone at MgO/GO modified carbon paste electrode, *Journal of Materials Science: Materials in Electronics* 31 (2020) 19728–19740. <https://doi.org/10.1007/s10854-020-04498-x>.
 - 32 L. Agüí, J.E. Lopez-Guzman, A. González-Cortés, P. Yanez-Sedeno, J.M. Pingarron, Analytical performance of cylindrical carbon fiber microelectrodes in low-permittivity organic solvents: determination of vanillin in ethyl acetate, *Anal Chim Acta* 385 (1999) 241–248.
 - 33 M. Luque, E. Luque-Pérez, A. Ríos, M. Valcárcel, Supported liquid membranes for the determination of vanillin in food samples with amperometric detection, *Anal Chim Acta* 410 (2000) 127–134.
 - 34 J.L. Hardcastle, C.J. Paterson, R.G. Compton, Biphasic sonoelectroanalysis: Simultaneous extraction from, and

- determination of vanillin in food flavoring, *Electroanalysis: An International Journal Devoted to Fundamental and Practical Aspects of Electroanalysis* 13 (2001) 899–905.
- 35 B.K. Chethana, S. Basavanna, Y.A. Naik, Determination of vanillin in real samples using lysine modified carbon paste electrode, *J. Chem. Pharm. Res* 4 (2012) 538–545.
- 36 P. A Pushpanjali, J. G Manjunatha, G. Tigari, S. Fattepur, Poly (niacin) based carbon nanotube sensor for the sensitive and selective voltammetric detection of vanillin with caffeine, *Analytical and Bioanalytical Electrochemistry* 12 (2020) 553–568.
- 37 M. Sivakumar, M. Sakthivel, S.-M. Chen, Simple synthesis of cobalt sulfide nanorods for efficient electrocatalytic oxidation of vanillin in food samples, *J Colloid Interface Sci* 490 (2017) 719–726. <https://doi.org/https://doi.org/10.1016/j.jcis.2016.11.094>.
- 38 J.K. Shashikumara, B.E. Kumara Swamy, S.C. Sharma, A simple sensing approach for the determination of dopamine by poly (Yellow PX4R) pencil graphite electrode, *Chemical Data Collections* 27 (2020) 100366. <https://doi.org/https://doi.org/10.1016/j.cdc.2020.100366>.
- 39 M.M. Foroughi, M. Noroozifar, M. Khorasani-Motlagh, Simultaneous determination of hydroquinone and catechol using a modified glassy carbon electrode by ruthenium red/carbon nanotube, *Journal of the Iranian Chemical Society* 12 (2015) 1139–1147. <https://doi.org/10.1007/s13738-014-0575-7>.
- 40 J. Tashkhourian, M. Daneshi, F. Nami-Ana, M. Behbahani, A. Bagheri, Simultaneous determination of hydroquinone and catechol at gold nanoparticles mesoporous silica modified carbon paste electrode, *J Hazard Mater* 318 (2016) 117–124. <https://doi.org/https://doi.org/10.1016/j.jhazmat.2016.06.049>.

	<p>Mr. Sumanth GS. MSc Chemistry in Chemistry from Kuvempu University during 2019 and qualified GATE examination 2020. Currently he is doing my Ph.D in Industrial chemistry department of Kuvempu University under the guidance of Prof. B E KUMARA SWAMY on the topic modified carbon paste electrode sensor for some drugs and published four papers in International Journals and his interest includes Nanoparticle modified sensors, Cyclic voltammetric studies.</p>
	<p>Prof. B.E,Kumara Swamy has obtained his Ph.D degree in Industrial Chemistry from Kuvempu University and National Science Foundation (NSF) Post-Doctoral Research Associate from Southern Methodist University, Dallas, Texas and Research Associate in University of Virginia, Virginia, USA. Presently working as, a Professor and Chairman of Industrial Chemistry at Department of Post Graduate Studies in Industrial Chemistry, Kuvempu University. His research areas are Development of Electrochemical Sensor for some neurotransmitters, Biosensors, Nanosensors, Electrochemical Sensors and Nanochemistry. He has published more than 348 research papers in peer-reviewed journals with h index of 58 and citations were more than 11500 with i10 index 248. His interest includes modified carbon paste electrodes for biomolecules. He is in Associate Editor in Science Letters Journal, World Research Journal of Analytical Chemistry, Academic Editor to Journal of Chemistry, Advisory Board member in Biopublications and worked as Guest Editor in Special Issue on Nanoparticle and Cancer Treatment. He is a Fellow of American Chemical Society, Life Member of Indian Society of Analytical Scientists, SAEST member and ICC member. He served as the Deputy Registrar in Development Section Kuvempu University from July 2015 to Sept 2020 and Deputy Director in IQAC, Kuvempu University. He is recipient of Prof.M.R.Gajendraghad Gold Medal, Young Scientist Award from ICC and Swadeeshi Science Congress and Distinguished Scientist Award. Presently, Chairman in Board of Studies in Dept of Industrial Chemistry, Kuvempu University Shankaraghatta, Karnataka, India</p>
	<p>Dr. Chetankumar K finished M.Sc in Industrial Chemistry from Kuvempu University in 2015 and obtained Ph.D from same Dept during 2021 in Development of electrochemical sensor under the guidance of Prof B E Kumara Swamy and has published 21 papers in high reputed Journals and interest includes modified carbon paste electrodes and Nanochemistry and at present working in Kuvempu university</p>

SOCIETYFORMATERIALSCHEMISTRY(SMC)

(Reg. No. - Maharashtra, Mumbai/1229/2008/GBBSD)

c/o ChemistryDivision

Bhabha Atomic Research Centre, Mumbai 400085

APPLICATIONFORMEMBERSHIP

Please enroll me as a Life member of the Society for Materials Chemistry (SMC).

My particulars are as follows:

Name : _____

Educational Qualifications : _____

Field of Specialization : _____

Official Address : _____

Telephone No. (Off.) : _____

Residential Address : _____

Telephone No. (Res.) : _____

Address for Correspondence : Home/Office (Please tick one of the options)

E-mail Address : _____

Subscription Details

Mode of Payment : Cheque/DD/Cash

(Cheque/DD should be drawn in favor of "Society for Materials Chemistry" for Rs. 1000/- payable at Mumbai. For out-station *non-multi-city* cheques, please include Rs.50/- as additional charge for bank clearance.

Number : _____

Dated : _____

Drawn on Bank & Branch : _____

Amount : _____

Place: _____

Date: _____ Signature _____

Registration Number: _____ (To be allotted by SMC office)

Printed by:

Ebenezer Printing House

Unit No. 5 & 11, 2nd Floor, Hind Service Industries

Veer Savarkar Marg, Shivaji Park Sea-Face, Dadar (W), Mumbai - 400 028

Tel.: 2446 2632 / 2446 3872 Tel Fax: 2444 9765 E-mail: outworkeph@gmail.com

In this issue

Sr. No	Feature Articles	Page No.
1.	Controlled Distance Electrochemistry (CDE) for High Temperature Oxidation Studies of nuclear materials in reactor simulated condition <i>Kiran K Mandapaka and Supratik Roychowdhury</i>	1
2.	Electrochemical Impedance Spectroscopy to elucidate the mechanism of Stellite #3 corrosion in permanganate based decontaminating formulations <i>Veena Subramanian, Sinu Chandran, S.V. Narasimhan, and T.V. Krishnamohan</i>	7
3.	Electrochemistry in Nuclear Fuel Cycle <i>Manoj Kumar Sharma</i>	15
4.	Rapid and sensitive redox speciation method for vanadium during electro-synthesis of V(II) formate <i>K. K. Bairwa and V. S. Tripathi</i>	27
5.	Advancing Green Hydrogen Revolution: A Comprehensive Review of Bifunctional Electrocatalysts and Hybrid Materials for Water Electrolysis <i>Naseem Kousar, Gouthami Patil, Lokesh Koodlur Sannegowda*</i>	33
6.	Fabrication of a voltammetrically effective Vanillin sensor at a ZnO-modified carbon paste electrode: A cyclic voltammetric study <i>G.S. Sumanth, B.E. Kumara Swamy*, K. Chetankumar</i>	42

Published by
Society for Materials Chemistry
C/o. Chemistry Division
Bhabha Atomic Research Centre, Trombay, Mumbai 40085
e-mail: socmatchem@gmail.com, Tel: 91-22-25592001